Resurrecting an Ancient Bite: Virtual Chewing Model Sheds Light on one of the Earliest Primates

by
Amanda Slade

A thesis submitted to Johns Hopkins University
in conformity with the requirements for the degree of
Master of Arts in Medical and Biological Illustration.

Baltimore, Maryland
March, 2018

Abstract

The first true primates in the fossil record are known from near the Paleocene-Eocene boundary, approximately 55 million years ago. The prevailing evidence suggests that these primates diversified rapidly, making the sequence of events which make up their evolutionary history challenging to navigate. (Kay et al., 2004; Rose, 2006). A powerful tool for enhancing the understanding of primate origin is deciphering early primate chewing anatomy, as it can help paleontologists to infer a range of features including diet, body form and function and evolution. (Perry, 2008). The study of such ancient anatomy is inherently difficult, however, due to their fossil remains often being damaged and distorted, having undergone eons of geological stress. Furthermore, soft tissue is usually completely absent from the fossil remains of this time period.

Perry and colleagues (2015; 2018), however, have developed a rigorous muscular reconstructive techniques using mathematical estimates of muscle size based on muscle-bone correlation in living analogs. These techniques can radically enhance the reconstruction of a specimen but can be hindered by sediment obscuring the necessary osteological measurement points. Additionally, these estimates, although novel, are entirely static numerical reconstructions making their implications and plausibility difficult to visualize.

This project used virtual visualization techniques to facilitate both the accessibility and dynamic reconstruction of chewing muscle data acquired from a specimen of one of the earliest primate species, *Smilodectes gracils*. The rigorous restoration of the virtual skull allowed for novel jaw adductor volume data to be collected and subsequently visualized through an interactive web application, featuring the virtually reconstructed 3D skull, chewing musculature, and an animated chewing simulation which brings static numerical data to life. This project contributes to the fields of virtual paleontology and biocommunication by using visualization to both extract and dynamically display hard data. These tools helps demystify a portion the often convoluted and controversial discussion of primate origins, and have implications for understanding the ecological history of our own species .

Amanda Slade

Chairpersons of the Advisory Committee:

Jonathan M.G. Perry, **MSc, PhD**, Assistant Professor, Center for Functional Anatomy and Evolution

Timothy Phelps, **MS, CMI**, **FAMI** Professor (Faculty Advisor), Art as Applied to Medicine

Acknowledgements

The completion of this thesis would not have been possible without support and assistance of so many people. Jonathan M.G. Perry, Msc, PhD, Assistant Professor in the Center for Functional Anatomy and Evolution at the Johns Hopkins University School of Medicine, proposed the idea for this project to our department. I have always been very interested in evolutionary biology and so I would like to start by thanking him for allowing me to work with him on such a fascinating project. I have learned more than I could have ever imagined. Dr. Perry, himself has been equally fascinating to work with. Our topics of conversations were never entirely about the project and ranged from Star Wars to how to measure "stickiness". I would like to thank him for being brilliant, while simultaneously being laid back and fun to be around. I hope to emulate his approach to work and life it my future.

I would like to thank Timothy Phelps, MS, CMI, FAMI, Professor of Art as Applied of Medicine who out of all the faculty has always made me feel the most as if he was on "my side" and truly fighting in my corner. His guidance, experience, understanding and "dad jokes" were valuable to me not only for this project but for my life in general.

In addition, I would like to thank the rest of the faculty: Cory Sandone, David Rini, Jennifer Fairman, and Juan Garcia. Each of them has had a direct part in shaping the artist I will be graduating as. I will constantly think back on their guidance and teaching and will always aspire to be a master in my craft as each of them are. Dacia Balch is another person in the department who needs acknowledgment. The experience I've had these past two years would have been radically different without her. She greatly contributed to my piece of mind by making me feel like I had someone to turn to for virtually any issue.

I would like to thank my amazing classmates: Hillary Wilson, Lauren Rakes, Mary Shi, Shawna Snyder and Tziporah Thompson. They're talent, intelligence and ambition has provided me with inspiration, conversation, and support. In a field and program, which can by its nature be competitive, I would like to congratulate our class on always being gracious and positive toward one another. I will deeply miss each of their unique personalities and particularly each of their unique senses of humor. I have never hoped more that a group of people will stay my friends for life.

I would also like to acknowledge my parents. My mom was always the first person I would call on the occasions of thesis related tears and would always find a way to make me feel confident again. My Dad

who would continually surprise me with packages on my door step throughout the year, he has always had a talent for knowing the value of small gestures. I want to acknowledge my community in Portland: my brother Aaron and close friends: Kenny, Danielle, Casey, and Carl for always making me feel missed and loved when I returned home to visit. The feeling is and was always mutual.

A constant rock during this project and during my time in Baltimore in general, has been Scott Thorpe. He has given me emotional support, laughs and a home away from home while I have been living here. His ability's as an artist himself continues to inspire me.

Finally I would like to acknowledge my cats Maybelline and Kit Walker Texas Ranger who generally got in the way most of the time but whom I am fond of anyway.

Table of Contents

Abstract I

Acknowledgements II

Index of Figures VI

Introduction 1

1. Early Primates 1

2. Chewing Anatomy and Biomechanics 2

    2.1 Chewing Musculature 4

    2.2 Chewing Biomechanics 5

3. Virtual Paleontology 6

4. Facial Approximation 9

5. Objectives 10

6. Significance of the Study 10

Material and Methods 11

1. Data Acquisition and Processing 11

    1.1 Segmenting and Isosurface Creation using AVIZO 11

    2. Virtual Skull Restoration using Z Brush 12

    2.1 Reference Techniques 12

        2.1.1 Aligning Dentition 12

        2.1.2 Model References 13

        2.1.3 Fracture Patterns 13

        2.1.4 Reference Photos 14

        2.1.5 Expert Opinion 14

    2.2 Digital Techniques 15

        2.2.1 Reorientation 15

2.2.2 Organizing Geometry 15

2.2.3 Removing Sediment 15

2.2.4 Recreating Missing Anatomy 15

3. Virtual Skull Reconstruction using Z Brush 16

3.1 Symmetrization 17

3.2 Smoothing Restored Skull 17

3.3 Sculpting Techniques 17

3.4 Recreating Dentition 17

4. Virtual Mastication Muscle Reconstruction using GEOMAGIC, Z Brush and Blender 18

4.1 Scale Verification 18

4.2 Surface Area Measurements in GEOMAGIC 18

4.3 Numerical Muscle Volume Estimates 20

4.4 Extracting Origin and Insertion Surface Areas in Z Brush 20

4.5 Sculpting Appended Objects in Z Brush 20

4.6 Subtracting Overlaps in Z Brush 20

4.7 Volume Verification in Blender 22

4.8 Adding Muscle Texture and Fiber Direction in Z Brush 22

5. Facial Approximation in Z Brush 24

6. Optimizing Meshes for a Web Application using Z Brush and Blender 25

6.1 Creating a Low Poly Model in Z Brush 25

6.2 Retopologizing Models 26

6.3 Creating UV Maps in Blender 26

6.4 Creating Normal Maps in Blender 29

6.5 Texture Painting in Blender 29

7. Creating a Chewing Simulation in Blender 29

7.1 Rigging the model 29

7.1.1 Creating Armatures 30
7.1.2 Parenting Armatures and Posing 32
7.1.3 Adding Muscles to Jaw Armature 32
7.1.4 Weight Painting 32
7.2 Animating a Gape cycle in Blender 34
7.2.1 Determining Maximum Gape 35
7.2.2 Choosing Key Frames 37
7.2.3 Simulating Gape Phases 41
7.3 Shape keys and Volume Conservation 41
7.4 Shape keys and Volume Conservation 41
7.5 Vertex Baking 45

8. Creating interactive applications using Blend4Web 46
8.1 Creating an Environment 46
8.2 Creating a Node Tree 47
8.3 Annotations 50
8.4 Exporting 50

RESULTS 51

1. Fossil Reconstruction Results 51
2. Muscle Reconstruction Results 56
2.1 Dimensional Data 56
2.2 Virtual Jaw Adductor Models 56
3. Chewing biomechanics Results 61
4. Facial Approximation Results 62
5. 3D Interactivity Results 63
6. Work Flow Results 66
7. Assets Referral 72

DISCUSSION 68

1. Fossil Reconstruction 68

2. Muscle reconstruction: 68

3. Chewing model and Animation 69

4. Facial approximation 70

5. Web application and Interactively 71

6. WebGL using Blend4Web 71

7. Working in Blender 72

8. Working in Z Brush 72

9. Reproducible Workflow 73

CONCLUSION 73

REFERENCES 74

VITA 78

List of Figures

Figure 1. Combined geologic time scale and Phylogenetic tree of primates. **3**

Figure 2. Smilodectes gracilis fossil specimen of cranium and mandible (DMNH 10000) 5

Figure 3. Screen shots of the (A) Isosurfaces of the mandibles and the (B) Isosurface of the cranium, within AVIZO software. 11

Figure 4. Screen shots showing the process of aligning the dentition of the jaw to the dentition of the cranium within Z Brush. The cranium has been "hidden" within Z Brush for clarity. 12

Figure 5. Photographs of reference models including, a (A) dental model of M1, M2, M3 on Cautius ralstoni (a close relative of Smilodectes) and a (B) cranium of Propithetcus coguereli (an extant lemur). Photo credit: Amanda Slade 2018. 13

Figure 6. Screen shot of a masked section of the specimen that follows a fracture pattern in Z Brush. 14

Figure 7. Screen shots of (A) a superior view of the cranium and jaw having been oriented in Z Brush and (B) a lateral view of the jaw having been oriented to fit the cranium. 15

Figure 8. Screen shots of the recreated anatomy of the virtual specimen in Z Brush. 16

Figure 9. Screen shot of an individual tooth being made into a Sub Tool, in Z Brush, so that it can be manipulated independently of the surrounding dentition. Transparency is enabled. 17

Figure 10. Screenshot in GEOMAGIC of the surface area for the origin of the medial pterygoid painted onto the mandible. 19

Figure 11. Screenshot in GEOMAGIC of (A) the Fill Holes function being performed on the origin of the medial pterygoid object, (B) the Fill Holes settings used, (C) the surface area being calculated on the origin of the medial pterygoid, and (D) the output of the Select by Area function. 19

Figure 12. The table lists each of the jaw adductors and their respective volume estimates in cm3. 20

Figure 13. Screenshots of (A) "origin" Sub Tool of the temporalis positioned correctly,

(B) the mask painted following the origin Sub Tool as a guideline, and (C) mesh extracted from the mask. 21

Figure 14. Screenshots of Blender interface showing 3D Print Plugin tab (A) the Volume output field. 22

Figure *15*. Screen shots of the (A) basic muscle shape, (B) Damien standard to make major muscle fiber groups and (C) finer muscle fiber detail. 23

Figure 16 Screenshots of (A) underlying anatomy visible within the transparent surface sculpt and (B) the basic surface anatomy sculpt of Smilodectes Gracilis. 24

Figure 17 Screen shot of ZRemesher settings in ZBrush 25

Figure 18. Screen shots of (A) Blender seam selection under (B) Edit mode 26

Figure 19. Screen shots of Blender interface showing a (A) UV Mapping menu and a (B) split screen with the UV map shown in the UV/Image Editor type. 27

Figure 20. Screen shots of (A) Normal map mapped onto the UV map and (B) the Bake menu with the Bake mode set to Normals. 27

Figure 21. Screen shots of Blender medial pterygoid muscle mesh showing the (A) high and low poly meshes before the normal map is applied to the low poly mesh and the (B) high and low poly meshes after the normal map is applied to the low poly mesh. 27

Figure 22. Screen shot of Blender showing the texture painting interface. Areas of interest are highlighted. Text not intended to be read. 28

Figure 23. Screen shots of Blender showing a Single Bone being added to the scene and the Armature Display options. Not all text is intended to be read. 30

Figure 24. Screen shots of Blender showing the three elements of a Bone. 31

Figure 25. Screen shots in Blender showing (A) the positioning the Root of the Bone in Octahedral display to align with the helical axis of the jaw and (B) positioning in the Bone to reside in the midpoint between the mandibular condyles along the helical axis shown in yellow. 31

Figure 26. Screen shots in Blender showing (A) frontal view of the jaw armature in Stick display (B) lateral view of the jaw armature with the helical axis of the jaw shown in yellow. 31

Figure 27. Screen shots in Blender showing (A) bones created for the medical pterygoid,

(B) bones created for the masseter, (C) bones created for the temporalis, and (D), (E) two views of the final armature including all bones and all muscles. 33

Figure 28. Screen shots in Blender in Weight Paint Mode showing a bone's influence on the masseter muscle mesh. Red indicates maximum influence: blue indicates no influence. 34

Figure 29. Screens hots in Blender showing condyle displacement set at 2mm. 35

Figure 30. Screens hots in Blender showing the condyle "contacting" the mandibular fossa (at 46.8). 36

Figure 31. Table showing the Maximum Gape in degrees from the vertical axis at different condyle displacement points. The average Maximum Gape is also shown highlighted in yellow. 37

Figure 32. Image depicting the elliptical shape the path of the jaw's vertical and horizontal path creates when the rostral most point at its midline is tracked during a gape cycle. The eight points chosen to represent this shape are indicated in white circles. The X axis represents lateral displacement in mm and the Y axis represents vertical displacement in mm. 38

Figure 33. Screen shots in Blender showing the recreated elliptical shape made of cube objects and the jaw being matched to one of them. 39

Figure 34. Screen shots in Blender showing (A) a close view of the jaw being moved to point 4 and (B) the Control Bone's coordinates that were key framed. Location Z indicates the condylar displacement of 1.5 mm within the mandibular fossa, Rotation X indicated the jaw rotation around the transverse axis, and Rotation Y indicates the jaw rotation about the vertical axis. 39

Figure 35. Screen shots in Blender showing the graph editor depicting the vertical displacement of the jaw (in degrees around the Transverse Axis). Colors and text are added over the screen shot to demonstrate how the graph is similar to actual data describing the four phases in the gape cycle (FC - Fast close, SC- Slow close, SO - Slow open, FO - Fast open) (Ross and Diaz 2014). 40

Figure 36. Table describing the keyframe data at each point in the gape cycle. The table shows the Rotation around the Transverse Axis, Rotation around the Vertical Axis, Number of frames between each point, and the Phase in the Gape Cycle. 40

Figure 37. Screen shots in Blender showing the volume being measured with the Volume Tool before and after the armature displaces the mesh. The volume is shown to be (A) 4.18 cm3 before being displaced and (B) 5.8535 cm3 after being displaced. This demonstrates how volume is not conserved. Not all text is intended to be read. 42

Figure 38. Screen shot in Blender of Shape Key interface demonstrating the Relative Value slide bar being adjusted. 43

Figure 39. Screen shots in Blender showing the volume being measured with the Volume Tool before and after the armature displaces the mesh. The volume is shown to be (A) 30.8732 cm3 before being displaced and (B) 26.4637 cm3 after being displaced, which matches its original value at rest. Not all text is intended to be read. 44

Figure 40. Screen shot in Blender showing Bake Vertex Animation settings. 45

Figure 41. Screen shot in Blender showing the Camera Limit's settings used. 47

Figure 42. Screen shot in Blender showing the Select Node used in creating the Node Tree, including (A) the hide object node, (B) the Switch Select node, and (C) the play animation node. 48

Figure 43: Screen shot in Blender showing the Node Tree used for the interactive application. Text is intended to be read. 49

Figure 44: Screen shot in Blender showing Annotation properties used for the Masseter annotation 50

Figure 45. Lateral view of original virtual fossil. 52

Figure 46. Lateral view of the virtually restored cranium and mandible. 53

Figure 47. Lateral view of the virtual reconstruction of the skull. 54

Figure 48. Posterior view of the virtual reconstruction of the skull. 55

Figure 49. Table of volume estimates of the jaw adductor muscles 56

Figure 50. Lateral view of the virtual muscle reconstruction. 57

Figure 51. Lateral view of the virtual muscle reconstruction with Masseter removed. 58

Figure 52. Posterior view of the virtual muscle reconstruction with Masseter removed. 59

Figure 53. Medial and Lateral views of the origin and insertion sites of the jaw adductor muscles 60

Figure 54. Still screen captures of the dynamic chewing simulation. 61

Figure 55. Virtual facial approximation. 62

Figure 56. Screen shots displaying the interactive chewing simulation in a web application 63

Figure 57. Screen shot displaying the interactive web application, displaying muscle interactivity. 64

Figure 58. Screen shot displaying interactive web application, displaying muscle interactivity. 65

Figure 59. Diagram of the project work flow. 66

INTRODUCTION

The study of primates has always had inherent interest and has been of special interest since Linneaus included humans in his classification of animals (Linneaus 1735). The human species has since been traced back 7.2 million years when the first hominin remains occurred (Burnet et al., 2002). The first primates, tiny lemur-like mammals, however, occurred almost 50 million years earlier. The study of these very early primates enriches our understanding of living primates and provides a more complete understanding of the primate evolutionary tree to which the human species belongs.

This project offers the unique opportunity of investigating one of the most ancient primate species, *Smilodectes gracilis*, by exploring a remarkably preserved fossilized skull and associated jaw discovered in Wyoming in 1993. Such well- preserved and near complete fossils are important to paleobiology because they permit a richer reconstruction of past ecological relationships than is true for most fossils. This project utilized the CT scan of the specimen (DMNH 10000, housed at the Denver Museum of Nature and Science) to study the chewing architecture and dynamics of early primates by virtually reconstructing a *Smilodeces gracilis* cranium, mandible and jaw adductor musculature and subsequently simulating its chewing movement.

1. Early Primates

The first true primates in the fossil record are known from roughly the Paleocene-Eocene thermal maximum, approximately 55 million years ago. Increased temperatures caused a cosmopolitan dispersal that included a thriving group of early primates (Rose, 2006, p. 343). These small creatures featured specific arboreal adaptations that set them apart from other tree dwellers including: a specialized grasping foot, a replacement of claws by nails on all digits, hind limb locomotor dominance, reduced olfaction, stereoscopic vision, and large brain to body size ratios (Cartmil, 1972; Sussman, 1978; Rasmussen, 2007)

These first euprimates (true primates) divided abruptly into two groups that are thought by some to represent today's basic dichotomy of all primates. The tarsier-like Omomyiforms which belong to the Haplorrhini (which includes modern tarsiers and simians), and the lemur like Adapiformes which belong to the Strepsirrhini (which include modern Lemuriformes.) (Kay et al.,2004; Rose, 2006). Currently there are no transitional forms that indicate a common ancestor between the Adapiformes and Omomyiformes, although several early primates from India are so primitive that they are difficult to allocate to either

group (Dunn et al., 2016). The prevailing evidence suggests that the earliest primates diversified rapidly and this makes the members of the two groups equally important in enriching the understanding of the origins of all primates. (Kay et al., 2004; Rose, 2006). **(fig 1).**

The Adapiformes group includes the most primitive and well known of all fossil primates the Notharctids (see Gregory's 1920 *Notharctus* skeleton study). Some of the most common species found in the early and middle Eocene deposits are of this group and thus their evolutionary history has been comparatively well documented and has even been used to support evolutionary gradualism (Rose 2006). This group contains six genera including *Smilodectes*.

Smilodectes is composed of three named species with *Smilodectes gracilis* being the most well documented. *S. gracilis* was a successful species from the middle Eocene Bridger Formation of Wyoming. Based on its dental morphology it is thought to have been a foliovore. They have the dental formula 2-1-4-3 and lacked a fused symphysis. This species has a more rounded frontal bone and shorter snouts compared to other Notharctids. *S. gracilis* also features comparatively reduced olfactory bulbs, an enlarged visual cortex, and relatively smaller eyes than their nocturnal counterparts, all of which supports the inference that it was a diurnal species. Its cranial capacity of 9.5 cubic centimeters and lower average body mass of 2kg, yields an encephalizaiton quotient relatively high for the Eocene although lower than any living primate (Gingerich, 1980) . From studies of its skeleton it is thought to have been a vertical climber and leaper.(Fleagle 1988).

Although the Notharctids features some fairly well described genera, including *Smilodectes*, there are still many questions left unanswered. A shallow knowledge of Notharctids behavior, diet, morphology, body form and function and evolutionary history warrants further study. A logical place to start is a study of the craniomandibular anatomy in that it can provide unique insight into each of these areas and can especially shed light on feeding behavior and diet. Dietary and oral processing of this group, in turn, can have the potential to illuminate the uncertain euprimate history of origin given that most reconstructions of extinct primates include some inferences about diet. (Cartmill, 1972 Sussman, 1991)

(Perry et al., 2015)")

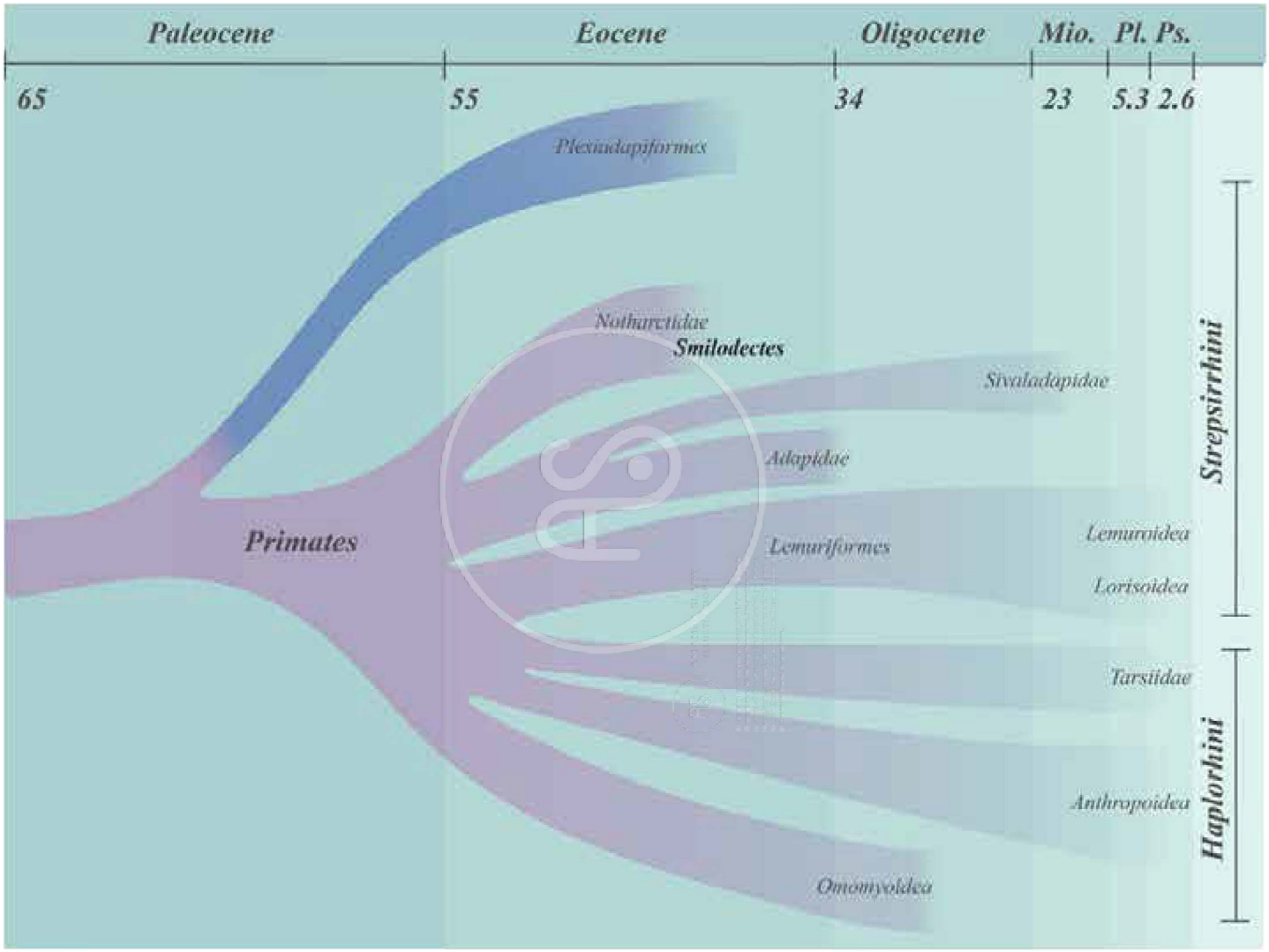

Figure 1. Combined geologic time scale and Phylogenetic tree of primates.

2. Chewing Anatomy and Biomechanics

Feeding behavior allows an organism to acquire the energy needed for sustaining survival and the ability to reproduce. Masticatory anatomy in primates should therefore be selected to improve their feeding performance. Ross and Diaz suggest, "Relationships among feeding system morphology, feeding behavior, and diet not only explain the morphological diversity of extant primates, but can also be used to reconstruct feeding behavior and diet in fossil taxa. (Ross and Diaz, 2014 p 104)".

2.1 Chewing musculature

The study of masticatory anatomy including jaw adductors allow for important inferences to be made about diet, body form and function, and evolution (Perry, 2008) This is because, "Diet and mastication are closely tied to hard anatomy" (Perry, 2008). Thus, access to data from living analogs make reconstructions of mastication especially justifiable for early primates (Perry, 2008)

Using mathematical estimates of muscle size based on muscle-bone correlation in living analogs, Perry and colleagues (e.g., Perry, 2008; Perry et al., 2015; Perry , 2018) have developed one of the most rigorous approaches to chewing muscle reconstruction. For the first time the dimensions of the chewing muscles have been estimated in early primates using correlations between muscle dimensions and bone dimensions. Although many suggestions had been presented on early primate diet (e.g., Covert, 1986; Ravosa, 1996), no study had produced any real dimensional data on chewing musculature.

Perry et al. (2015) utilized living strepsirrhines as analogs for early primates. A sample of extant strepsirrhine cadavers was used to "compare the osteological proxies of muscle dimensions to the actual dimensions of the muscle they represent (Perry 2011)". These same proxies were then made on adapid specimens to make estimates for jaw adductor muscle mass, physiological cross-sectional area, fiber length, muscle leverage, bite force and gape. These estimates were able to provide another source of dietary inference in adapids and was able to strengthen the previous dental-dietary hypothesis that they were foliovores and cast uncertainty on the hypothesis that they were gougers of tree exudates.

This study (Perry et. al., 2015) selected Adapidae as subject of analysis due to the quality of the skull specimens because feeding behavior inferences on this group have the potential to illuminate euprimate origins. The nothartids, which existed simultaneously, would have equal potential to shed light on euprimate origins. Using the jaw adductor muscle estimate techniques on this similar group would be beneficial providing a more complete picture of euprimate phylogeny and origins as well as validate or invalidate the current dentition based hypotheses about Notharctid diet and feeding behavior. *S. gracilis*

would be a particularly apt species to utilize these techniques, in that a remarkably well preserved specimen with an associated jaw is available **(fig 2)**, along with a complete micro CT scan of the fossil**.**

Applying these muscle reconstruction techniques to the *S. gracilis* specimen would dramatically increase the value of its reconstruction. Even these advanced reconstruction techniques, however, have their limitations. Fossils themselves can be difficult to measure due to their distorted state and sediment blocking the view of an osteological site of interest. The act of handling the fossil can also damage it. Numerical reconstructions also lack visual verification of their feasibility. A volume of a muscle for instance, may seem reasonable until it is recreated physically and applied to the bony anatomy, where flawed proportions can suddenly become very obvious. Numerical muscular reconstruction estimates also cannot demonstrate how the muscles interacted with the skull and one another, or how they behaved during jaw movement. A virtual 3D model of the musculature based on real volumetric data would have clear potential in resolving some of these issues.

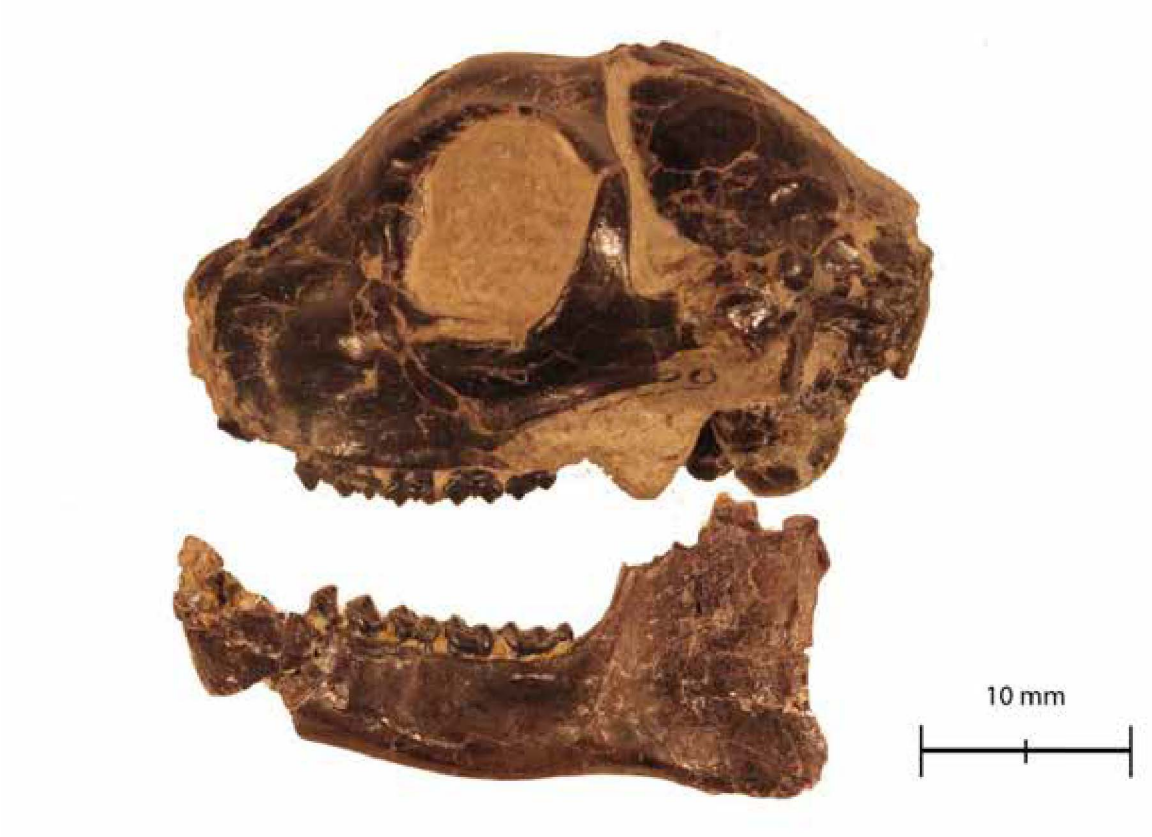

Figure 2. Smilodectes gracilis *fossil specimen of cranium and mandible (DMNH 10000).*

2.2 Chewing Biomechanics:

Ross and Diaz's review of primate feeding biomechanics suggests that biomechanics "develops and tests hypotheses relating morphological to behavioral variation and using physical principles … applied through mathematical models of biological system." (2014, p 105) This process is difficult in the field of extinct primate biology in that the behavior of extinct primates cannot be observed and thus any mathematical models must be based entirely on morphology.

Furthermore, historically the field of primate jaw morphology and biomechanics have been dominated by mathematical modeling, experimental investigations, and anatomical descriptions. Most of these are complicated and difficult to follow for the uninitiated student or beginning researcher. The development of powerful digital tools for visualizing and communicating biomechanical and anatomical data have become not only helpful, but perhaps pedagogically necessary, for educating students on the complexities of masticatory biomechanics. In this project, I have combined data from strepsirrhine osteological correlates, the anatomy of the skull in *Smilodectes gracilis*, and 3D digital tools to generate a soft-tissue, moving model of chewing in this early fossil primate. This model, to the extent possible, is also informed by experimental data on chewing movements in mammals in an effort to bring these experimental studies to life.

3. Virtual Paleontology

Within the last decade, the field of paleontology has experienced a "CT revolution" (Sutton, 2014 p.6) which coincides with the increased availability of Computed Tomography scanning. In a field devoted to the study of delicate three dimensional specimens, the advantages of CT and other non destructive scanning technology, are obvious. Studying fossils requires extracting information from delicate, 3D structures. Traditional methods of preparing fossils for study all require physical handling and processing which risk damage and lost data. CT scanning allows for the Paleontologist to analyze, isolate, segment and immortalize fossils without ever touching them. Despite its advantages, the techniques involved in virtual paleontology are not as widely used as they might be, in part, because they are considered, "too difficult" (Sutton 2014) and time consuming. Although digital processing a fossil is generally faster, a good quality virtual fossil of a complicated specimen can still take days to prepare (Abel et al., 2012). Creating models and animations which clearly display a novel fossil finding, can take even longer.

Before the rise in CT scanning technology and virtual paleontology, paleontologists heavily relied

on, and still rely on fossil "preparators" in order to make a fossil ready to study (Brown, 2009).

The occupation of a preparator, involves the preparation and conservation of fossils for the purposes of research by scientists. (Brown et al., 2009) In a text book describing paleontological techniques, the author writes, "vertebrate paleontology...is a field of study where the accuracy of collection and preparation of specimens and data is the foundation that determines the ultimate quality of the science" (Leiggi and May, 1994, vxiii). This notion has not changed with the shift from physical to digital studies, however, the needs of a virtual paleontologist have shifted to require the addition of a "virtual preparator" as well as a traditional one. The skills of a biocommunicator are apt for filling this role and pioneering this convention shift, by bridging the gap between raw CT data, and polished, easily accessible, and interactive 3D models. This project will document novel workflow of a virtual fossil preparation of as well as the creation of interactive virtual models, based on the data collected from the reconstructed virtual specimen.

In addition to the virtual preparation of fossils themselves, accurate digital models have become vital in advancing research, resolving contrasting hypothesis, and assisting in exhibiting findings to a wide audience. (Molnar 2009). Visualization has traditionally been an excellent way to provide a complete reconstruction of an extinct species. Illustrations and models have historically played a major role in forming concepts of extinct animals and how they behaved in life (Molnar, 2009). 3D modeling and animation software takes this role to an even higher level. Physics based software such as **Cinema 4D, Blender** and **Maya** have the capability of realistically mimicking biomechanics using rigging and constraints (Molnar, 2009). Forensic reconstructive methods can be applied digitally using **Z Brush** which permits digitally sculpting musculature and surface detail over a skull base. Web based interactivity allows the digital models to be viewed and studied in a three dimensional platform.

These advances in virtual paleontology as well as digital imaging have opened a new world for paleontology and specifically for early primate studies and chewing mechanics. Previously inaccessible brain cavities surrounded by fragile skulls and sediment have been able to produce virtual endocasts of three different adapiforms (including *Smilodectes gracilis*) by using CT scans and digital processing (Harrington et al., 2016; Gilbert and Jungers, 2017) .A Hadropithecus (giant lemur) skull, was also recently virtually reconstructed to near completion; accurately displaying this rare species for the first time (Ryan et al., 2008). The first volumetrically accurate 3D print of the phelangeroid masticatory apparatus featuring removable muscle layers, was created using 3D scans and sculpting software at Johns Hopkins University (Reback, 2017; St Clair et. al. 2018). T. Ross and Diaz have created virtual models of

primate jaws during their respective gape cycles, demonstrating the actual displacement magnitudes in real time (Ross and Diaz 2014). These projects demonstrate the increase value paleontology, and specifically primate biology have placed on digital imaging.

With the increased production of virtual 3D specimens and models digital sharing has become increasingly important. Researchers have been using the internet to share data more directly (**ispeCT appl**et on **DigiMorph**, for example (Abel et al., 2012)). Organizations such as The Smithsonian Natural History Museum have been sharing data as well as publicly providing an online interactive 3D collection of fossils, artifacts, primates and other animals ("Human Evolution Evidence, 3D Collection", 2018). **Sketchfab** is a platform that uses **WebGL (Web Graphics Library)** technology to publish, share, buy and sell 3D **Virtual Reality (VR)** and **Augmented Reality (AR)** content and supports a growing population of paleontologists who use it to upload fossil content. However, a method of sharing that allows public accessibility, high quality resolution of the models, and full interactivity has not been established. Technical issues involved in sharing data has still been problematic for scientists and can even be said to be holding back CT based morphological research (Abel et al., Sutton et al., 2016)

In this project I will utilize **WebGL** technology through **Blend4Web** to share the virtual 3D models and animations created in this project. **WebGL** a **JavaScript** application programming interface for rendering interactive 3D graphics within any compatible web browser without the use of software component add-ons (Tavares, Gregg, 2012). This technology is remarkable in that it makes a 3D model accessible to anyone with internet access. **Blend4Web** is an open source framework that utilizes the power of **WebGL** for creating and displaying interactive 3D computer graphics within web browsers. A 3D model can be exported as a single self-contained **HTML** (**Hyper Text Markup Language)** file and embedded within a web page using a standard **i-frame HTML element** (Kovelenov, 2014). This program is unique in that it provides more powerful interactive options than programs such as **Sketchfab** without requiring any coding knowledge. Embedding an **HTML** file within a publication is entirely plausible. In this project I use **WebGL** technology through **Blend4Web** software to share high resolution, virtual, 3D chewing models and simulation within a fully interactive online application. This project will serve as a model for the possibilities of utilizing **WebGL** and specifically **Blend4Web** as a mechanism for sharing fossil data.

To create the first dynamic fully articulated, manipulable, animated and interactive model of an extinct primate for the study of chewing biomechanics, this project will have harness the full range of digital processing software and integrate information from different fields. The model incorporates

data from comparative anatomy, functional morphology, and biomechanics. The project utilizes the full range of digital processing possible moving through CT imaging, 3D sculpting, rigging, animation and finally online interactive software. This project will not only push the boundaries of the study of early primate chewing architecture and dynamics but will also document a novel workflow that utilizes the full breadth of digital imaging and that demonstrates a future direction of virtual paleontology.

4. Facial Approximation

The Society of Vertebrate Paleontology has awarded the John J. Lanzendorf PaleoArt Prize for achievements in the field of paleo art since 1999. The society maintains that paleoart, "is one of the most important vehicle for communicating discoveries and data among paleontologists, and is critical to promulgating vertebrate paleontology across discipline and to lay audiences." (Society of Vertebrate Paleontology, 1999).

The field of paleoart has been heavily dominated by subject matter concerning developments in dinosaur biology. Large quantities of dinosaur art ranging from 2D illustrations, to physical 3D models, to virtual 3D animations exist to assist in communicating data in the field. Such a variety of artistic representation does not exists for extinct primates, save for those that are direct evolutionary precursors of humans. The artistic representations for early primates are generally reduced to flat 2D illustrations. A virtual 3D reconstructions of an early primate using reproducible forensic style facial approximation techniques has not been achieved.

An accurate and scientific based facial approximation for early primates becomes especially justifiable when the work of bony and muscular reconstruction is already done. The basis for accuracy in facial construction is already halfway there. The adductor muscles, skull and jaw make up most of the animal's facial silhouette. The relative size and orientation of the eyes can be inferred from bony orbit size. The external acoustic meatus being intact allow for a reasonable indicator of ear location. Any subsequent decision making on detail can be made based of off living analogs whose relevance as accurate references is backed by phylogeny.

This project created a unique opportunity to utilize the virtual reconstruction products created for more rigorous scientific purposes, as a means of producing a facial approximation of an early primate that is uniquely backed by anatomically justified decision making. This creates a further example of the capabilities of paleontological imaging.

5. Objectives:

This project aims to contribute to the study of early primate origins by presenting an interactive web based application featuring a polished set of virtual three dimensional reconstructions of one of the earliest primate species, *Smilodectes gracilis,* including a rigorously refurbished skull, 3D representations of novel chewing muscle data, and an animated chewing simulation which brings the static numerical data to life. The contribution of these visualization tools will hopefully illuminate a portion of the often convoluted and controversial discussion of primate origins as well as demonstrate the full potential and value of virtual planetological imaging. The specific goals include the creation of:

A virtual 3D model of a fully restored skull of *Smilodectes gracilis* derived from the CT data of an individual fossil specimen.

Virtual 3D jaw adductor muscle models based on muscle size estimates gleaned from measurements taken off the restored skull.

An animated a chewing simulation of the muscles and jaw engaged in a typical gape cycle based on documented primate biomechanical chewing data.

A virtual 3D facial approximation using sculpting software and basic forensic reconstruction techniques.

A fully interactive online application to display the previously described models and simulations. The application will be allow full manipulation of the models and include: control of individual muscle visibility, highlighted muscular origins and insertions, and zoom, pan, and rotate features.

A reproducible workflow detailing the steps of moving from CT fossil data, to virtual reconstruction, to rigging and animation, to web optimization and finally online accessibility.

6. Significance of the Study:

This project brings new understanding of ancient primate chewing architecture and dynamics by creating a digital 3D reconstruction of a *Smilodectes* skull, chewing musculature, and chewing behavior and thus contributes to the continued study of, and education about, the primate evolutionary tree. The interactivity of the model and simulation will set a standard for how fossils and 3D reconstructive work are presented within the scientific community. The project also contributes to the biocommunication field by bridging the gap between raw CT data, and polished, easily accessible, and interactive 3D models.

Materials and Methods:

1. Data Acquisition and Processing

A fossil specimen of *Smilodectes gracilis* was borrowed by the Department of Functional Anatomy and Evolution, Johns Hopkins, from the Denver Museum of Nature and Science in 2014. The specimen (DMNH 10000) includes a fossilized cranium, mandible (both sides) and proximal tibia. Three dimensional data were obtained from computer tomography at a slice resolution of 0.1063 mm using an Industrial High Resolution CT/S Ray Scanner located at the Duke University Shared Materials Instrumentation Facility. 2065 images resulted from the scan of the cranium and 1603 images of the jaws and proximal tibia.

1.1 Segmenting and Isosurface Creation using AVIZO

AVIZO 7.0 software (FEI Visualization Sciences Group) was used to view and process CT data. The images were viewed by importing the data sets **(Open > select all images in stack),** right clicking on the data set and selecting **Orthoslice.** The contrast and brightness were adjusted in the **Data window** to visualize the data. The data were segmented by selecting the data set and using the magic wand tool to select the bone while eliminating background and other sediment surrounding the bone **(Magic wand tool > Check box all slices, Add selection to current material > save data as).** A surface model was created using the Generate surface function **(select .tif-lable data set > Generate surface > Apply, Surface tab > view > shaded).** The final model was exported as an OBJ file. The process was repeated with the jaw data **(fig 3)**.

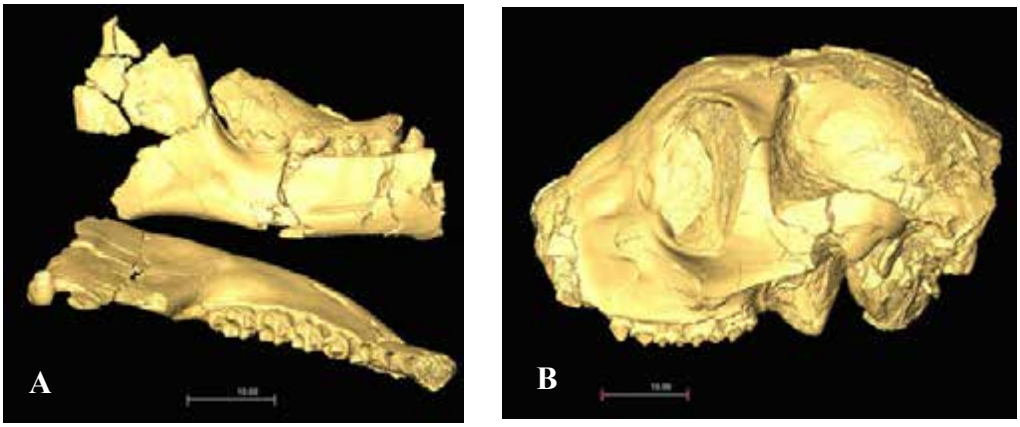

Figure 3. Screen shots of the (A) Isosurfaces of the mandibles and the (B) Isosurface of the cranium, within AVIZO software.

2. Virtual Skull Restoration using Z Brush

The digital three dimensional cranium and jaw of the *Smilodectes graclis* specimen was virtually restored using the **Z Brush**; a polygonal-based 3D modeling software. Much of the sediment surrounding the bony structures had been segmented from the bone during the pre-processing in the **AVIZO** software. The resulting fossil, however, was still highly fragmented, distorted and significantly encumbered with sediment. Several strategies were used in making educated decisions on what changes would be appropriate in order to restore the specimen as accurately as possible. These strategies were in line with fossil preparatory literature, which documents best practices in the physical preparation of a fossil for the purpose of research. It is believed by some preparators that when preparing a fossil "as much information as possible is conserved in the natural object" (Brown et al., 2009). This conservative approach was used during the digital "preparation" of the specimen in that only the most necessary changes were made, in order to keep as much of the original data intact as possible The changes themselves were made using a variety of techniques in **Z Brush**. The major strategies and techniques used in refurbishing the skull and jaw are divided into **Referencing Techniques** and **Digital Techniques**, which are listed in the following sections.

2.1 Reference Techniques

2.1.1 Aligning Dentition

No major fractures or distortion could be identified on either the upper or lower teeth on the specimen. The teeth could therefore be aligned and used as a starting point for making conclusions about where other anatomical landmarks should be located **(fig 4).** The jaw, for instance, was relatively complete and undamaged; therefore, once the teeth had been aligned a confident estimate of the location of the

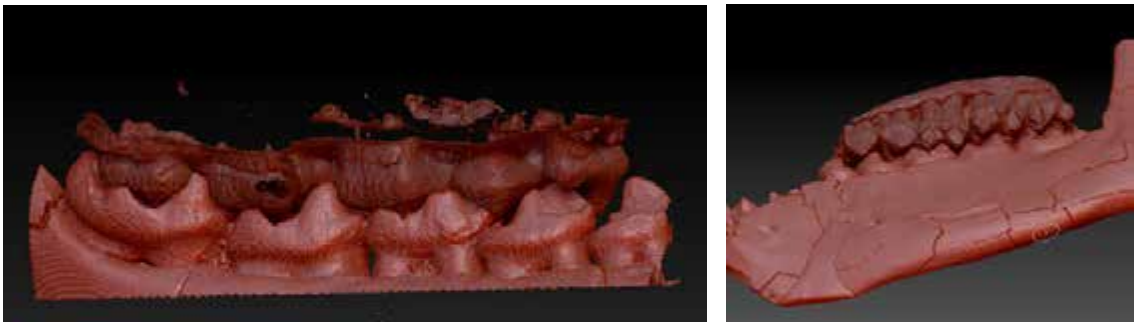

Figure 4. Screen shots showing the process of aligning the dentition of the jaw to the dentition of the cranium within Z Brush.. The cranium has been "hidden" within Z Brush for clarity.

temporomandibular joint point could be made. The articular surface of the mandibular fossa of the temporal bone was almost 10mm more rostral than the condyle of the jaw. A clear fracture could also be seen across the surface of the cranium with sections of the posterior portion were overlapping the anterior portion. Based on these observations, the decision was made to move the posterior portion of the skull (following the overlapping fracture) caudally until the articular surface of the mandibular fossa aligned with the condyle of the jaw.

2.1.2 Model References

A specimen of *Propithetcus coquereli* was provided for reference as well as an enlarged dental model of MI, M2, M3 of *Cantius ralstoni* **(fig 5)**. These physical three dimensional references were useful gaining in understanding of overall dimension and shape as well as specifics as too tooth alignment and jaw articulation.

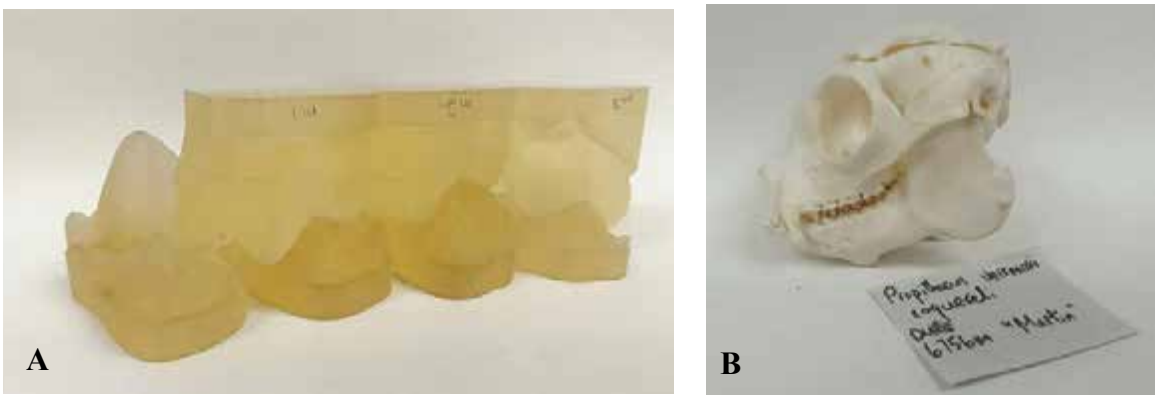

Figure 5. Photographs of reference models including, a (A) dental model of M1, M2, M3 on Cautius ralstoni (*a close relative of* Smilodectes) *and a (B) cranium of* Propithetcus coguereli (*an extant lemur).* Photo credit: Amanda Slade 2018.

2.1.3 Fracture Patterns

By following the fracture patterns in the specimen, fragments could be isolated and moved individually. Segments of the cranium were clearly overlapping each other. By following the fracture patterns these segments could be moved back into place. Other segments were spread apart and could be brought back together and fit as if a puzzle. By paying particular attention to these and other fracture patterns the specimen could be adjusted in a logical way **(fig 6).**

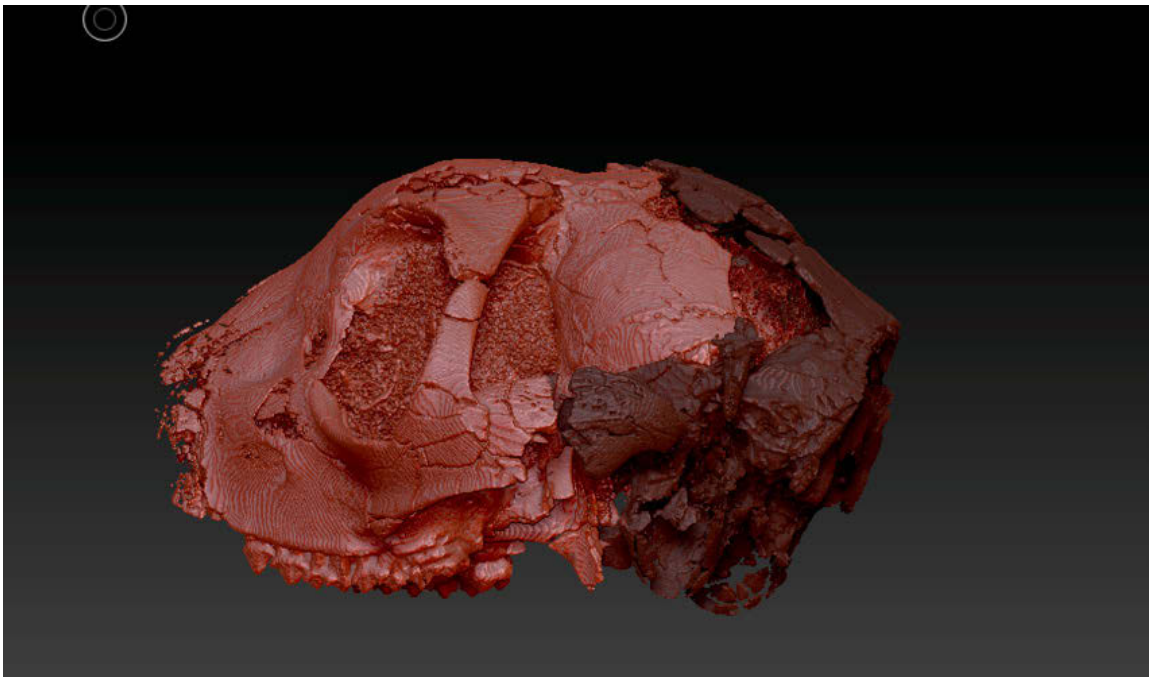

Figure 6. Screen shot of a masked section of the specimen that follows a fracture pattern in Z Brush.

2.1.4 Reference Photos

Detailed photographs of five other fossilized specimens of *Smilodectes gracilis* were available for reference, provided by the Johns Hopkins Department of Functional Anatomy and Evolution. Each of these specimens was damaged and distorted in distinct ways and had other features that were more or less preserved. By comparing each of these images to the digital specimen, as well as to one another, decisions on changes to make on the specimen, were made confidently. Features that were checked when making these comparisons included:

(1) Comparing the ratio of jaw to skull length (if a jaw was available).

(2) Measuring relative distances between bony landmarks.

(3) Referencing common features such as orbits, temporomandibular joints, and major foramina.

4) Referencing how the "bite" of the specimen and how their dentition aligned.

(5) Referencing missing anatomy.

2.1.5 Expert Opinion

Dr. Jonathan Perry, of the department of Functional Anatomy and Evolution at Johns Hopkins, studies the chewing anatomy of primates. He was able to use his background and years of training and research to give feedback on how the cranium was to be altered, as well as to check the progress along the way.

2.2 Digital Techniques

2.2.1 Reorientation

When OBJ files of the segmented CT cranium and jaw data were imported into **Z Brush** they were oriented in a skewed position and not aligned in relation to one another. Using the **Move Transpose** tools, the cranium was rotated and moved to align with the program's orthogonal orientation. The jaw was placed in a logical position in relation to the cranium **(fig 7)**.

2.2.2 Organizing Geometry

Polygroups and **Sub Tools** allow a mesh to be organized with visual grouping within **Z Brush**. **Sub Tools** create separate pieces of geometry and **Polygroups** create separate selection areas within a piece of continuous geometry. These organization tools were used to separate fragments of anatomy and move and rotate them individually.

2.2.3 Removing Sediment

The **Lasso tool** was used to select portions of the mesh that appeared to be sediment, this geometry was then deleted **(Hide Geometry > Delete Hidden)**. If any holes in the mesh were created from the process, then **Close Holes** was used to fill the missing geometry.

2.2.4 Recreating Missing Anatomy

Significant portions of the jaw and cranium were missing entirely. The nasal region, interior of the orbits, and several teeth were missing data. These areas were recreated by creating a new **Sub Tool** of a sphere **(Sub Tool < Append < Sphere)**. The sphere is then moved and scaled using the scale and move tools to the area needing reconstruction. Using the **Move** brush the sphere is reshaped to resemble the

A  **B** 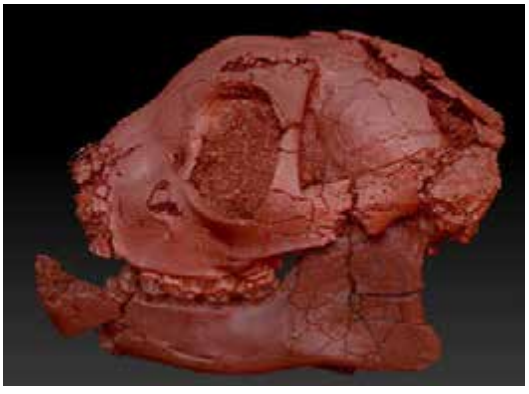

Figure 7. Screen shots of a (A) superior view of the cranium and jaw having been oriented in Z Brush and a (B) lateral view of the jaw having been oriented to fit the cranium.

anatomy of a reference (**see 2.1.2, 2.1.4**). The **Standard brush** and **Smooth tool** were used for detail refinement. Shapes were kept fairly general and fine detail was avoided to ensure that features being recreated would not be assumed to be real **(fig 8)**.

The changes made to the digital specimen were made only when an educated reason could be given based on the previously listed strategies. The resulting model's deformations and distortions are corrected, and almost all of the information the original fossil contained is preserved.

Figure 8. Screen shots of the recreated anatomy of the virtual specimen in Z Brush

3. Virtual Skull Reconstruction using Z Brush

A full reconstruction of the specimen was creating with the intention of recreating the anatomy of an average member of the species rather than preserving the anatomy of an individual (as in the restoration of the selected specimen (see section **2.)**. The full reconstruction utilized much more artistic license and created an approximation as to what a completely undamaged skull of an average *Smilodectes gracilis* would look like. All reconstruction was done within **Z Brush**. The techniques used for this process are listed in the sections below.

3.1 Symmetrization

To ensure the reconstructed model's symmetry the refurbished model was cut in half along the midsagittal plane. Subsequent sculpting and adjustments were then made to only one half of the model. When sculpting and refinement was complete the half was duplicated **(Tools > Sub Tools > Duplicate)**, mirrored **(Tools > Deformation > Mirror)**, and merged **(Tools > Sub Tools > Merge > Merge Down).**

3.2 Smoothing Restored Skull

The refurbished model was used as a starting point. All **Sub Tools** of individual fragments as well as the reconstructed areas of missing anatomy were merged into a single **Sub Tool**. The jaw and cranium were kept separate pieces of geometry. The fissures and fractures were then repaired using the **Smooth** tool.

3.3 Sculpting Techniques

A sphere was appended, moved to the appropriate location and sculpted over the refurbished model. A new version of the anatomy was sculpted on top of the refurbished specimen's anatomy, which allowed for the refurbished model to be used as a guide for reconstructing the model. Once the appended object was sculpted in a way that appeared correct, it could be merged down and incorporated into the model. This method allowed for the model to be recreate piece by piece ensuring a thorough approach.

3.4 Recreating Dentition

Because the reconstructed model was ultimately used as a chewing model, recreating an accurate "bite" was important. Each tooth was made into its own **Sub Tool** so it could be manipulated independently **(fig 9)**. Each tooth was sculpted to ensure that it fit within among the surrounding teeth and to ensure that it preserved a realistic "bite" with the occluding teeth during mastication.

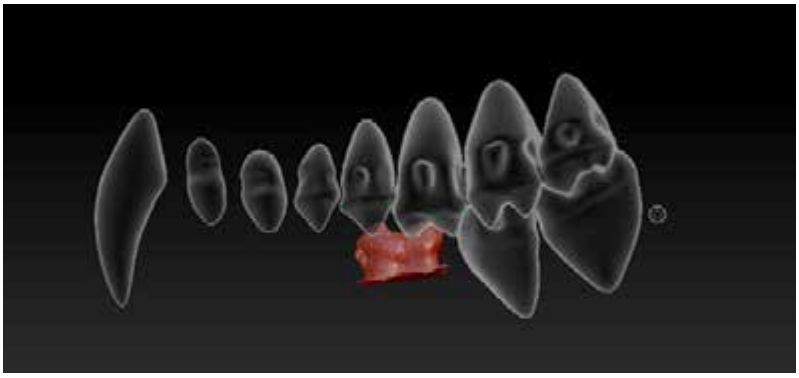

Figure 9. Screen shot of an individual tooth being made into a Sub Tool, in Z Brush, so that it can be manipulated independently of the surrounding dentition . Transparency is enabled.

4. Virtual Mastication Muscle Reconstruction

The three jaw adductor muscles were chosen for the reconstruction; the masseter, temporalis, and medial pterygoid. A method of estimating muscular volume developed by Dr. Perry was utilized for making the measurements. The estimates are based on the bony features of the skull and jaw that indicate origins and insertions of the musculature. Accurate measurements could not be made on the physical specimen due to sediment impacting potions of the necessary osteological landmarks, distortion of the specimen, and other damage. Measurements were able to be made on the refurbished digital skull within **GEOMAGIC** software. **GEOMAGIC** software is a professional engineering software which has an emphasis on 3D scanning and surface manipulation..

4.1 Scale verification

Real life scale within **Z Brush** stays consistent with the imported OBJ file. Any processing within **Z Brush** was to scale with the physical specimen. After exporting the refurbished digital specimen, the relative scale was unaltered when the object was imported into **GEOMAGIC**. This was verified by making dimensional measurements on the physical specimen and comparing them with the digital specimen's scale in **GEOMAGIC.**

4.2 Surface Area Measurements in GEOMAGIC

The digital skull was loaded into **GEOMAGIC.** The **Paint tool** was used to paint the surface area of the origins and insertions of each muscle **(fig 10).** The surface areas of the painted regions were then isolated from the rest of the anatomy. The **Fill Holes** function was used to fill any major holes or gaps in the surface that were created by fractures in the fossil **(fig 11 A, B)** or imperfections in the transfer from CT data to surface model. Some holes were left unfilled because filling them resulted in major distortions of the original anatomy**.** The area of the surface was then calculated using the **Selected By Area** function **(fig 11 C, D).** The surface areas of each origin and insertion were saved and exported as OBJ. files to be used for reference during muscle sculpture.

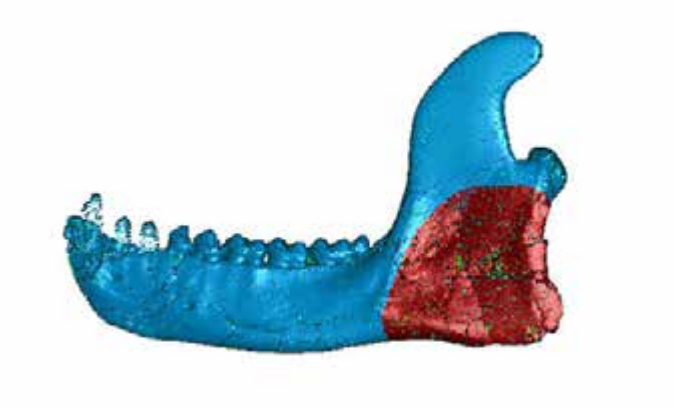

Figure 10. Screenshot in GEOMAGIC of the surface area for the insertion of the masseter painted onto the mandible.

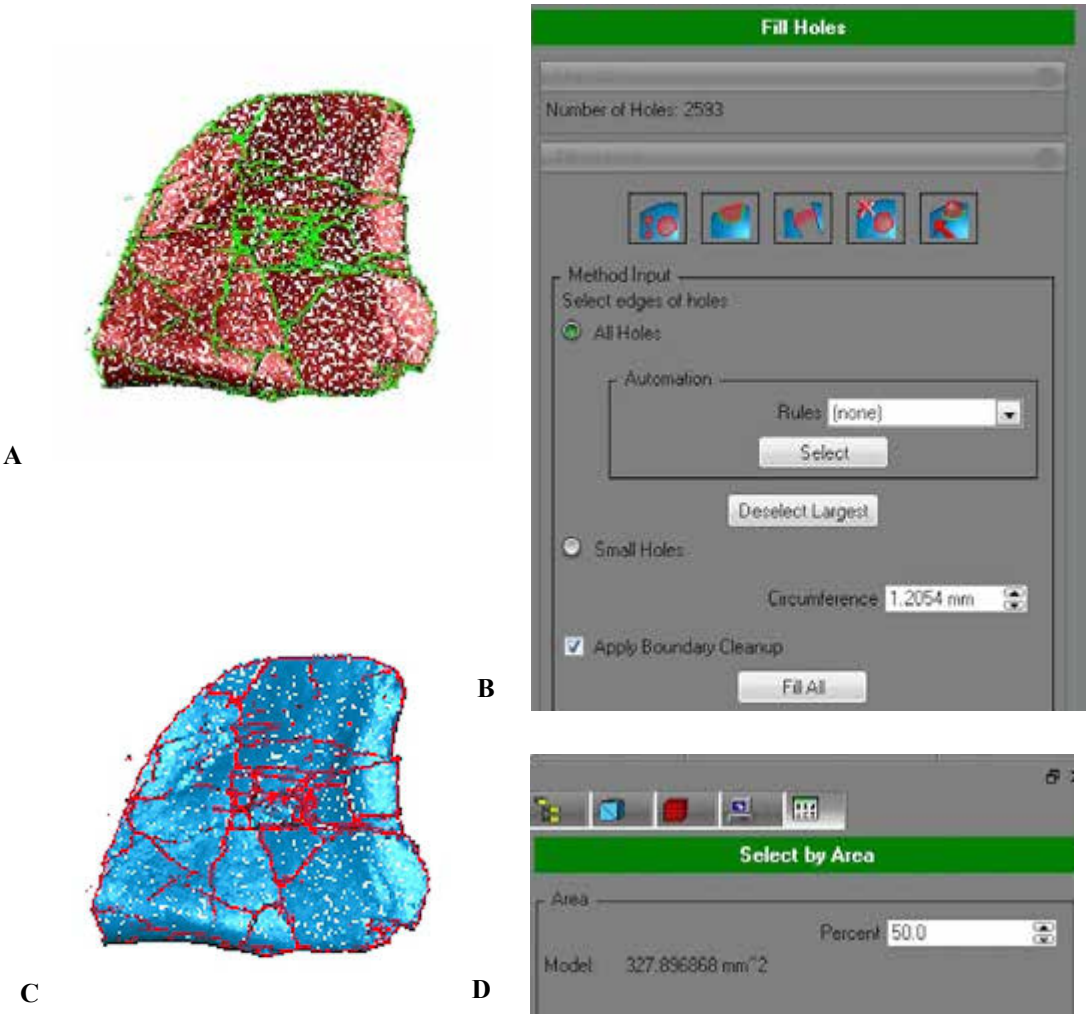

Figure 11. Screenshots in GREOMAGIC of (A) the Fill Holes function being performed on the insertion of the masseter object, (B) the Fill Holes settings used, (C) the surface area being calculated on the origin of the medial pterygoid, and (D) the output of the Select by Area function.

4.3 Numerical Muscle Volume Estimates

Dr. J Perry, of the Department of Functional Anatomy and Evolution at Johns Hopkins University used the surface areas extracted in **GEOMAGIC** to calculate volume estimate of each of the three adductor muscles. The resulting volumes are listed in (**fig 12.)**

Jaw Adductor Muscle	Volume Estimate (cm^3)
Masseter	4.18
Temporalis	4.74
Medial Pterygoid	2.75

Figure 12. Table listing the jaw adductor muscle estimates in centimeters cubed.

4.4 Extracting Origin and Insertion Surface Areas in Z Brush

OBJ files of the surface area for the origin and insertions for each muscle were uploaded into **Z Brush** and appended into the reconstructed skull file. Each of these were made into a separate **Sub Tool** and positioned over the skull model using transparency mode so that the shape could be accurately placed **(fig 13 A).** A mask was applied to the area using the origin/insertion **Sub Tool** as a guideline **(fig 13 B)**. A new mesh was extracted **(Tools > Sub Tools > Extract > Apply; Smt = 5, Thick = .05) (fig 13 C).**

4.5 Sculpting Appended Objects in Z Brush

A sphere **Sub Tool** was appended and sculpted into the general shape of the muscle using the **Move brush**, **Dyna Mesh** and **Smooth tools**. The origin and insertions of each shape were matched with the origin and insertion meshes extracted; these **Sub Tools** were then merged into single piece of geometry.

4.6 Subtracting Overlaps in Z Brush

Boolean subtracting operations were performed to eliminate overlaps between layers of adjoining meshes. With the selected **Sub Tool** in **Dyna Mesh** mode and the **Sub Too**l to be merged assigned the White **Polygroup (Group As Dyna Mesh Sub**) a merge down operation **(Tool > Sub Tool > Merge Down)** was used to subtract the merged mesh from the current one. This allowed the junction between the muscle and the bone to fit perfectly.

A

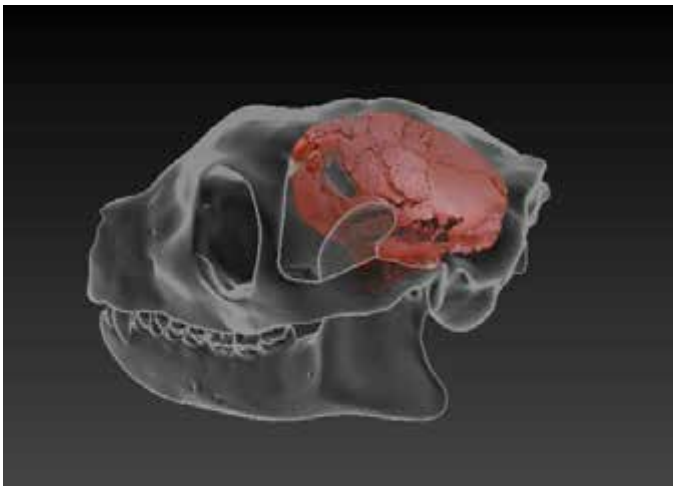

B

C

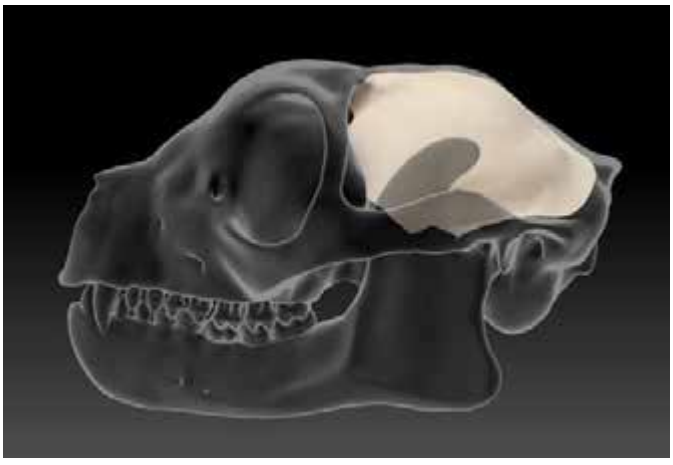

Figure 13. Screen shots of the (A) "origin" Sub Tool of the temporalis positioned correctly, the (B) mask painted following the origin Sub Tool as a guideline, and the (C) mesh extracted from the mask.

4.7 Volume Verification in Blender

The muscle **Sub Tools** were exported as OBJ files and brought into **Blender** for volume determination. The 3**D Print Plugin** was installed in order to use the volume feature in **Blender (fig 14).** In **Object Mode** the object was selected and a volume operation was performed (**3D print > Statistics > Volume)**. The volume in cm^3 appears in the **Output.** Adjustments were made within **Blender** under **Sculpt Mode**. The **Grab tool** was used to make bulk adjustments.

Care was taken to ensure the borders and surfaces of the origin and insertions sites remained unaltered. When the volumes were roughly the correct, the muscle objects were exported from **Blender** and imported back into **ZBrush** for additional detailed sculpting. When the models were complete they were exported and measured a final time within **Blender**.

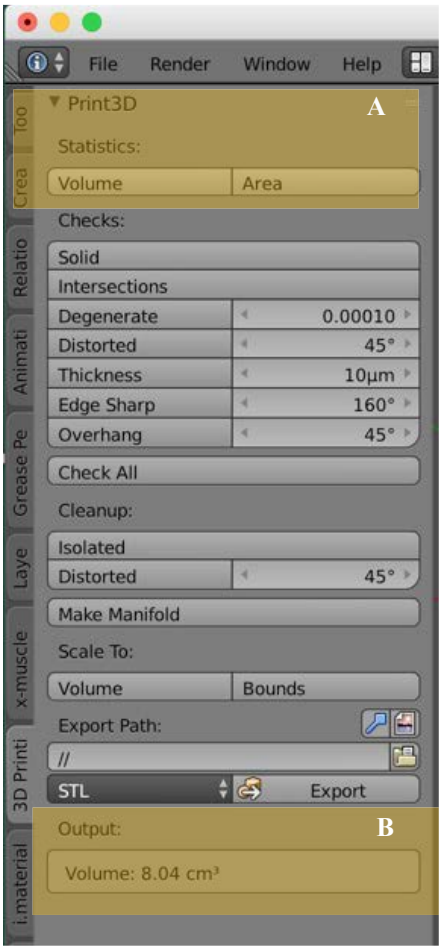

Figure 14. Screen shot of Blender interface showing 3D Print Plugin tab including the (A) Volume button and (B) the Volume Output field.

4.8 Adding Texture and Fiber Direction in Z Brush

The **Clay Buildup** brush was used to create raised topology of the muscles fiber and **Damien Standard** brush was used to indicate more precise lines and creases, as well as finer muscle fibers. **Dyna Mesh** was used to continuously adjust the topology of the mesh **(fig 15).**

Reference photos and illustrations were used while sculpting the musculature. Details such as typical muscle shape, fiber direction and typical connective tissue patterns were closely observed in these references to ensure the reconstructions were as accurate as possible.

A

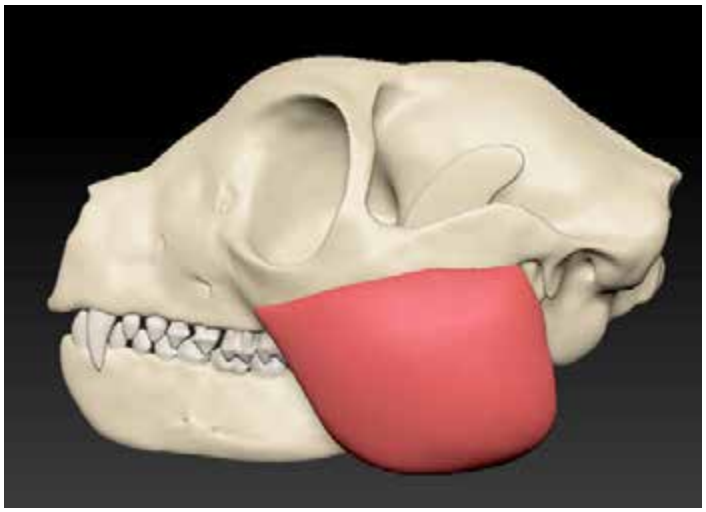

B

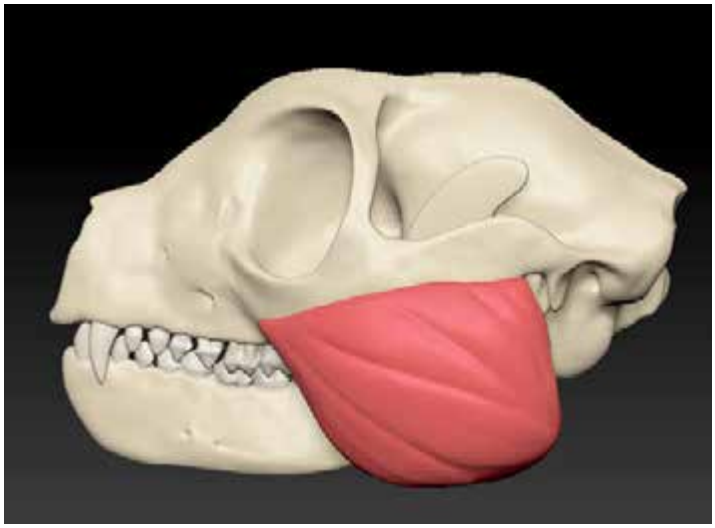

C

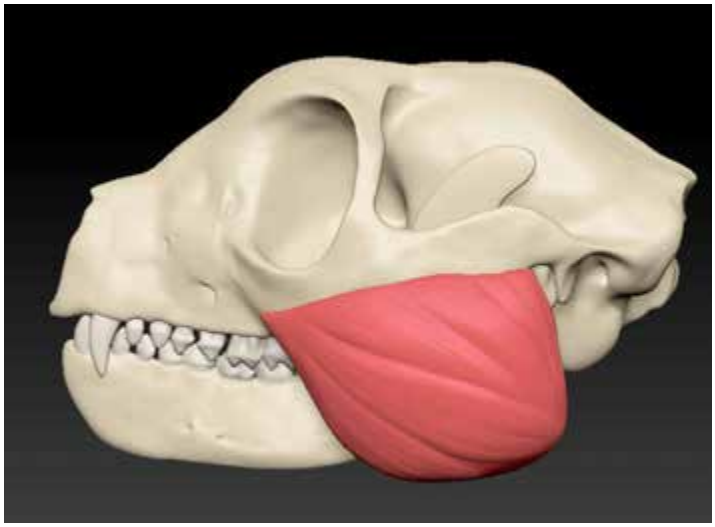

Figure 15. Screen shots of the (A) basic muscle shape, (B) Damien standard being used to make major muscle fiber groups and (C) finer muscle fiber detail.

5. Facial Approximation in Z brush

3D digital reconstruction of *Smilodectes gracilis* surface anatomy was created using **Z Brush.** Although facial musculature, fatty deposits, vasculature, and glandular tissue were not reconstructed, the major underlying anatomy was enough to give an estimate of what the surface features could have looked like.

Using the transparency option, the reconstructed skull, jaw and musculature were visualized as surface sculpting took place **(fig 16).** A sphere was appended and the **Move brush** was used to create a surface layer surrounding the underlying anatomy. The **Standard and ClayBuildUp** brushes were used for establishing larger features. **Damien Standard** brush was used for creating lines and creases. The **DynaMesh** tool was used throughout the sculpting process to retopologize the mesh.

The ears and eyes were created as separate **SubTools** and placed based on landmarks on the skull. The sculpts of the ears were placed in relation to the external auditory meatus and the eye balls were placed within the orbits with enough space surrounding them to account for the extraocular musculature and other anatomy (e.g., fat and fascia).

Once the major features and details were sculpted, and fur was added around the areas based on reference photos of living analogs. Other details were also included like eyelids, whisker indentations and texture on the nose.

A  **B** 

Figure 16. Screenshots of (A) underlying anatomy visible within the transparent surface sculpt and (B) the basic surface anatomy sculpt of Smilodectes Gracilis.

The photographs used as references were photos of *Smilodectes gracilis's* most direct living equivalents such as the Brown Lemur (*Eulemur fulvus*). Artistic interpretations of *Smilodectes gracilis* were also used along with those of closely related extinct genera including *Adapis* and *Notharctus.*

6. Optimizing Meshes for a Web Application using Z Brush and Blender

All the models created were designed to be ultimately inserted into an interactive online application. The speed of loading such an application is linked to the size of the file. In order to ensure that the application could be loaded in a reasonable amount of time without sacrificing any quality of detail the models needed to be prepared for the web. This process involves using a high to low poly workflow. A low polygon model is created using the original high polygon sculpt using tools provided in **Z Brush**. The low polygon and high polygon models are both exported into blender and the detail of the high polygon model can be "baked" onto the low polygon model by **UV unwrapping** the models and creating a **normal map**. Using the normal map as a texture, the low polygon model can have the same level of detail as the high polygon model while vastly reducing the amount of render time. The reconstructed cranium, jaw, masseter, temporalis and medial pterygoid were all brought through the process outlined below.

6.1 Creating a Low Poly Model in Z Brush

The **Decimation Master** is simple way to reduce the level of polygons in a mesh in a way that maintains the integrity of the original model. Decimating by 40-100% will leave the detail almost entirely intact (100% means no decimation and .01% means maximum decimation), while below 40% will begin to reduce the resolution significantly. Creating a low poly model requires only that the silhouette of the model remain relatively unchanged while the detail does not need to be maintained as it will be baked into the model at a later time. With the **Sub Tool** selected for decimation the model was preprocessed **(Z Plugin > Decimation Master > Preprocess current)**. When the preprocessing was complete, the model was decimated to 30% **(Z plugin > Decimation Master > Decimate).**

Figure 17. Screen shot of ZRemesher settings in ZBrush.

6.2 Retopologizing Models

Decimating the model reduces the number of polygons quickly however the topology created can be messy and make the following step of unwrapping the mesh difficult. The **ZRemesher (Tool > Geometry > ZRemesher)** is used to create cleaner topology that is easier to unwrap. The default settings were used in each case **(fig 17).**

6.3 UV Maps in Blender

To unwrap the low poly meshes to create **UV maps** they are imported into **Blender**. Seams are created in the mesh to facilitate unfolding into a flat shape. To create a seam, the object is put into edit mode and edges are highlighted using the edge select tool and pressing shift while clicking edges. When a seem is complete it is marked using the **Mark Seam** function **(Shading / UVs < UV Mapping < Mark Seam) (fig18).** When the seams are complete the mesh is unwrapped by selecting the entire mesh **(hotkey < A)**, accessing the unwrap menu **(hotkey < U)**, and selecting **Unwrap**. To view the resulting **UV map** the screen is split and the **UV / Image Editor** is selected under **Editor type (fig 19)**. The resulting image shows depicts the mesh unwrapped into a flat image along the selected seams.

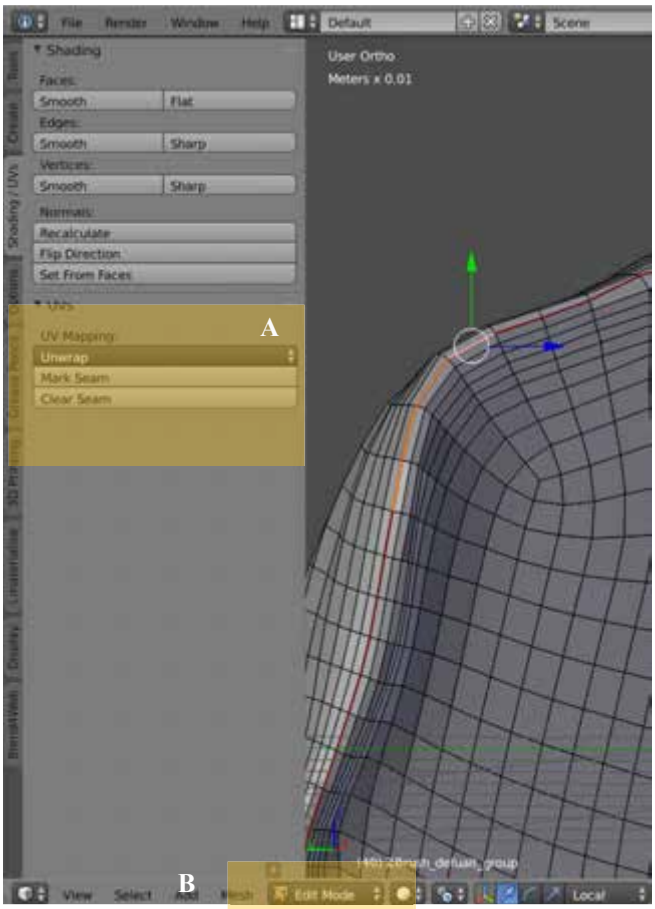

Figure 18. Screen shots of (A) Blender seam selection in (B) Edit mode.

6.4 Normal maps in Blender

With the **UV maps** created, the normal map can now baked onto the low poly mesh from the high poly mesh. The high poly mesh is imported into **Blender** and positioned in the exact same position as the low poly mesh. In the **Outliner panel**, the high poly mesh is selected first and the low poly mesh second, by holding shift and selecting. Within the **Bake** menu, **Normal** is selected as the **Bake Mode** and the **Bake** button is pressed **(Properties < Render < Bake) (fig 20)**.

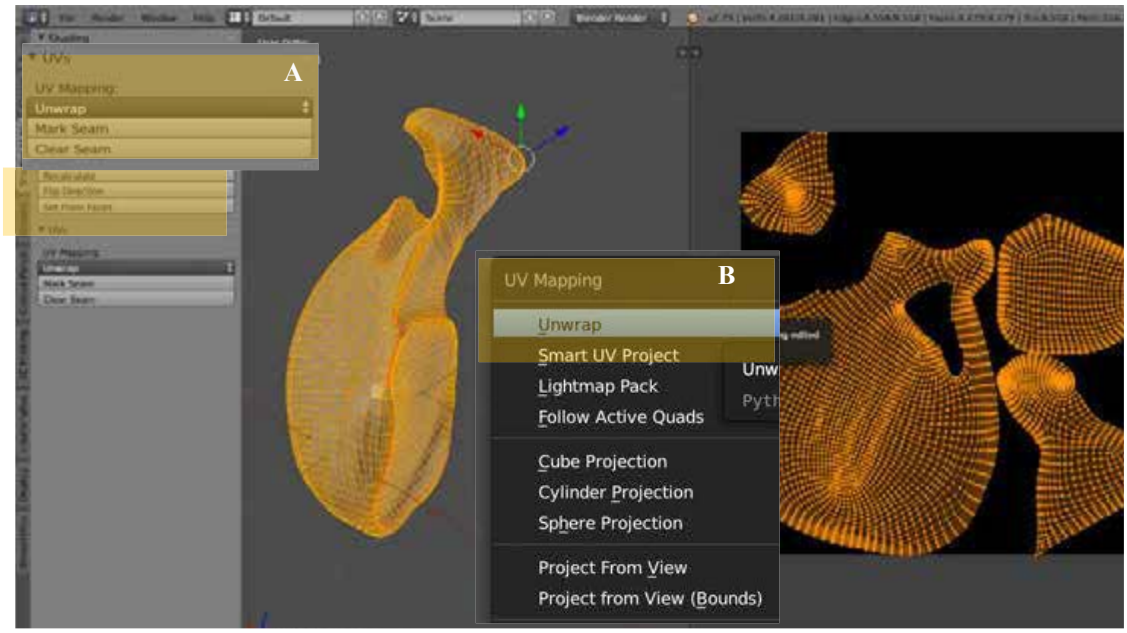

Figure 19. Screen shot of Blender interface showing a (A) UV Mapping menu and a (B) split screen with the UV map shown in the UV/Image Editor type

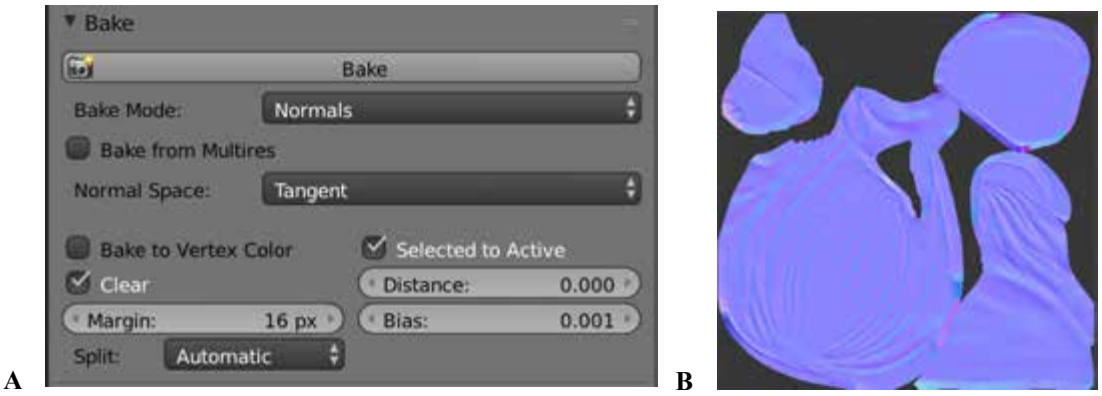

Figure 20. Screen shots of (A) Normal map mapped onto the UV map and (B) the Bake menu with the Bake mode set to Normals.

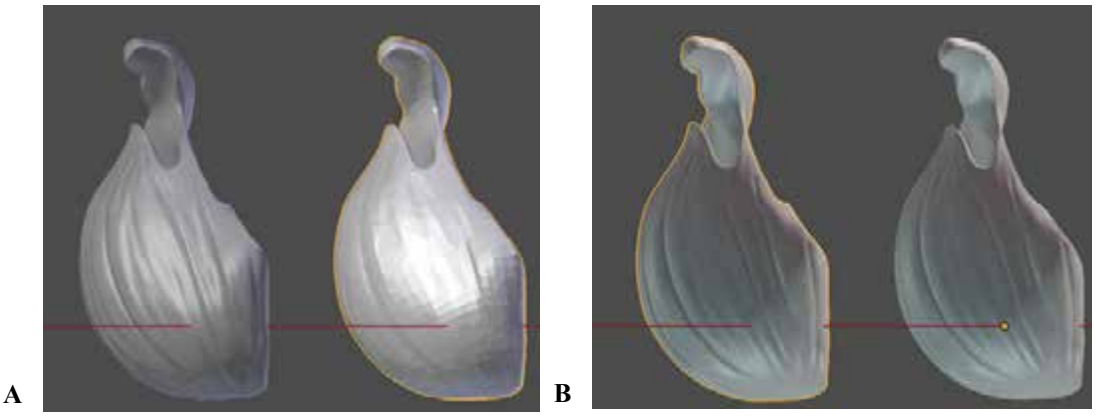

Figure 21. Screen shots of Blender medial pterygoid muscle mesh showing the (A) high and low poly meshes before the normal map is applied to the low poly mesh and the (B) high and low poly meshes after the normal map is applied to the low poly mesh.

.

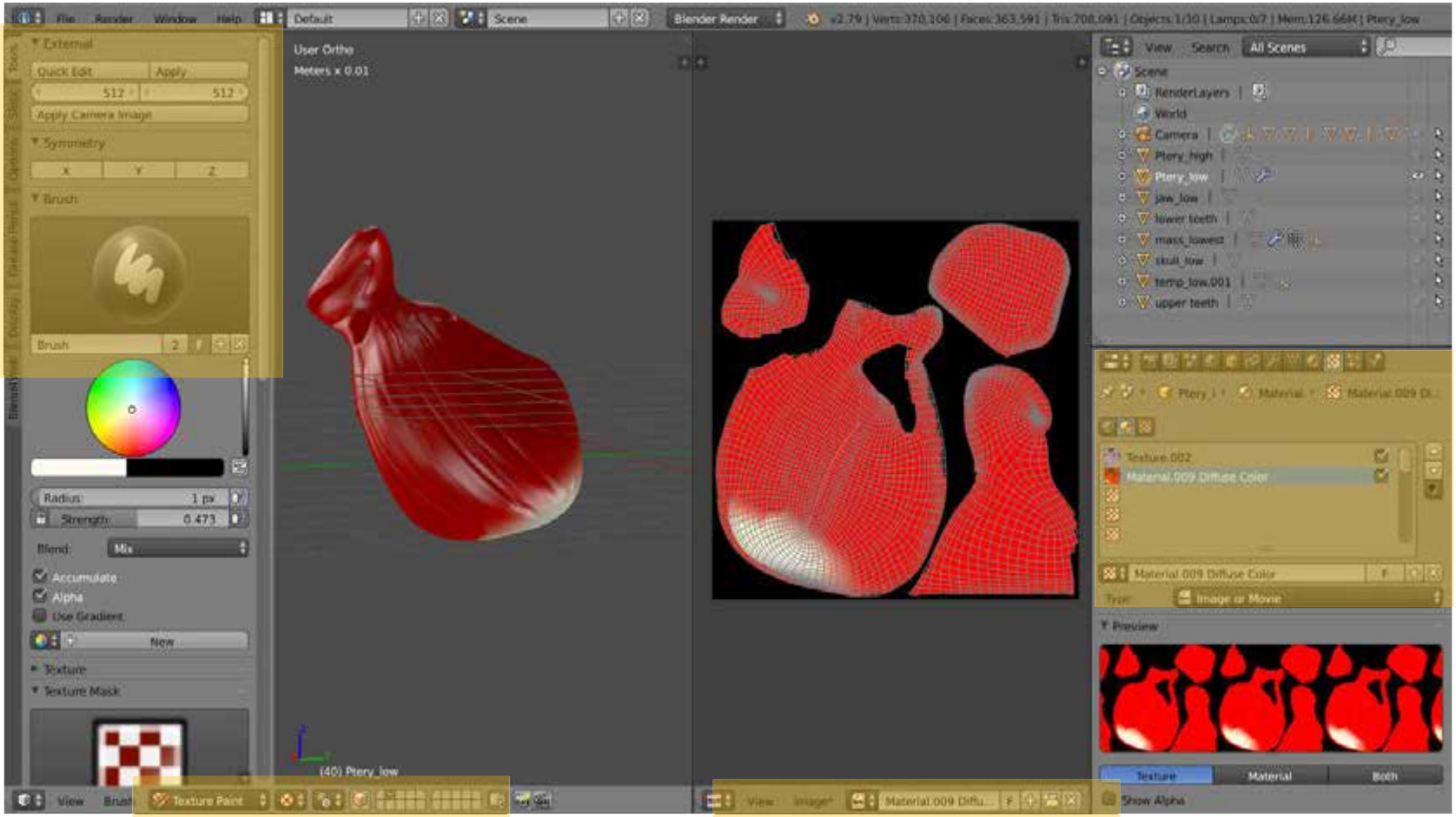

Figure 22. Screen shot of Blender showing the texture painting interface. Areas of interest are highlighted. Not all text is intended to be read.

Within the **UV / Image Editor** the normal map will appear mapped out onto the UV map previously created. The normal map should be saved as a png. **(Image < Save As Image).**

To apply the normal map to the low poly mesh the saved png file is loaded as a texture. A new material is created under the material tab in the **Properties editor**, a new texture is then created under the texture tab. The normal mapped previously saved is then loaded into the texture **(Texture < Type < Image or Movie, Image < open).** In order for the normal map to be seen on the low poly mesh, the **Normal map** check box must be checked under **Image Sampling**, and **Color** must be unchecked and **Normal** checked under **Influence.** The normal map appears on the low poly object and is almost indistinguishable from the high poly mesh **(fig 21).**

6.4 Texture painting in Blender

Each of the objects was individually painted using **Blender's** texture painting tool **(fig 22**). This feature allows painting to occur directly onto the mesh. It is also possible to keep the texture activated and details of the sculpt can be viewed while painting the model. The texture painting feature is accessed in the **Texture Paint edit mode**. With a split screen, the second screen is set to the **UV / image editor** and **painting** can be seen on the UV map and the mesh simultaneously. A new texture is added by selecting a new material under the **Slots tab**. This texture appears under the **Available Paint Slots** and is selected. The mesh turns to a default black color and is able to be painted on using the brushes and color selector in the **Tools tab**. Detailed textures were hand painted onto each of the muscles as well as the skull, jaw and teeth.

7. Creating a Chewing Simulation in Blender

To create an accurate chewing simulation, armature animation was used to recreate the chewing movements. This methods utilized the software's kinematic system to simulate the physical capabilities and limitations of actual craniomadibular movement.

7.1 Rigging the model

Rigging is a process used in armature animation in which a"skeleton" is created out of a set of interconnected "bones" which is then attached to the vertices of a mesh model. This armature can then be posed and keyframed and the vertices of the mesh will follow it. The armature itself serves as nothing more than an intuitive handle for the animation process and does not appear in any rendering. (Soriano, 2011.)

7.1.1 Creating Armatures

In order to ensure that all muscles moved in response to the jaw, the rigging was created in a systematic way. The jaw movement was rigged first and each muscle was then added subsequently to the rig. Specialized armatures were then added to modify each muscle's movement.

An armature was created by adding a **Single Bone (Add > Armature > Single Bone)** into the scene. The display of the bone can be adjusted by selecting the options in the **Armature** tab under **Properties (Properties > Armature > Display).** The X-Ray option was used to allow for the bone to be seen through the model. While initially constructing the model the Octahedral display was chosen and, as the armature became more complex, the Stick display was used **(fig 23)**.

In order to add to the **Single Bone** and create a full armature the **Bone** was selected and the mode was switched to **Edit Mode**. Here the armature will always remain in a "rest" position, whereas in **Object Mode** and **Pose Mode,** the current "pose" of the armature will show. A **Bone** is made up of three elements **(fig 24):** The **Root** or "start joint", the **Body**, and the **Tip** or "end joint". Each of these elements are able to be manipulated. To add bones to an existing bone either then Tip or Root can be selected and

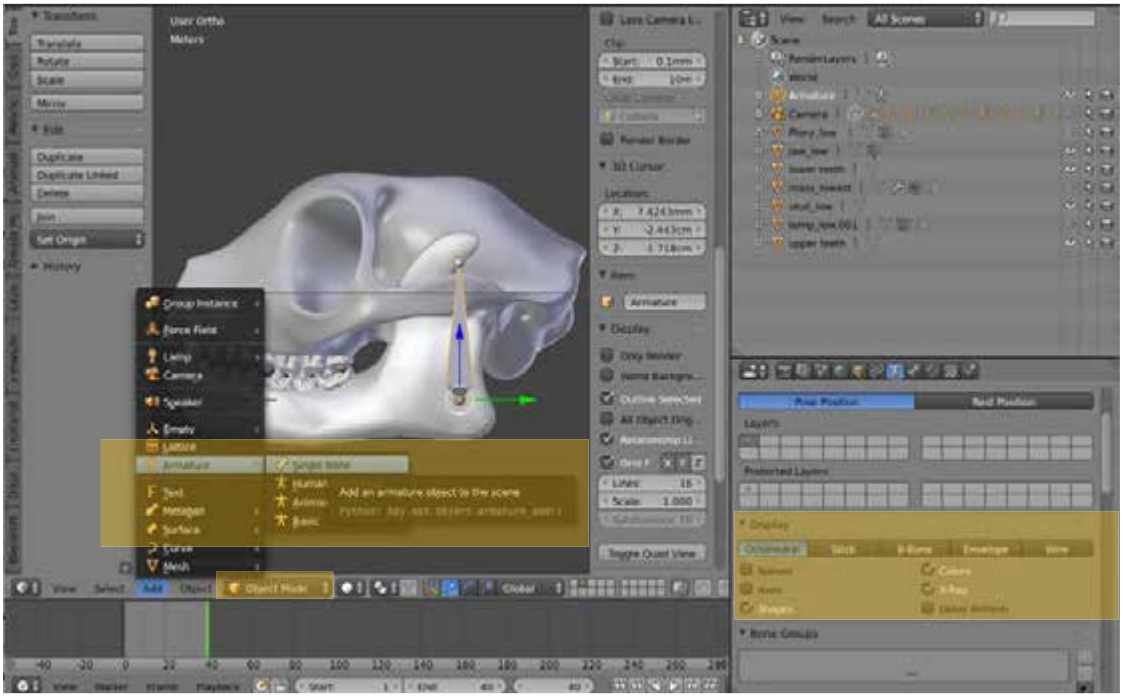

Figure 23. Screen shots of Blender showing a Single Bone being added to the scene and the Armature Display options. Not all text is intended to be read.

Extrude a new bone **(Armature > Extrude**). The new bone will be the "child" of its **Tip** owner and connected to it. When the original bone is moved its child will move with it.

The armature used to move the jaw was created in such a way that all bones within the armature were children of a single parent (or "**Control**") bone. When this "**Control Bone**" is moved, all bones connected to it would move with it. The **Control Bone** was placed in the midpoint between the condyles of the mandible and positioned so that its **Root** was perpendicular to the helical axis of rotation of the jaw **(fig 25).**

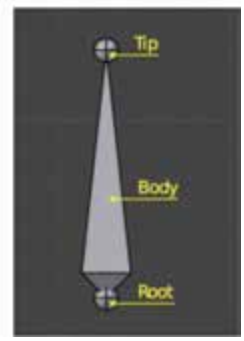

Figure 24. Screen shots of Blender showing the three elements of a Bone.

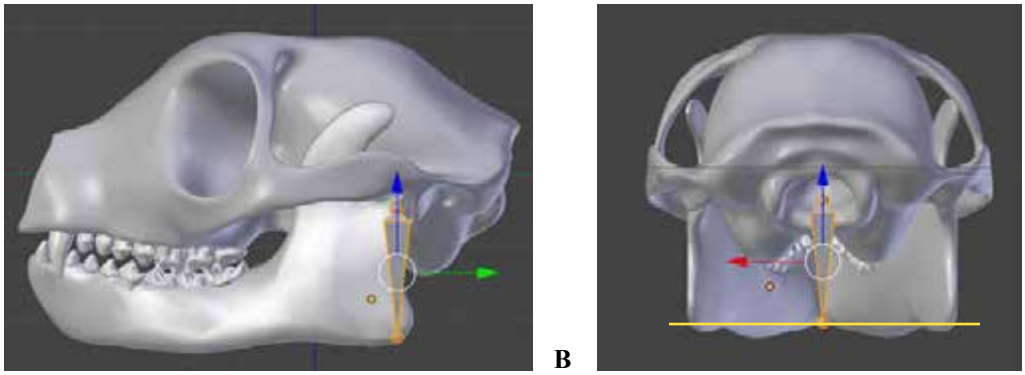

A **B**

Figure 25. Screen shots in Blender showing (A) the positioning the Root of the Bone in Octahedral display to align with the helical axis of the jaw and (B) positioning in the Bone to reside in the midpoint between the mandibular condyles along the helical axis shown in yellow.

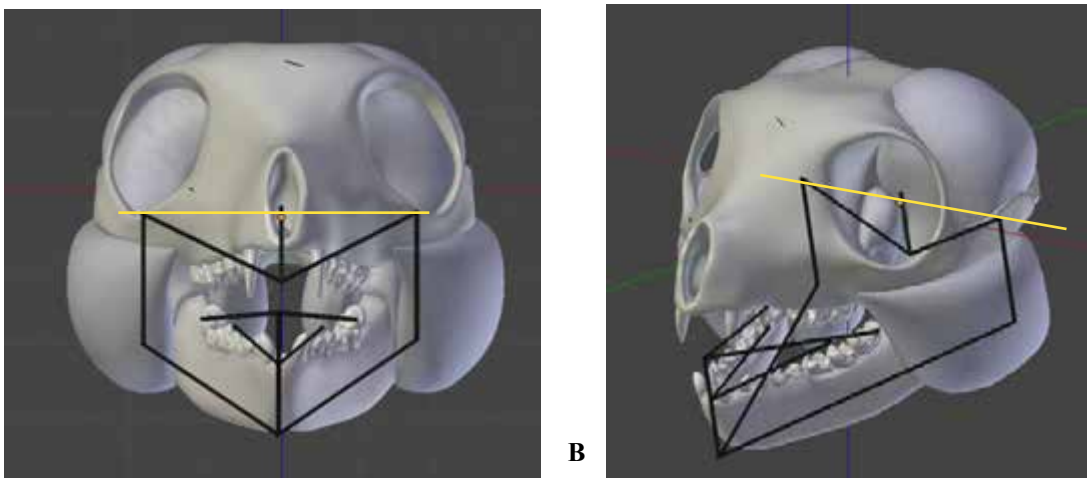

A **B**

Figure 26. Screen shots in Blender showing (A) frontal view of the jaw armature in Stick display (B) lateral view of the jaw armature with the helical axis of the jaw shown in yellow.

Connecting bones were then assembled using the **Extrude** function to follow the form of the jaw and lower teeth. The joint points of the mandibular condyles were carefully aligned with the **Root** of the **Control Bone** along the helical axis.

7.1.2 Parenting Armatures and Posing

The armature was then attached to the mesh of the jaw by parenting the armature with the the mesh. In **Object** mode the jaw mesh was selected and then by holding shift the armature was also selected. The parent **With Automatic Weights** function was performed **(Object > Parent > With Automatic Weights)**. In order to ensure that the armature was affecting the mesh in the desired way the mode was switched to **Pose Mode** and the **Control bone** was selected and rotated around the Z axis. If the parenting was successful, the jaw would move in unison with the armature. **(fig 26).**

7.1.3 Adding Muscles to Jaw Armature

Once the armature for the jaw movement was established, the muscles were parented to the armature so that they would respond to the jaw as it was posed. The muscles were parented systematically and additional bones were created to adjust how each muscle responded. These additional bones added to the armature were added for one of two purposes:

(1) To anchor part of the muscle to ensure it would not be affected by jaw movement.

(2) To assist the initial jaw armature to ensure a part of the muscle would be affected by jaw movement.

The bones added specifically for each muscle are shown in **figure 27** as is the completed armature.

To simplify the animation process and due the limitations of the **Blend4Web** software in the interactivity stage, the jaw, lower teeth, and all three adductor muscles were joined into a single object **(shift select all objects > object > join)** and re-parented to the completed armature. The jaw was rotated using the control bone to test if all armatures were working in the same way that they were when the objects were separated. If one bone was affecting a muscle it was not supposed to, then the bone's position would be adjusted.

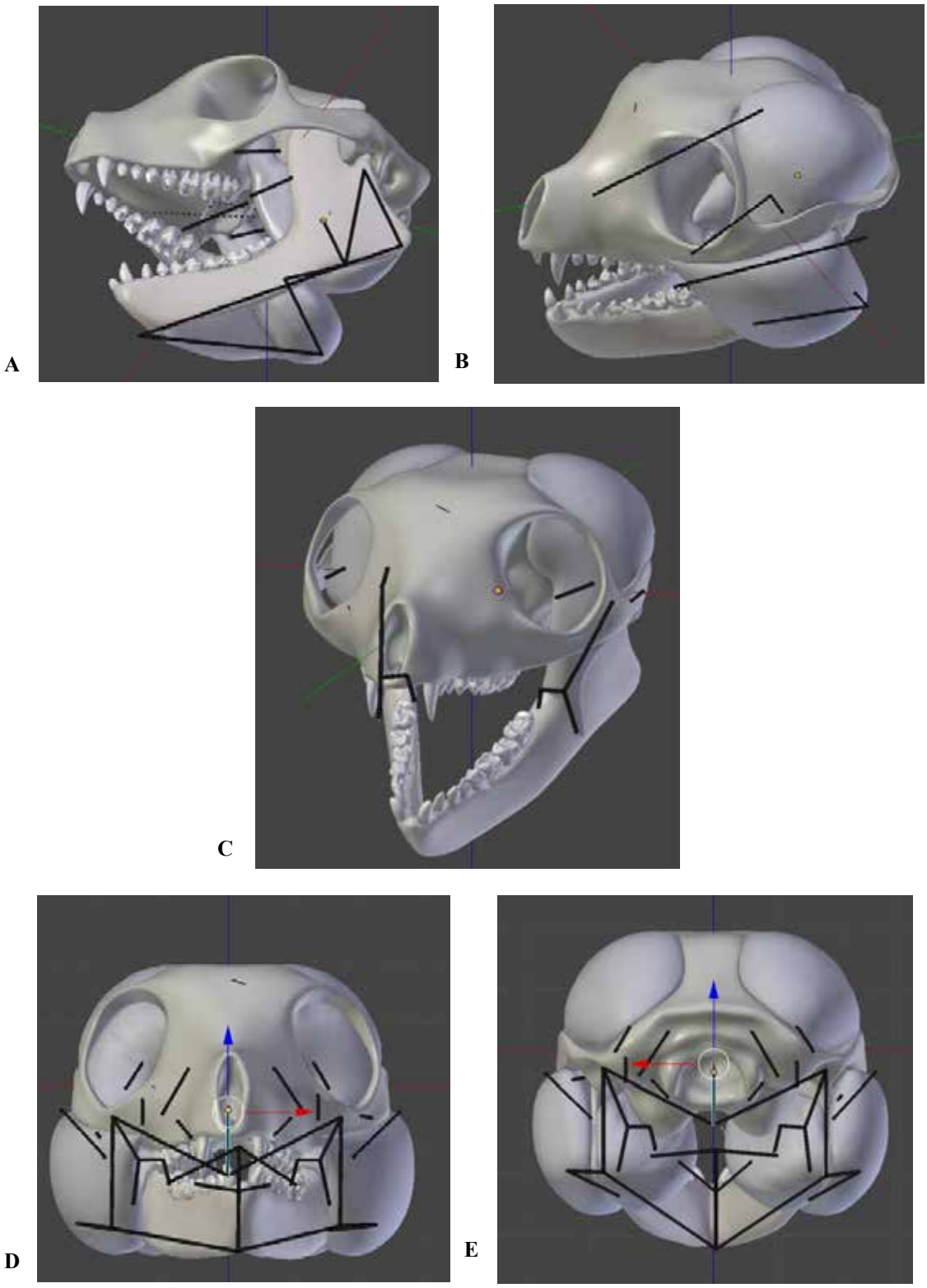

Figure 27. Screen shots in Blender showing (A) bones created for the medical pterygoid, (B) bones created for the masseter, (C) bones created for the temporalis, and (D), (E) two views of the final armature including all bones and all muscles.

7.1.3 Weight Painting

The effect each individual bone had on a mesh could be checked by viewing the mesh in **Weight Painting mode**. Here the amount of influence a particular bone had on a mesh was depicted in a color scale, where blue indicates no influence and red indicates maximum influence. By checking the weights of each mode, it could be confirmed that each muscle was only being influenced only by the bones intended for it. As seen in the **figure 27** a bone designed to influence the masseter should have no influence on the temporalis. The temporalis should therefore be entirely blue in weight paint model.

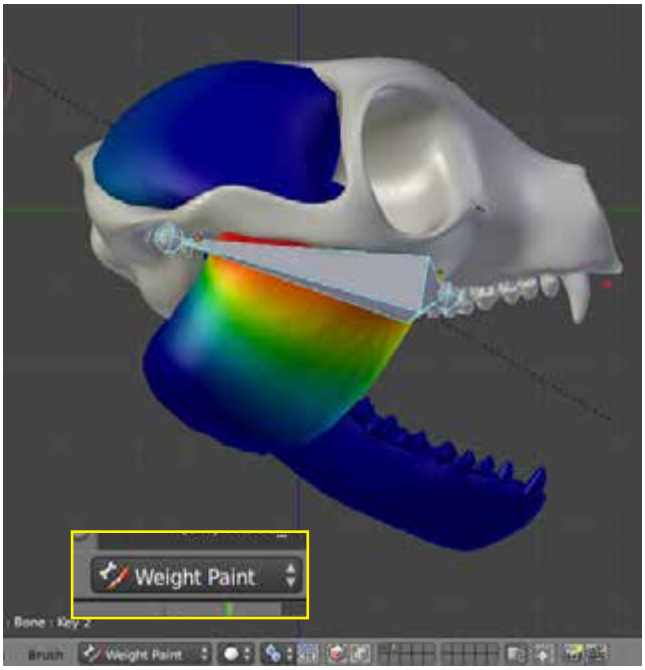

Figure 28. Screen shots in Blender in Weight Paint Mode showing a bone's influence on the masseter muscle mesh. Red indicates maximum influence: blue indicates no influence.

7.2 Animating a Gape cycle in Blender

To date, no studies have been published on the chewing biomechanics of *Smilodectes gracilis* specifically. The chewing mechanics of living primates in general, however, have fortunately been well documented. In order to simulate a believable chewing simulation for this species, a chewing gape cycle depicting Hiiemae's (1976) four gape-cycle phases were simulated based on data for a "typical" primate. A gape cycle is defined as "the cyclical elevation or depression and medial or lateral movements of the jaw defined from maximum gape to maximum gape. (Ross and Diaz, 2014 p. 106)". Hiiemae's four gape-cycle phases make up each cycle and mark the key jaw kinematic events (Ross and Diaz, 2014).
These phases include:

(1) **A Fast close (FC)**, in which the mandible moves upward to contact the food.

(2) **A Slow close (SC),** in which the mandible slows to due to making contact with the food.

(3) **Slow open (SO),** in which the tongue is adjusting the food.

(4) **Fast open (FO),** in which the jaw opens quickly to begin the cycle again.

(Ross and Diaz, 2014, Hiiemae 1976). **Minimum gape** occurs at the **SC-SO** transition and **Maximum gape** occurs at the **FO-FC** transition.

In order to simulate a gape cycle and gape phases, figures and literature were used as visual reference primarily from Ross and Diaz review "What Does Feeding System Morphology Tell Us About Feeding?" (2014) and Kay and Hiiemae's study "Jaw Movement and Tooth Use in Recent and Fossil Primates" (1976).

To ensure that jaw movement was as accurate as possible, the muscles were not attached to the jaw during animation due to the fact that they block visibility of the temporomandibular joint. A copy of the jaw mesh was created and parented to the same skeleton as the mesh of combined muscles and jaw . When the animation was complete the proxy jaw was removed.

7.2.1 Determining Maximum Gape

Because the major stages of a gape cycle involve a minimum and maximum gape the first step in simulating a chewing cycle was to determine the maximum gape of the virtual *Smilodectes* model.

To determine the maximum gape, the jaw was rotated using the **Control Bone** of the armature to rotate it around the transverse axis. When the condyle of the jaw "made contact" with the anterior portion of the mandibular fossa, maximum gape was considered to be reached. Because the objects are virtual and cannot actually make contact with one another "making contact" was determined to be just before the jaw mesh began merging with the edge of the posterior mandibular fossa, on cranial mesh, while in **"right orthographical view"** in **Blender**. **(fig 29, 30)** This is similar to published techniques for estimating maximum gape (Dumont et al., 2011; Fricano and Perry, in press).

When a primate opens its jaw to a maximum gape the condyles slide rostrally within the mandibular fossa. (Ross Diaz 2014) The further the condyle is displaced rostrally the wider the gape is. As it is unknown how far the condyles would have displaced in *Smilodectes,* a series of different condyle displacement figures were tested to document a range of gapes. At ~2mm the condyle of the jaw mesh began making "contact" with the cranial mesh **(fig 29)**, therefore this was considered the maximum displacement. The was measured at 0mm, 1mm, 1.5 mm and 2mm.. For the simulation the average of the four gape angles was used; this was found to be **33.8°. (fig 31)**

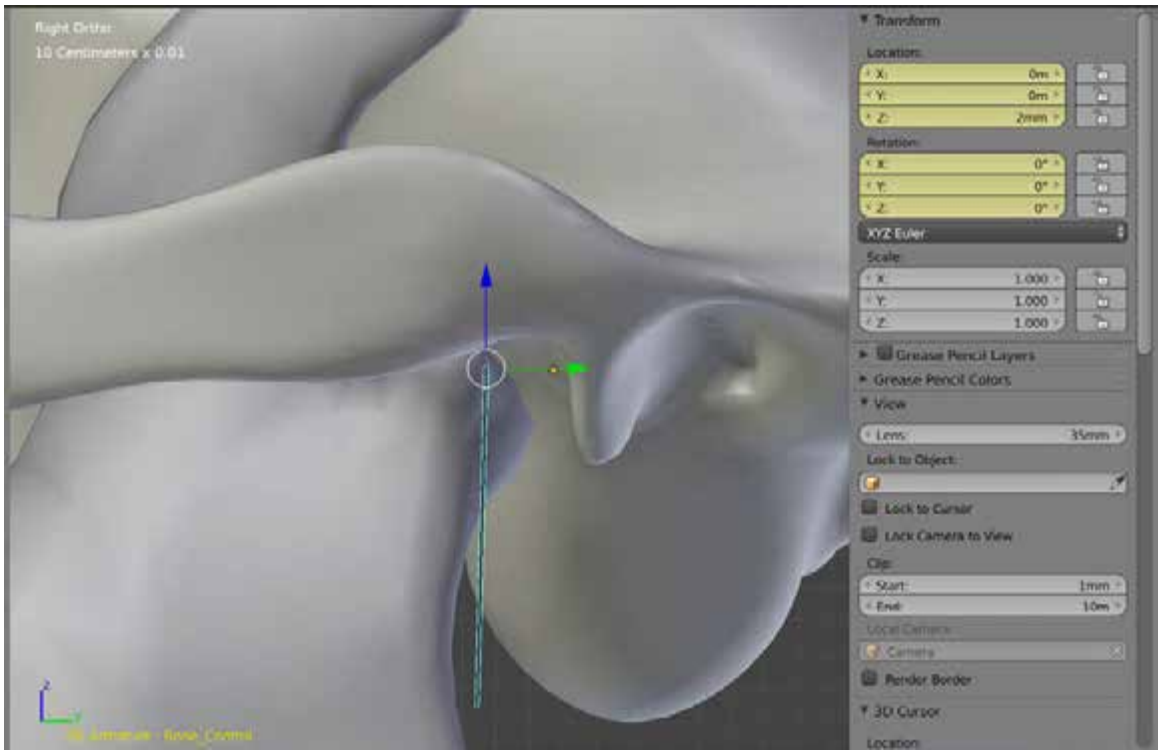

Figure 29. Screens hots in Blender showing condyle displacement set at 2mm.

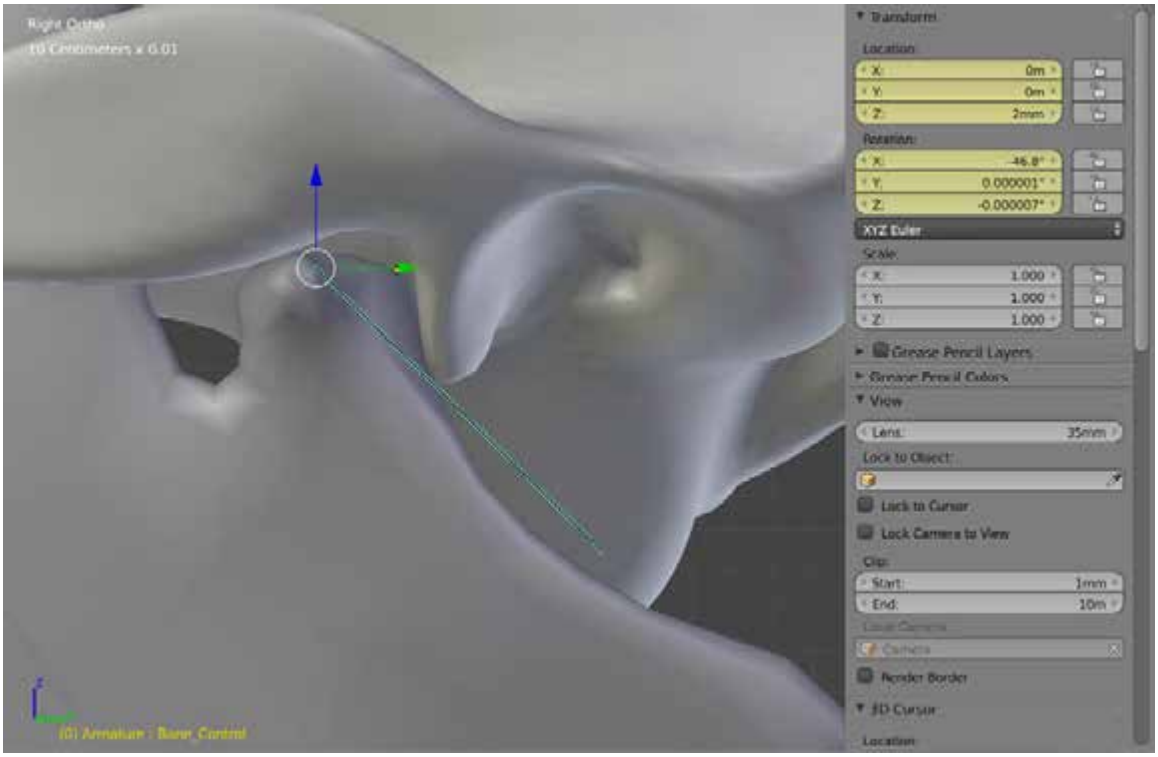

Figure 30. Screens hots in Blender showing the condyle "contacting" the mandibular fossa (at 46.8º).

Displacement of Condyles Along X axis (millimeters)	Maximum Gape (Degrees from vertical axis)
0mm	-15°
1 mm	-33.5°
1.5 mm	-40.2°
2 mm	-46.6°
Average:	-33.8°

Figure 31. Table showing the Maximum Gape in degrees from the vertical axis at different condyle displacement points. The average Maximum Gape is also shown highlighted in yellow.

7.2.2 Choosing Key Frames

In order to simulate a typical primate gape cycle, a diagram of the jaw displacement in a macaque was used as reference for the basic pattern. When the rostral most point at the midline of the jaw is tracked over time during a gape cycle, an elliptical shape is made from the points' vertical and horizontal displacement **(fig 32).** In order to simulate this effect in an animation, specific jaw displacement points were chosen along the elliptical path of the macaque diagram being referenced, and recreated in **Blender** to use as a reference **(fig 33).** The displacement of the jaw mesh at those points was then key framed.

Eight points were chosen to recreate the elliptical pattern in the *Smilodectes* virtual jaw. Each point represented the most rostral point of the jaw at its midline.

One point was chosen to account for the maximum gape (5) and another for the minimum gape (1). Two more points were chosen to indicate the midpoints between minimum and maximum gape (one when the jaw is opening (3) and one for jaw closing (7)). Finally, two points where chosen to recreate the shape of the top of the ellipse (2, 8) and two were chosen to produce the shape of the bottom of the ellipse (4, 6). Once these points were chosen they were recreated digitally in **Blender** by adding eight cubes in the **"front orthogonal view"** in **Blender**, and moving them into the desired elliptical pattern **(fig 34)**. The jaw was then moved to match these points and its position would be key framed.

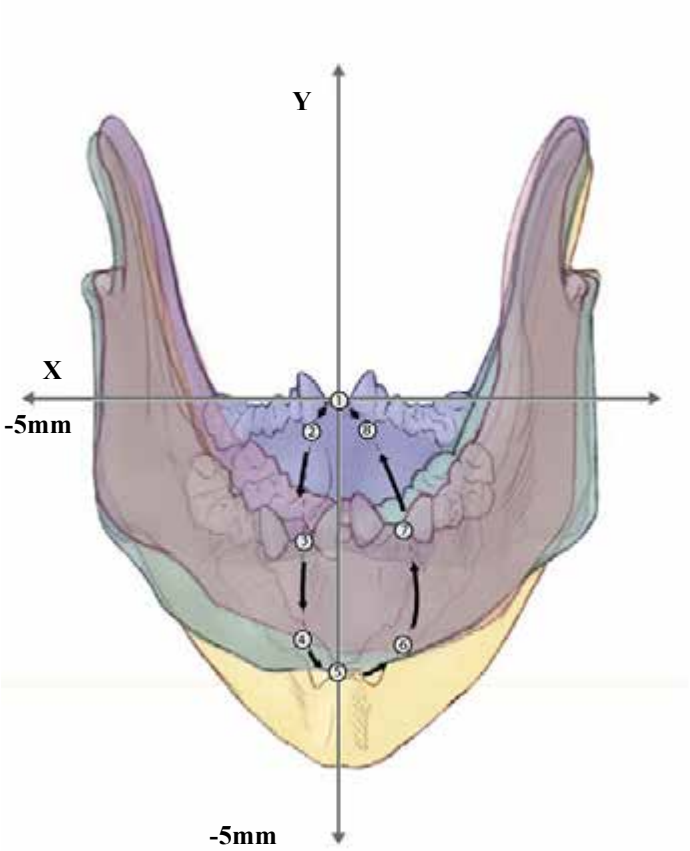

Figure 32. Image depicting the elliptical shape the path of the jaw's vertical and horizontal path creates when the rostral most point at its midline is tracked during a gape cycle. The eight points chosen to represent this shape are indicated in white circles. The X axis represents lateral displacement in mm and the Y axis represents vertical displacement in mm.

In order to move the virtual jaw to coordinate with these reference points, the jaw needed to be rotated about the transverse axes to produce jaw depression and elevation, and rotation about the vertical axes to produce the mediolateral movements of the teeth and anteroposterior movements of the condyles (Ross and Diaz 2014).

Jaw depression and elevation were achieved in **Blender** by rotating the **Control Bone** of the armature, along the X plane in **Blender** under the setting **XYZ Euler** in the **Transform section (fig 34)**. In order to achieve the mediolateral movements and the anteroposterior movements of the condyles, the **Control Bone** of the armature moved along the Y plane in **Blender**. Once the jaw was in position the **Control Bone's Location** and **Rotation Coordinates** were key framed at that point.

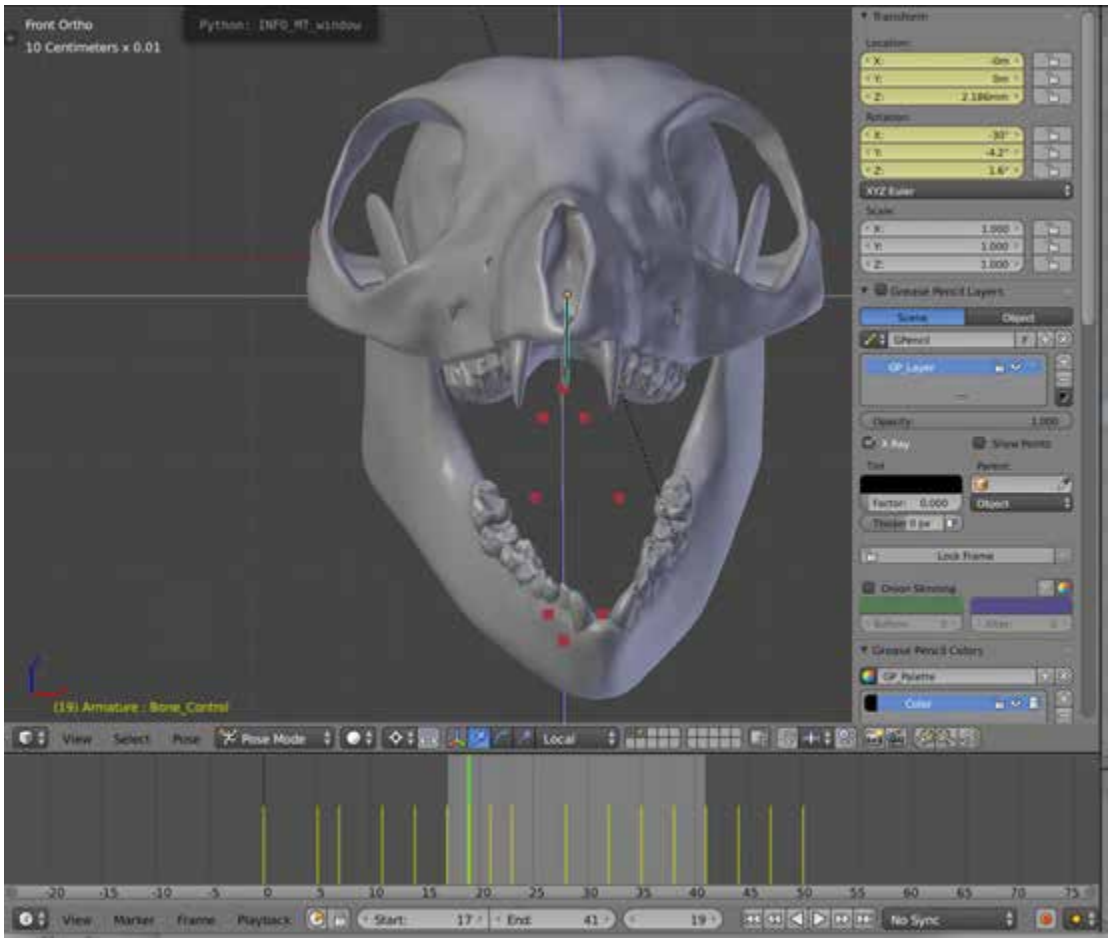

Figure 33. Screen shots in Blender showing the recreated elliptical shape made of cube objects and the jaw being matched to one of them.

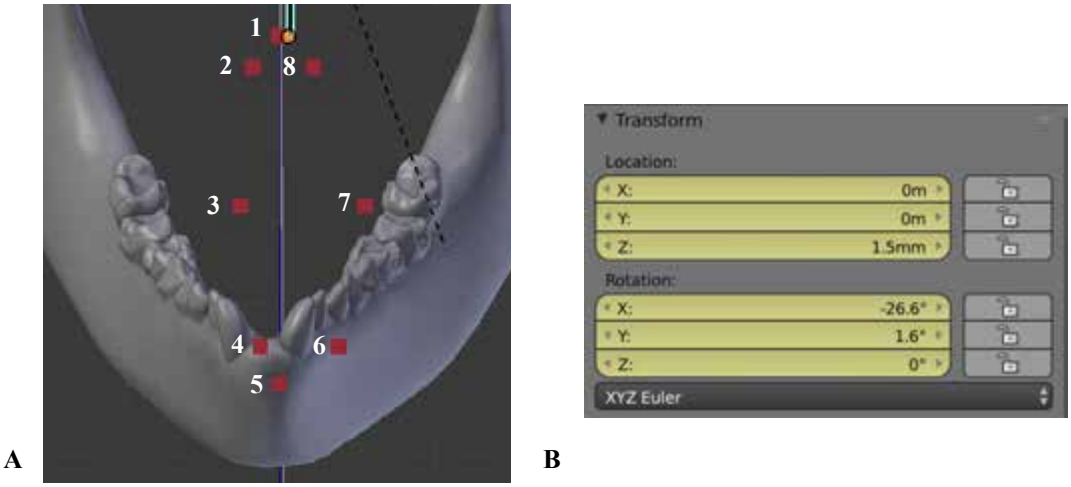

A **B**

Figure 34. Screen shots in Blender showing (A) a close view of the jaw being moved to point 4 and (B) the Control Bone's coordinates that were key framed. Location Z indicates the condylar displacement of 1.5 mm within the mandibular fossa, Rotation X indicated the jaw rotation around the transverse axis, and Rotation Y indicates the jaw rotation about the vertical axis.

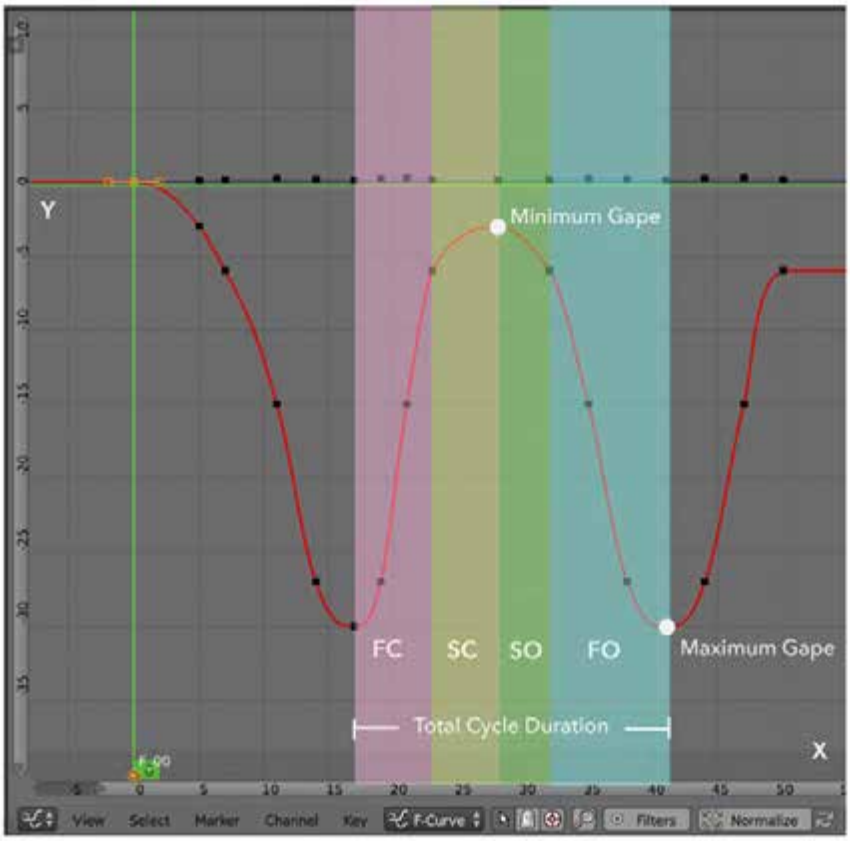

Figure 35. Screen shots in Blender showing the graph editor depicting the vertical displacement of the jaw (in degrees around the Transverse Axis). Colors and text are added over the screen shot to demonstrate how the graph is similar to actual data describing the four phases in the gape cycle (FC - Fast close, SC- Slow close, SO - Slow open, FO - Fast open) (Ross and Diaz 2014).

Point number	Rotation around Transverse Axis (Degrees)	Rotation around Vertical Axis (Degrees)	Time between points (Number of Frames)	Phase in Gape Cycle (FC, SC, SO, or FO)
1	-3°	0°	4	SO
2	-5°	-2.2°	3	FO
3	-15°	-3.6°	3	FO
4	-27°	- 2.2°	3	FO
5	-30°	0°	2	FC

Figure 36. Table describing the keyframe data at each point in the gape cycle. The table shows the Rotation around the Transverse Axis, Rotation around the Vertical Axis, Number of frames between each point, and the Phase in the Gape Cycle.

7.2.3 Simulating Gape Phases

To simulate the four Gape Phases within a Gape cycle the key frames within each cycle were given more or fewer frames depending on how fast the action was supposed to be. The number of frames given to each phase is listed in **figure 36.** The graph editor was used to confirm that the shape of the graph depicting the vertical displacement of the jaw, was similar to those created from actual data (Ross and Diaz 2014). The general shape of the displacement matched the four phases. **(fig 35)**

When playing back the animation a realistic chewing cycle is achieved. Each of the four phases can be identified and no part of the anatomy is intersecting other parts of anatomy in impossible ways.

7.4 Shape keys and Volume Conservation

When an armature is attached to the vertices of a mesh model the vertices will move with the armature when it is posed. Posing the armature can therefore make a mesh distort and move in a variety of ways, ho;ever, it should not be assumed that the volume of the mesh is conserved as it is manipulated. As seen in **figure 37** the mesh of the masseter begins with a volume of 4.18cm^3 before the armature is posed and ends with a volume of 5.85 cm^3 when the armature is posed. The volume of the mesh is not conserved during its transformation.

The solution for conserving the meshes volume involves the use of **Shape Keys** as a corrective tool. A **Shape Key** is a tool that stores the positions of a mesh's vertices. If the vertices are deformed into a new position a shape key will allow a mesh to be returned to that stored position. By key framing **Shape Keys** it is possible to animate an object morphing from one shape to another. **Shape Keys** were used as a corrective tool to ensure that a muscles' mesh maintained its volume during the armature animation through series of steps:

A

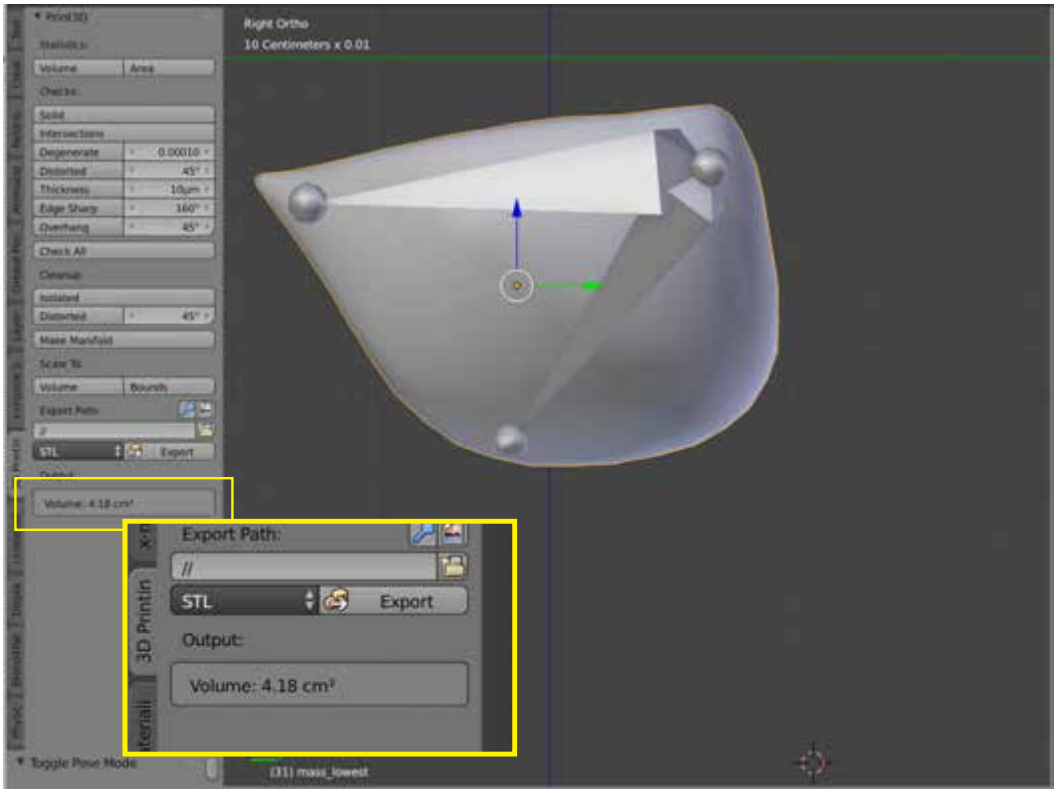

B

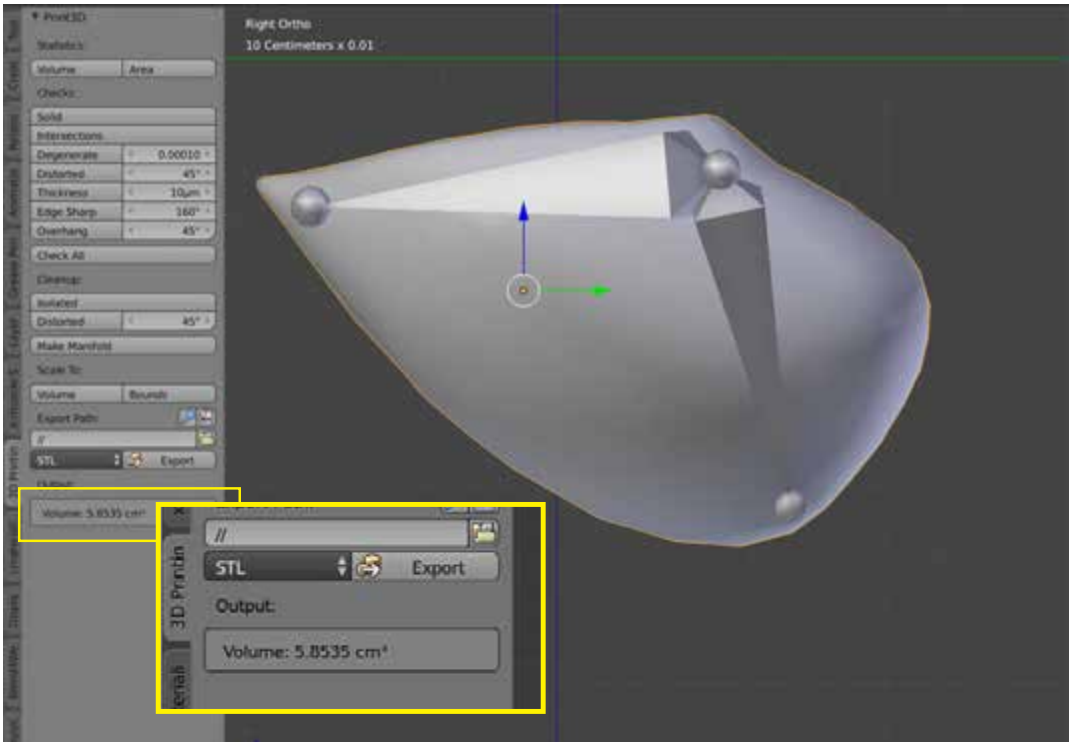

Figure 37. Screen shots in Blender showing the volume being measured with the Volume Tool before and after the armature displaces the mesh. The volume is shown to be (A) 4.18 cm^3 before being displaced and (B) 5.8535 cm^3 after being displaced. This demonstrates how volume is not conserved. Not all text is intended to be read.

Shape keys were used to correct muscle volume conservation by through the following steps:

(1) The mesh is selected and while in **Object Mode** a **Basis Shape Key** was stored **(Object Data > Shape Key > +)**.

(2) Using the **Volume tool (3D Print > Statistics > Volume)**, the volume of the mesh at rest was measured. (Due to the individual muscle meshes being combined with the mandible and lower teeth mesh's the volume was equal to the sum of those parts, ~ 27 cm^3 **(fig 39)**).

(3) The armature was selected and, while in **Pose Mod**e, was posed to the previously determined position of maximum gape

(4) The mesh's volume was checked again using the same process as step 1. (It was noted that the mesh's volume was nearly 5cm^3 greater than at rest).

(5) A second **Shape Key** was created and named "**Jaw Open**". The **Relative Value** slide bar was turned to **1.00**. Any changes made to the mesh would now be stored at that value.

(6) The **Sculpt tools** (in **Sculpt mode**) were used to correct the muscle's volume by "pushing" the mesh back into a reasonable shape and subsequently checking its volume, until it matched the original volume measured in step 1 **(fig 39).**

(7) The mesh could then be "morphed" between the **Basis Shape Key** and the **"Jaw Open" Shape Key** by sliding the **Relative Value** slide bar between the values of 0.000 and 1.000 **(fig 38)**.

(8) The **Relative Value** was then key framed to coincide with the movement of the jaw during the animation of the gape cycle. For example, when the jaw was at full occlusion the **Relative Value** was key framed at 0.000 and when the jaw was at maximum gape the **Relative Value** was key framed at 1.000.

Figure 38. Screen shot in Blender of Shape Key interface demonstrating the Relative Value slide bar being adjusted.

A

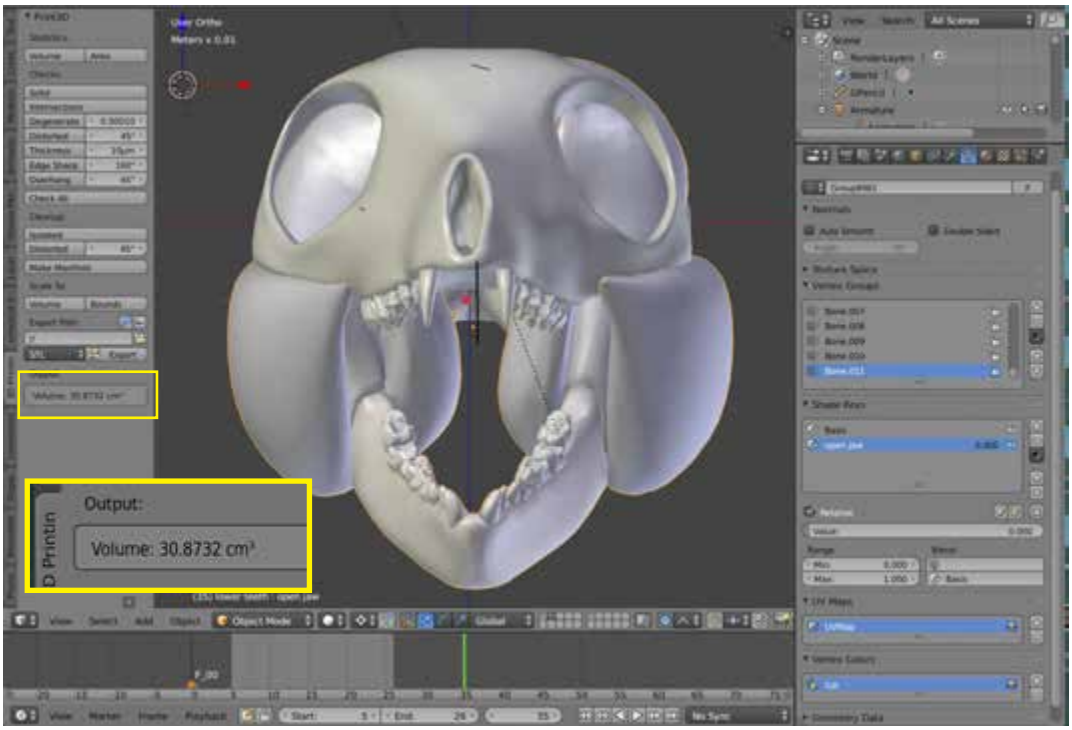

B

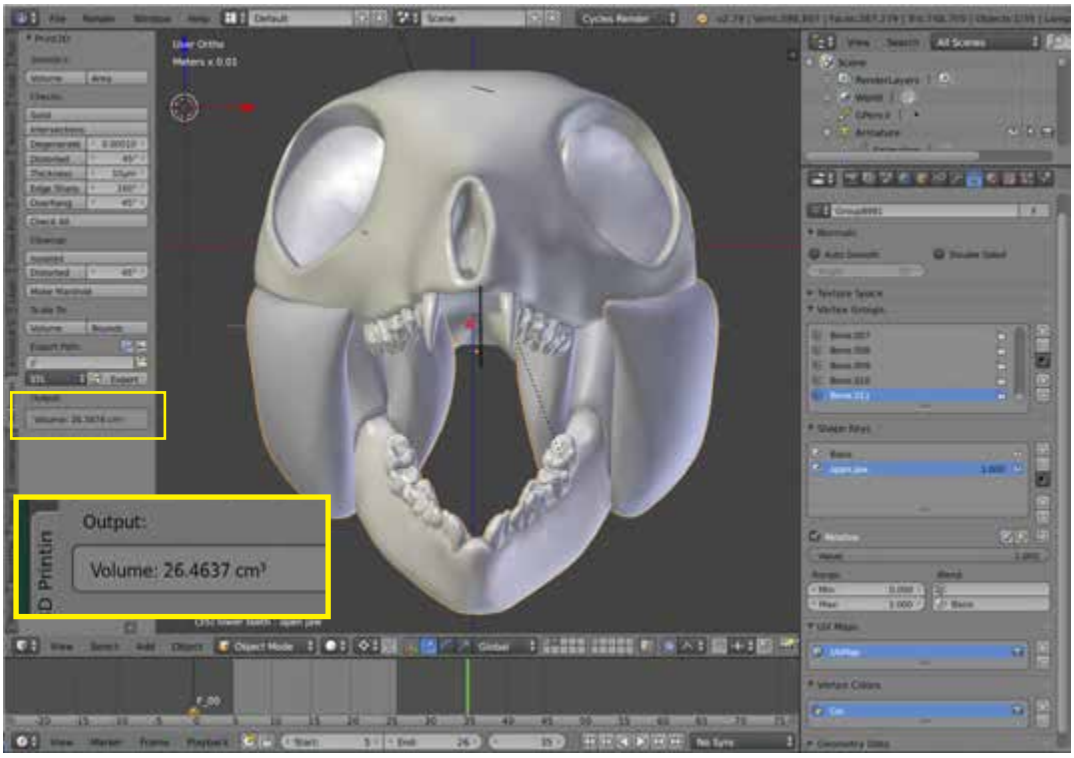

Figure 39. Screen shots in Blender showing the volume being measured with the Volume Tool before and after the armature displaces the mesh. The volume is shown to be (A) 30.8732 cm³ before being displaced and (B) 26.4637 cm³ after being displaced, which matches its original value at rest. Not all text is intended to be read.

By using **Shape Keys** to correct volume conservation and the **Volume tool** to verify that volume; the animation of the muscles responding to the jaw's movement during chewing was achieved in a smooth, realistic, and accurate way.

7.5 Vertex Baking

Blend4Web does not currently support the use of **Shape Key** animation controls and **Armature animation** controls, acting on the same mesh simultaneously. The workaround to using these controls while preserving the ability to play an animation in within a **Blend4Web** interactive application, is to **Vertex Bake** the animation prior to upload. **Vertex Baking** is a tool that stores the positions of all the vertices of a mesh, within a selected range of key frames. Once an animation is baked, it will play in **Blend4Web**, without the use the **Armature** and **Shape Key** controls that were used to create it.

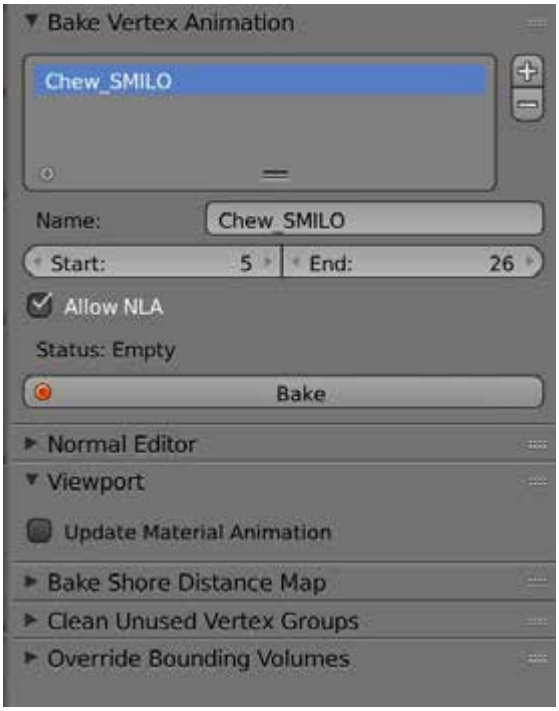

Figure 40. Screen shot in Blender showing Bake Vertex Animation settings.

The **Vertex Bake** tool was used by selecting the "combined jaw and muscle object" in **Object Mode** and by creating a new V**ertex Bake Animation (Blend4Web tab > Bake Vertex Animation > name "Chew_ SMILO" > Bake)**. One complete cycle, including the four phases of the gape cycle, was chosen to Bake. The duration was set by inputting the frame range of the cycle into the **Start** and **End** fields within the **Vertex Bake** settings. The settings used for the **Vertex Bake** of the chewing animation are shown in **fig 40.**

8. Creating interactive applications using Blend4Web

Blend4Web, a **WebGL** framework and a 3D content creation suite based on the 3D engine **Blender** was used in this project to create interactive application to display the virtual models created and to share them online. This project created interactive applications for the virtual reconstructed skull and chewing musculature of *Smilodectes gracili*s as well as the chewing simulation. It created a separate interactive for the facial approximation model. The environment, lighting, and camera set up was the same for both interactive applications.

8.1 Creating an Environment

A background, and lighting, and a camera were added to the scene to set the models' environment. The background was created by adding a flat plane **(Add > Mesh > Plane)** to the scene and modeling it into a curved plane that served as the floor and backdrop of the scene. The color of the plane was set to white **(Properties > Material > Diffuse**).

To light the scene, one **Sun light** and four **Point lights** were placed in the scene. A **Sun light** propagates from an infinite plane in one direction without attenuation (Yao, 2017). This light was used to light the entire scene. **Point lights** propagate from one source to all directions with gradual attenuation. These lights were used as fill lights and to create highlights on the model. The **Sun light** was the only light that was allowed to produce shadows. Shadows were enabled in the light properties (**Properties > Object Data > Shadows)**. The model was also set to cast shadows **(Properties > Object > Shadows > Cast Shadows).** The view of the scene was set by adding a **Camera (Add > Camera)**. The camera was moved to a location that framed the model in an aesthetic way.

To create interactive buttons, **Planes** were added to the scene, modeled into the desired shape, and given a color. Text is treated the same as any other mesh in Blender. Each word was added as a separate object and moved to the desired location in the scene. One "on button" and one "off button" were created for each of the muscles as well as for the chewing animation.

In order to keep the background, lights, buttons, and text static within the scene, they were parented to the **Camera (Object > Parent).** By doing this, the model becomes the only object that can moved in the scene.

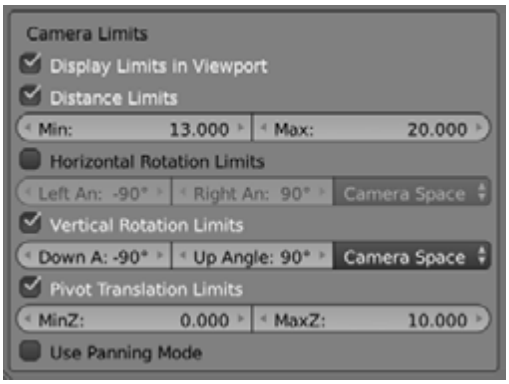

Figure 41. Screen shot in Blender showing the Camera Limit's settings used.

The movement of the model itself was also restricted using the **Camera Limits** parameters in the **Camera properties** tab. The **Camera Limits** used in the interactive application for this project are show in **figure 41.**

8.2 Creating a Node Tree

To create interactivity, the **Node Editor** was used. To activate logic on the scene the **Logic Editor** property under the **Scene tab** was selected and an **Active Node Tree** was appended. **The Logic Tree** was edited by selecting the **Blend4Web Logic Tree** type and selecting the appropriate node tree.

Nodes are logic blocks which are executed from an **Entry Point** node which has no inputs and only one output. All the other nodes have both inputs and outputs which are used to by inserted anywhere in the tree. The **Select, Hide Object and Show Object Nodes** were used to create a **node tree** that allows the interactive functionality of turning on and off the individual muscles on the model, when a corresponding button is clicked. The **Select node** was used to trace the selection of any object from the object list. The **Hide Object Node** hides an object if its condition is met, and the **Show Object Node** shows an object if the condition is met **(fig 42).** To play the chewing simulation the **Play Animation node** was used **(fig 42).** The full node tree can be seen in **figure 43.**

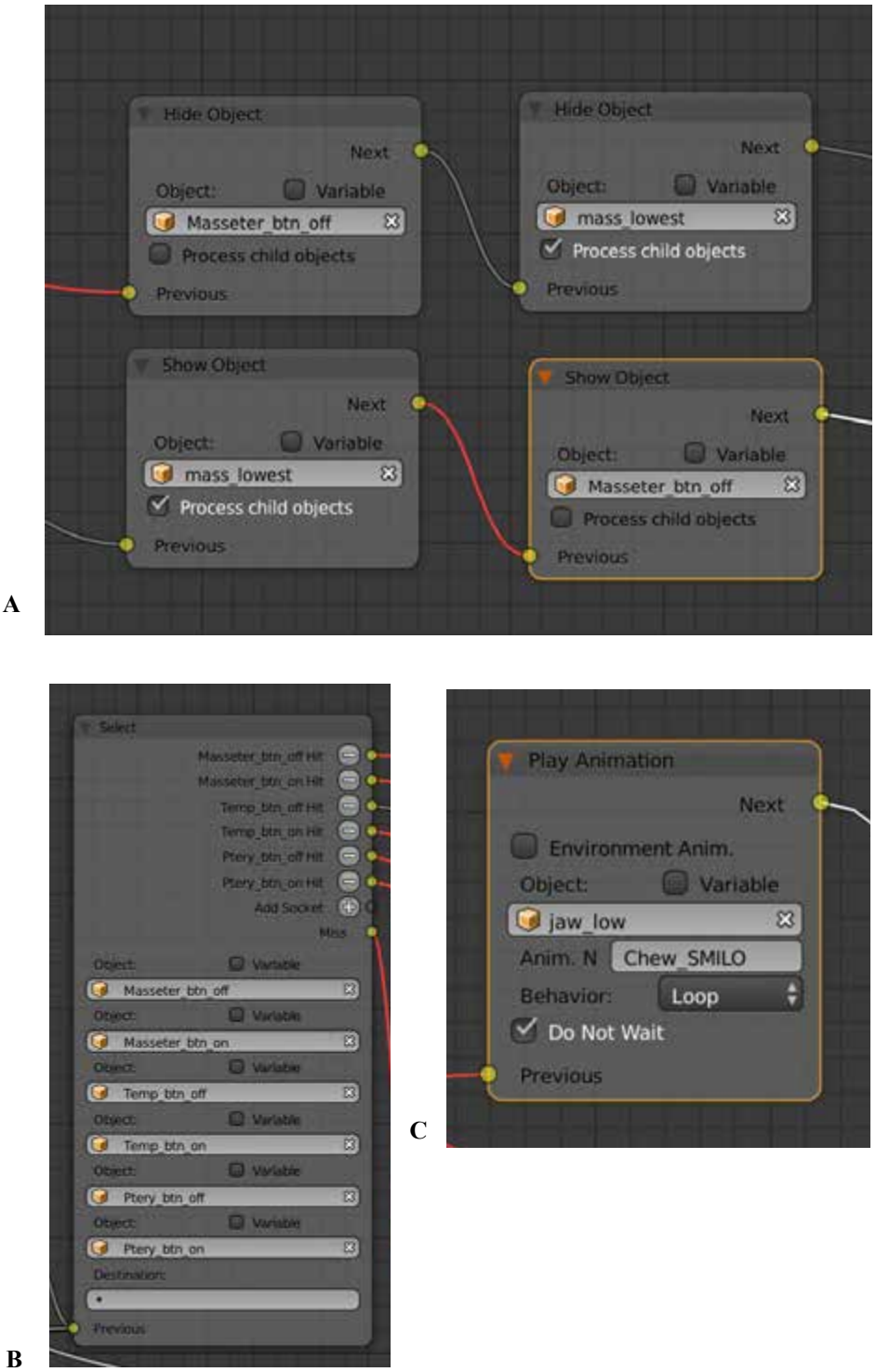

Figure 42. Screen shot in Blender showing the Select Node used in creating the Node Tree, including (A) the hide object node, (B) the Switch Select node, and (C) the play animation node.

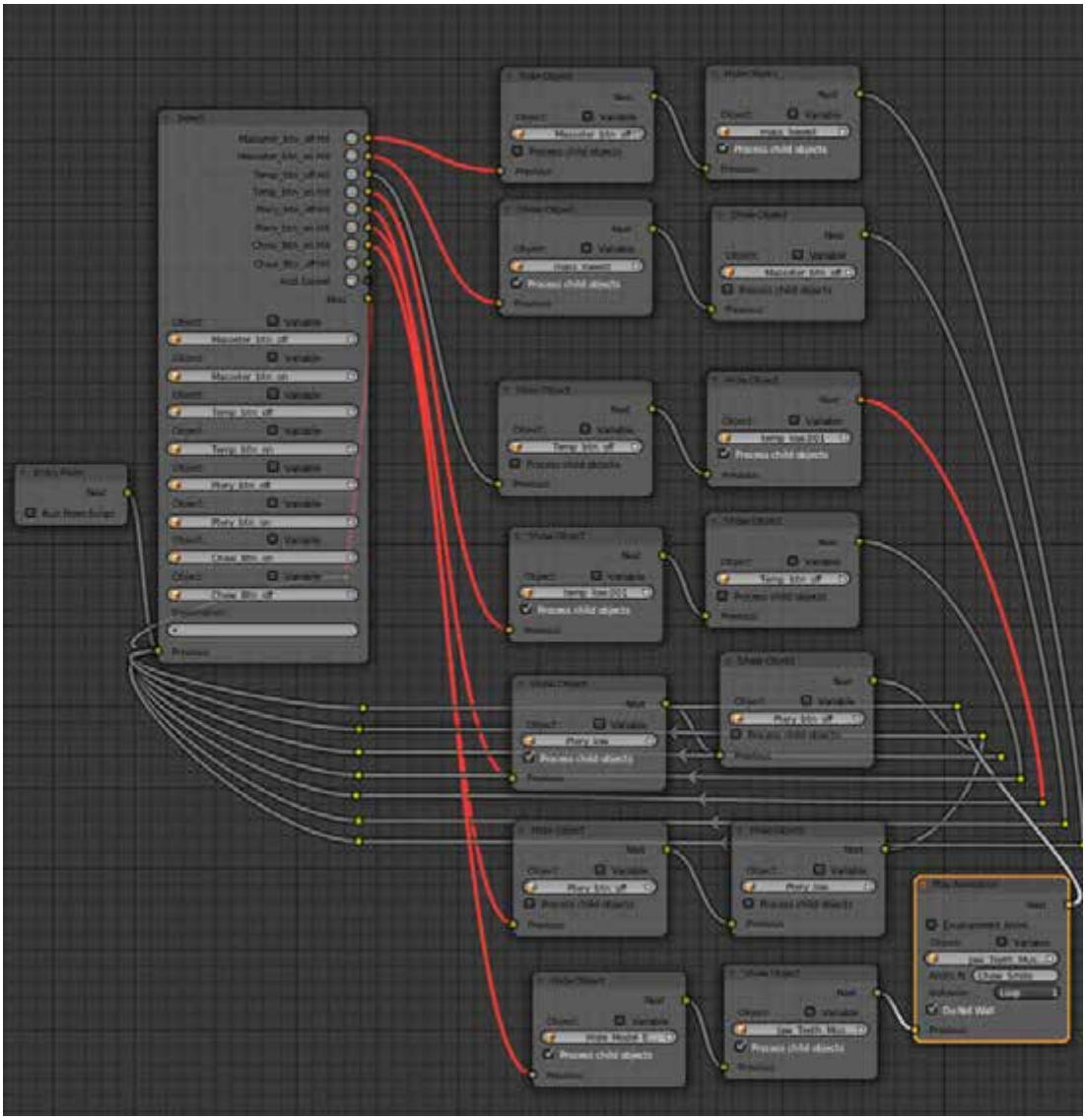

Figure 43. Screen shot in Blender showing the Node Tree used for the interactive application. Text is intended to be read.

8.3 Annotations

Labels and annotations are valuable tools for the biocommunicator and scientist. **Blend4Web** offers a useful built in annotation system. The annotation tags are 2D HTML elements, which follows particular positions of the 3D model. Positions were created for the 2D annotation element to track by creating an **Empty Plane Axes** and moving them to the position where an annotation was desired. The **Anchor** was then enabled in the **Object panel (Properties > Object > Enable Anchor)**. These **Anchors** also contain an interactive property which permits additional content to be added that drops down within the anchor when the anchor is clicked. The additional content could include text or an image and is added in the **Object properties** tab **(Properties > Object > Meta Tags > Description) (See fig 44)** This project utilized the **Anchors** to create annotations that labeled each muscle and when clicked provided more information about that muscle.

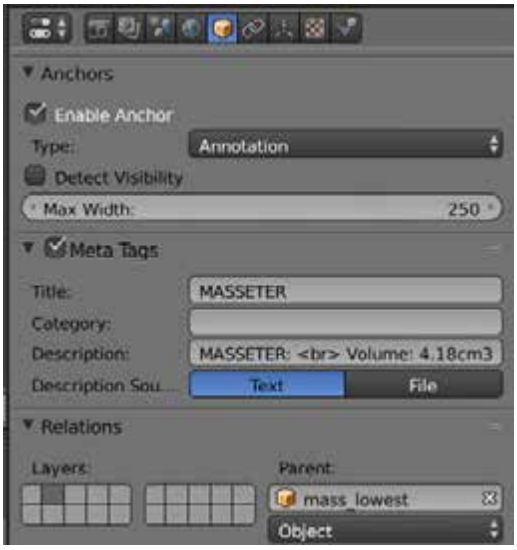

Figure 44. Screen shot in Blender showing Annotation properties used for the Masseter annotation

8.4 Exporting

The interactive web application was launched by exporting its HTML file and loading it onto a personal server as a test. The application ran smoothly and all interactive elements worked as designed.

RESULTS

1. Fossil Reconstruction Results

The reconstruction of the fossil specimen of *Smilodectes gracilis* had three stages each which yielded results useful in improving the study of the species and more specifically the study of the species' chewing architecture. The first stage resulted in a virtual, segmented fossil freed of much of the sediment it was impacted by and reoriented in an anatomically correct position. The second stage resulted in a virtual, restored fossil whose distortions and fragmentations were corrected and missing anatomy accounted for. The third stage resulted in a virtual, fully reconstructed, model of the specimen with realistic texture and detail added. These stages are shown in the following labeled diagrams:

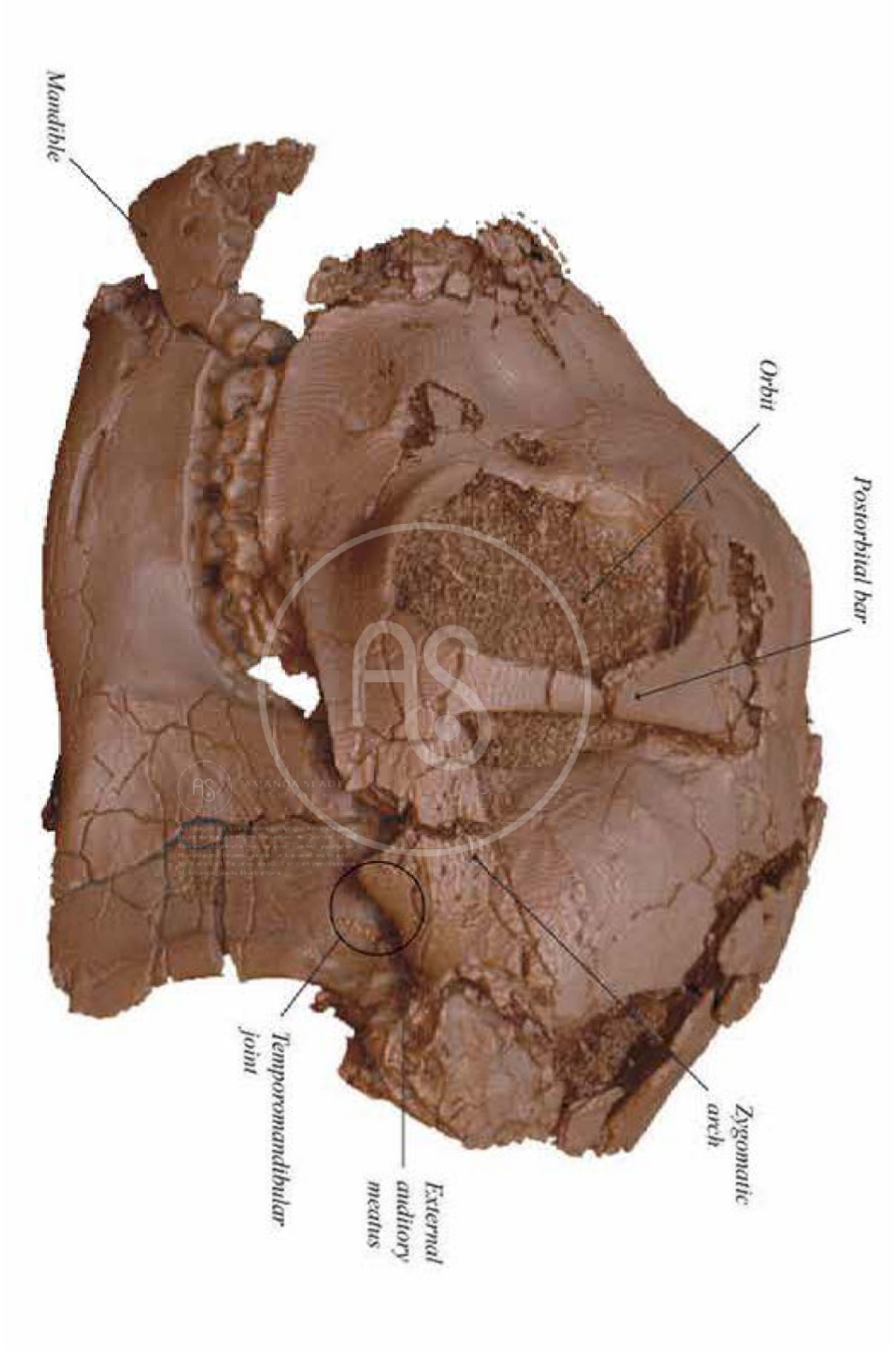

Figure 45. Lateral view of original virtual fossil.

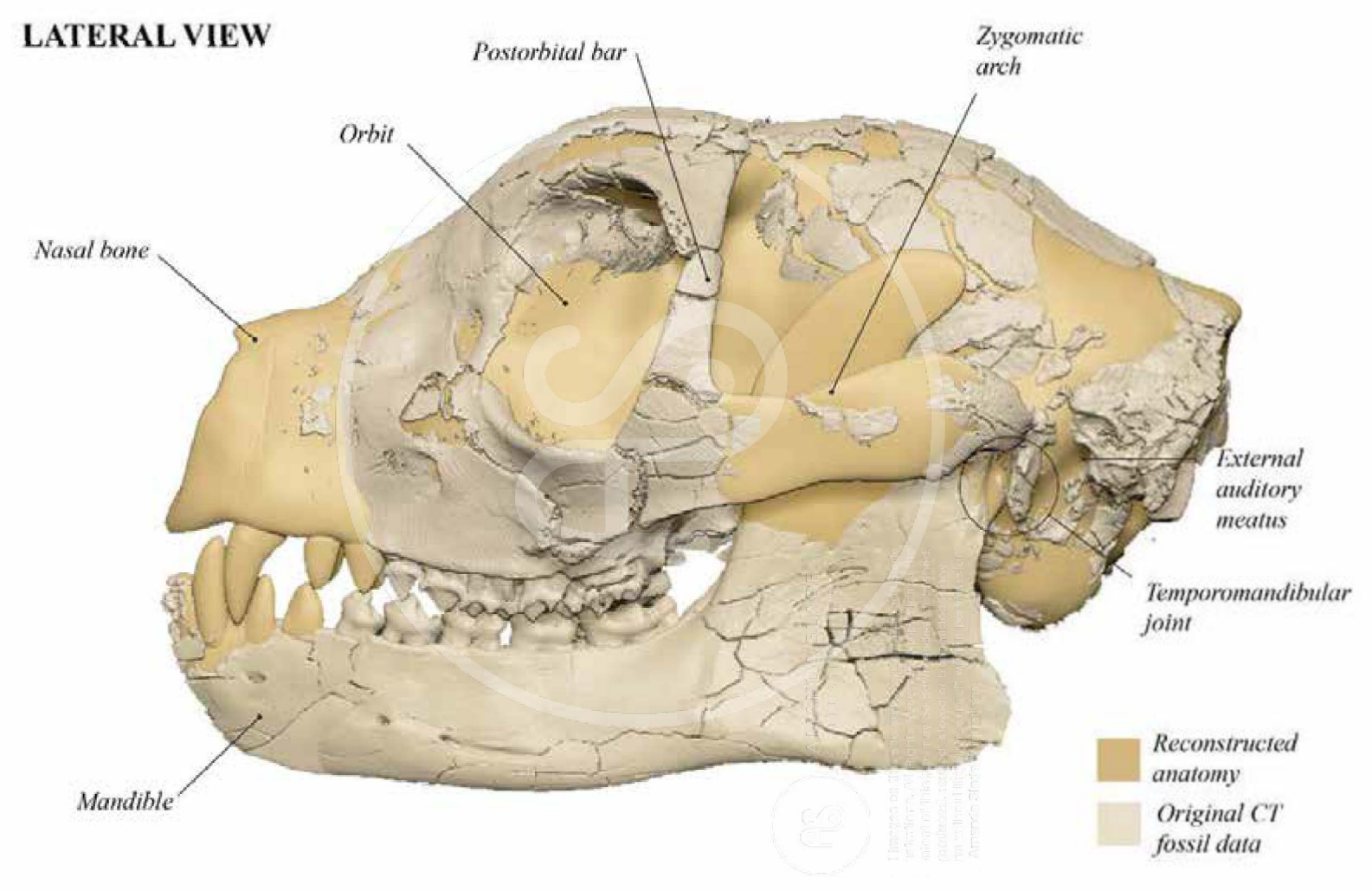

Figure 46. Lateral view of the virtually restored cranium and mandible.

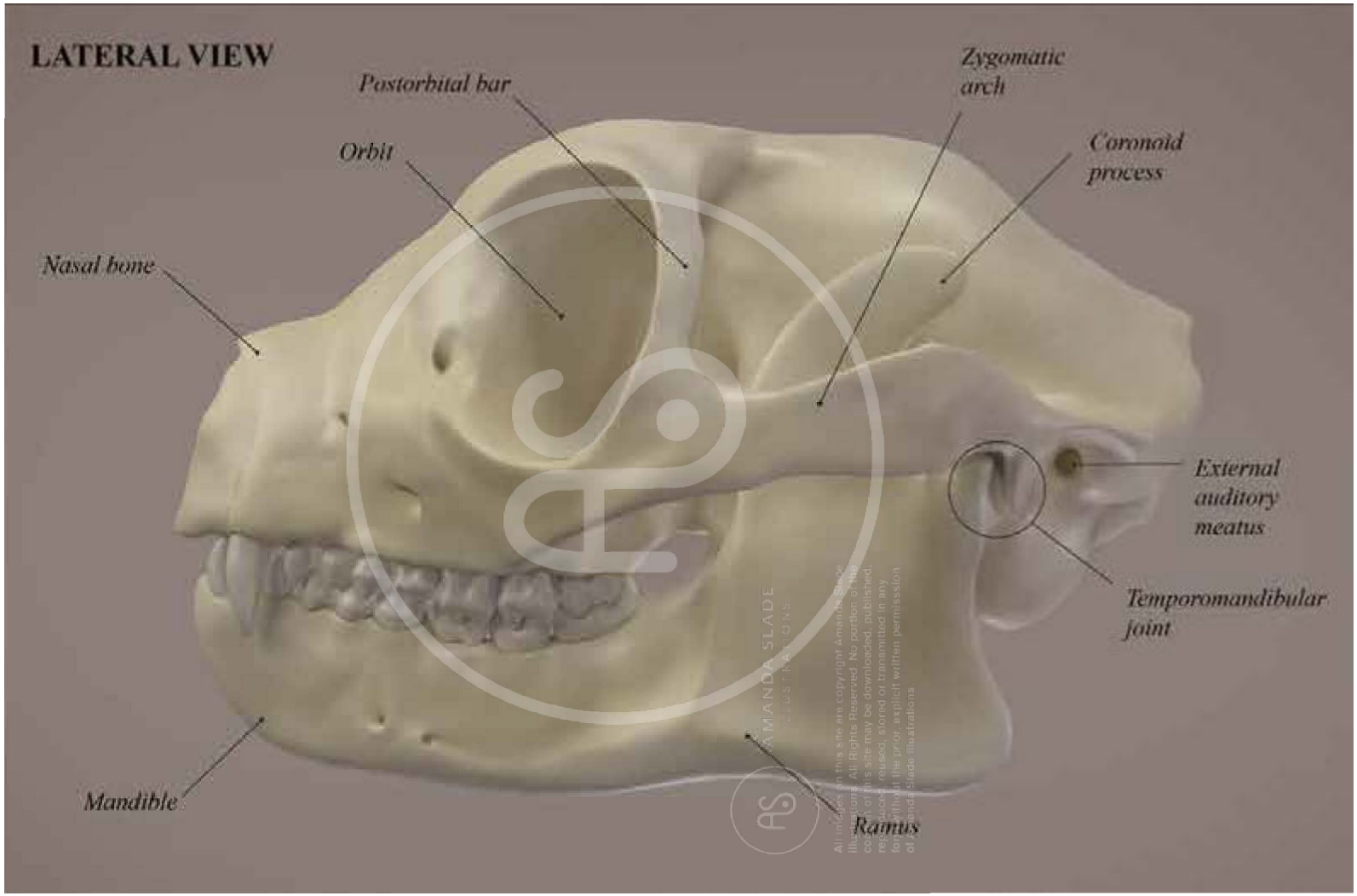

Figure 47. Lateral view of the virtual reconstruction of the skull.

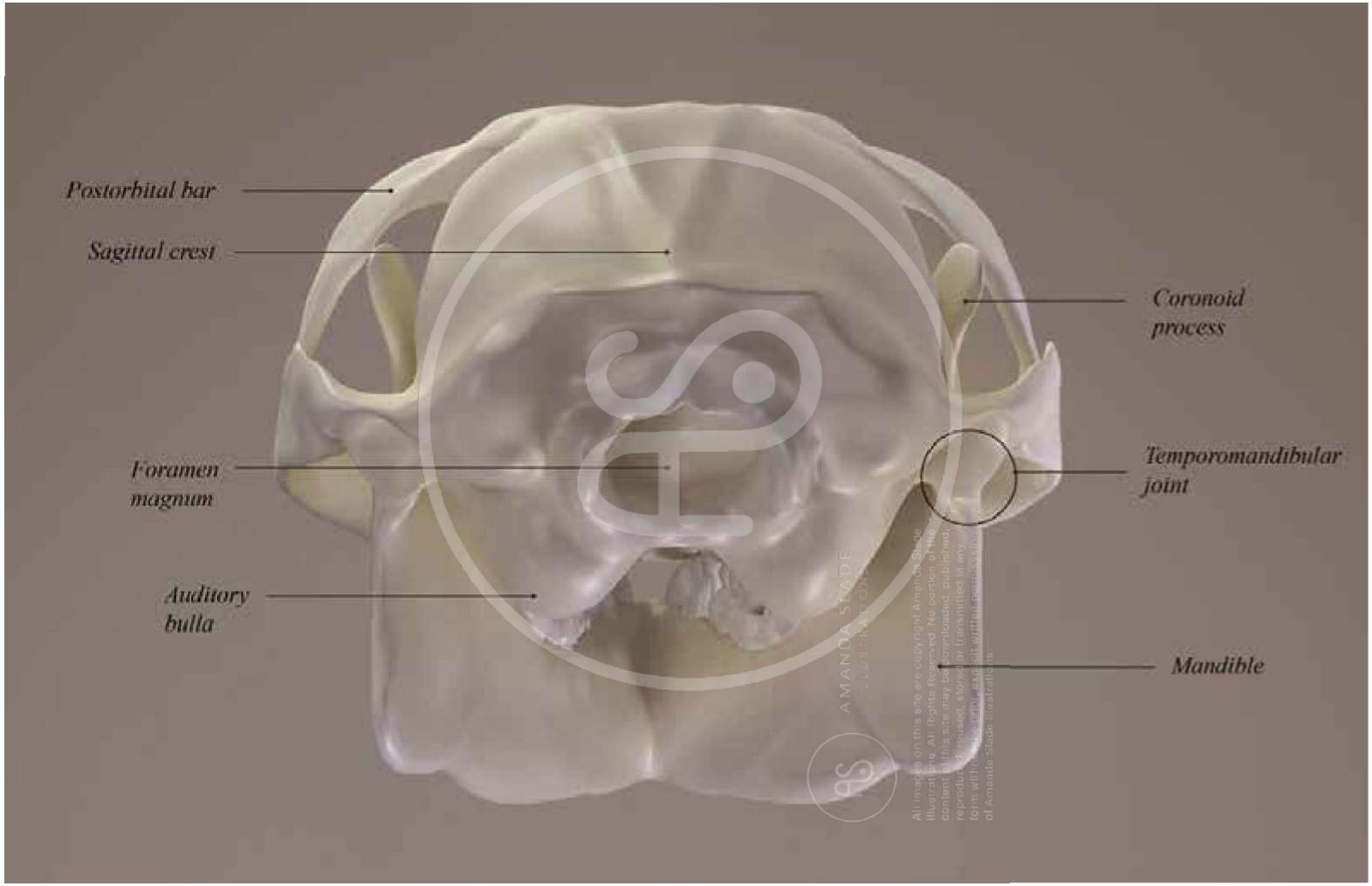

Figure 48. Posterior view of the virtual reconstruction of the skull.

2. Muscle Reconstruction Results

The jaw adductor muscles of *Smilodectes gracilis* were reconstructed both numerically and virtually. Dimensional data was calculated from osteological measurements taken from the virtually restored fossil specimen. Volumetric estimate of the sizes of the masseter, medial pterygoid and temporalis muscles were found. The dimensional data was then used to create virtual models that could attach to the virtual skull and mandible model previously created.

2.1 Dimensional Data

Jaw Adductor Muscle	Volume Estimate (cm3)
Masseter	4.18
Temporalis	4.74
Medial Pterygoid	2.75

Figure 49. Table of volume estimates of the jaw adductor muscles.

2.2 Virtual Jaw Adductor Models

The volumetric estimates of the jaw adductor muscles were used to digitally recreate virtual muscle models which are presented in the following labeled diagrams (fig 49, 50).

2.3 Origin and Insertions sites

The muscles were recreated based on their origin and insertion sites. Diagrammatic interpretations of these sites were created on the skull and mandible. (fig 51)

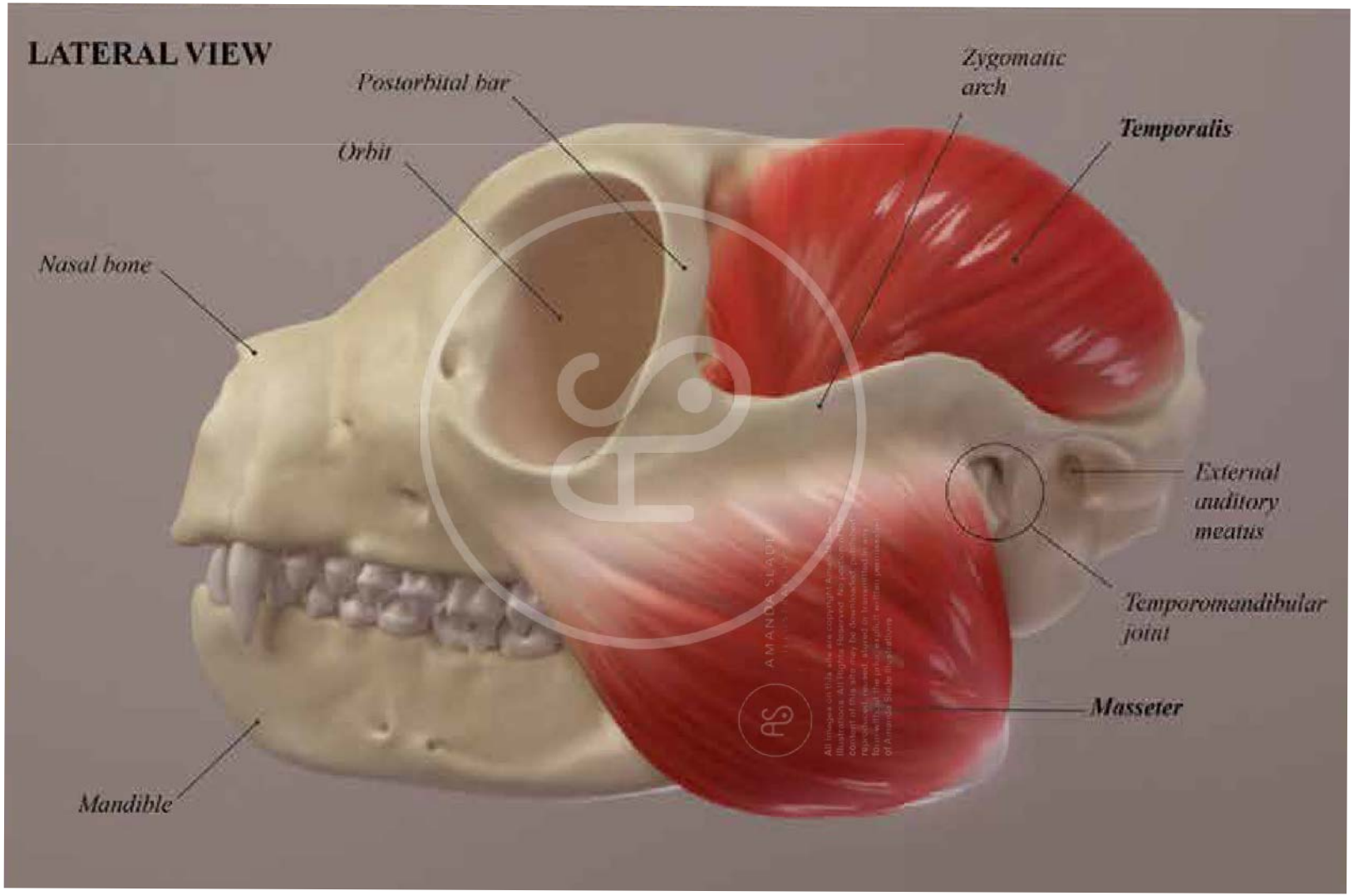

Figure 50. Lateral view of the virtual muscle reconstruction.

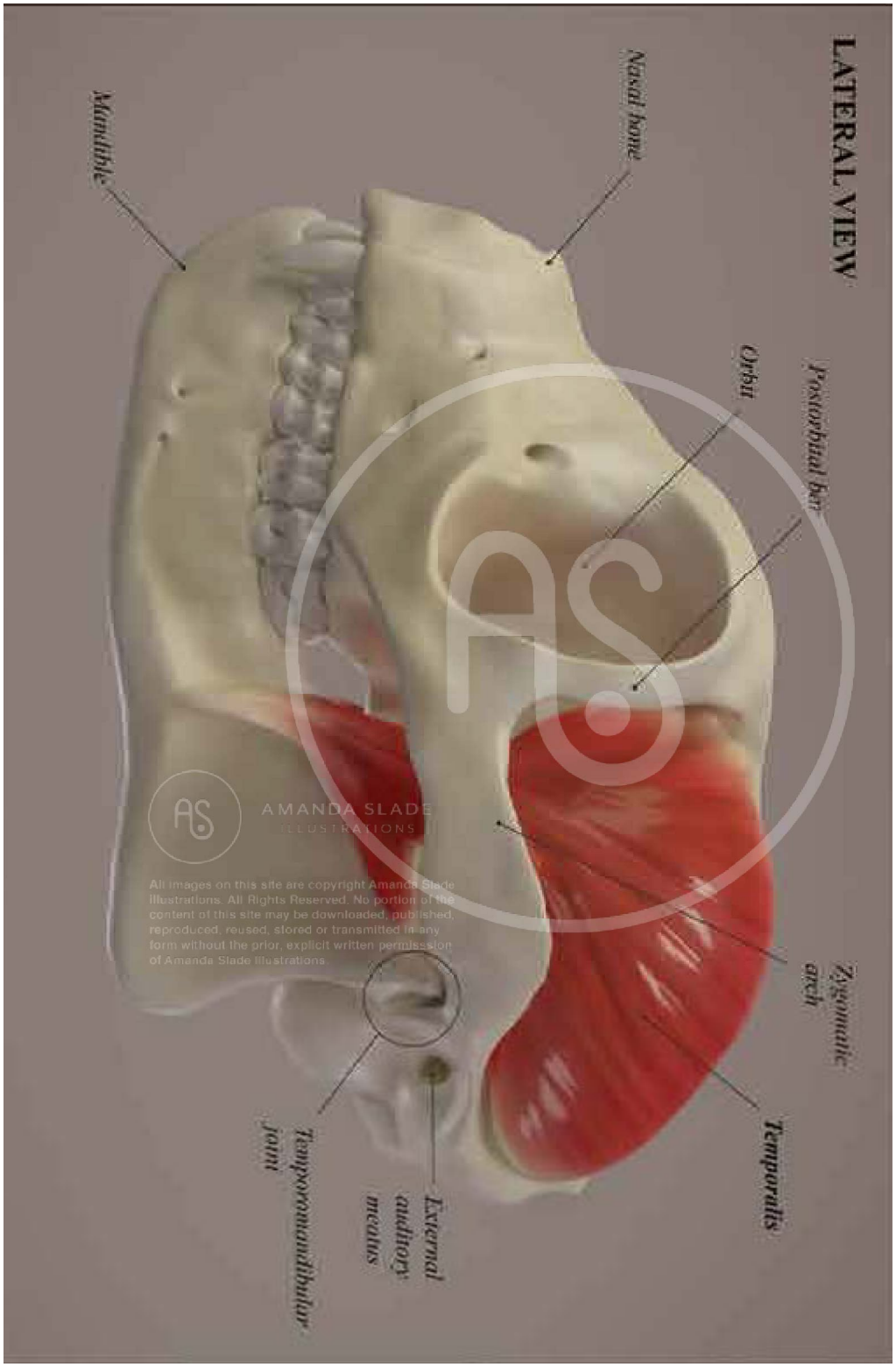

Figure 51. Lateral view of the virtual muscle reconstruction with Masseter removed.

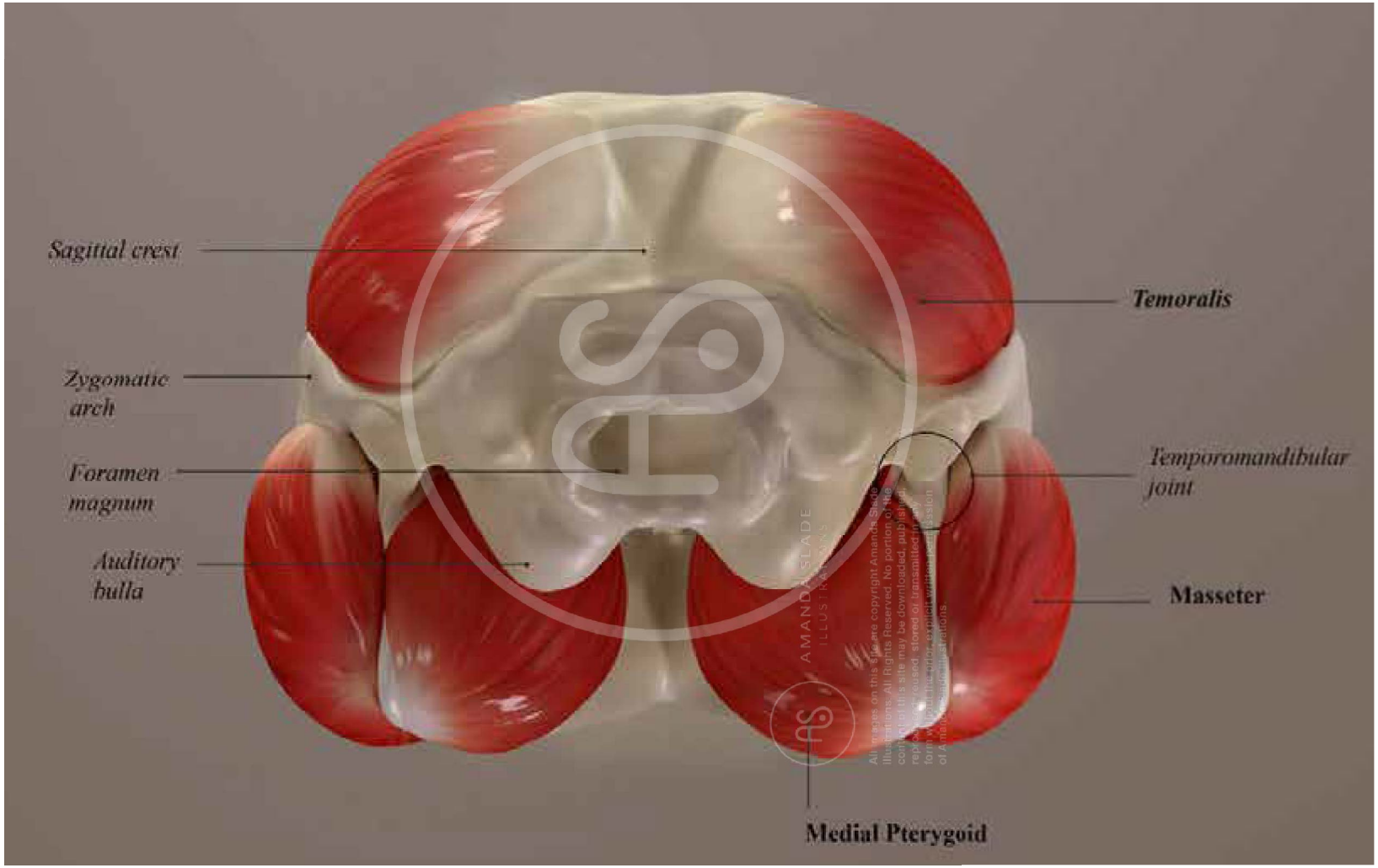

Figure 52. Posterior view of the virtual muscle reconstruction with Masseter removed.

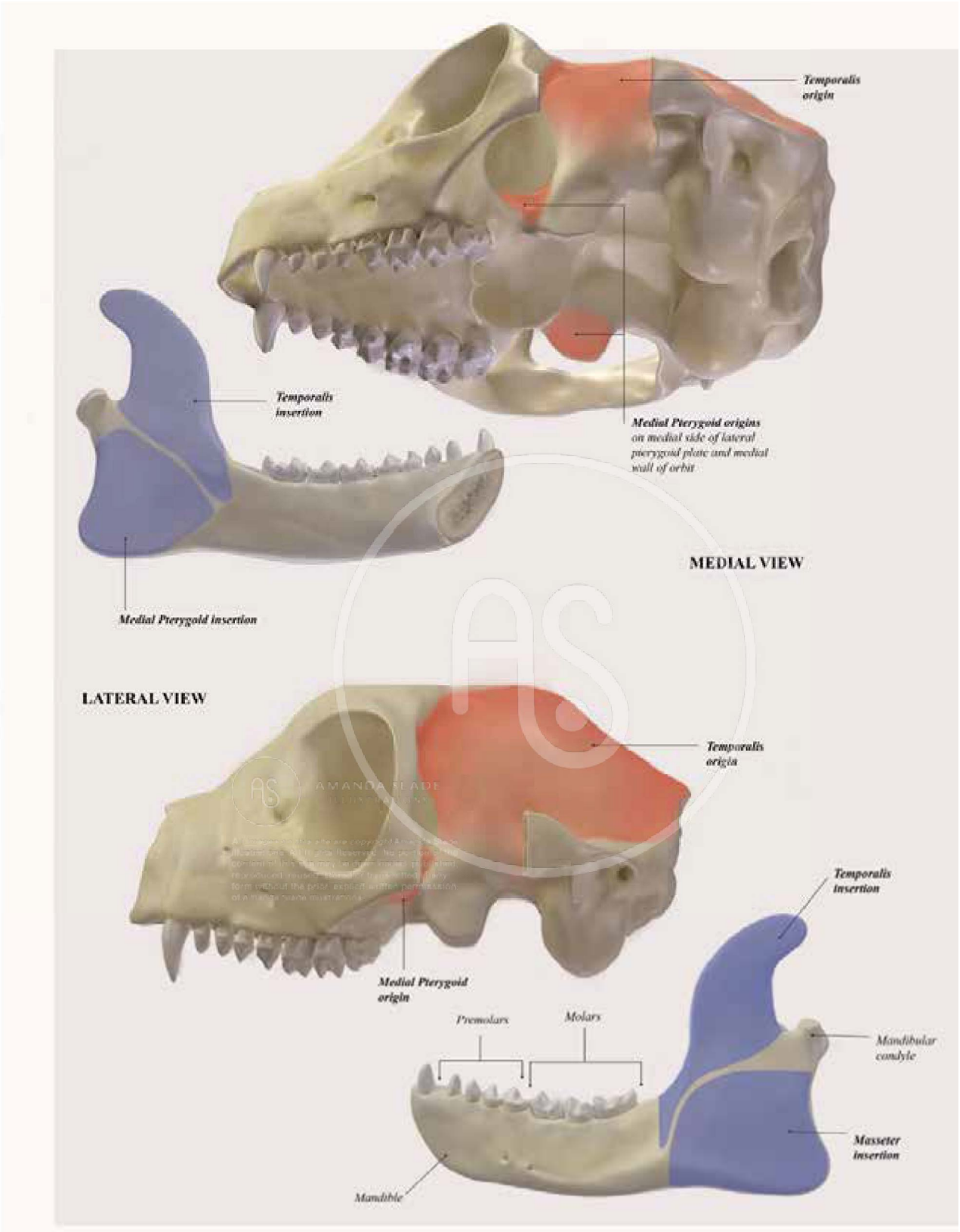

Figure 53. Medial and Lateral views of the origin and insertion sites of the jaw adductor muscles.

3. Chewing biomechanics Results

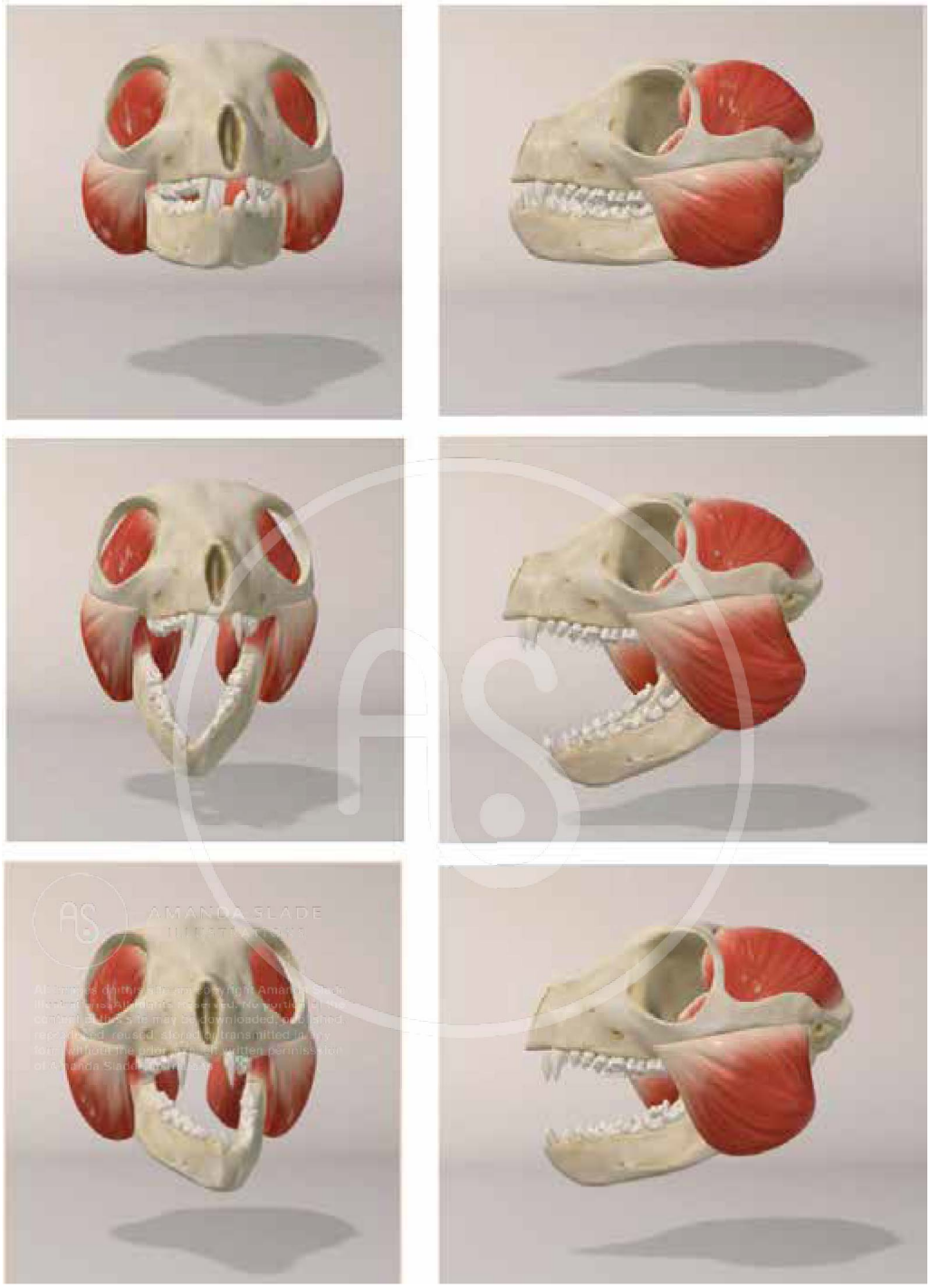

Figure 54. Still screen captures of the dynamic chewing simulation.

4. Facial Approximation Results

A virtual 3D facial approximation sculpture was created. The stages are documented. Underling skeletal and muscular anatomy were used from the previous models.

Figure 55. Virtual facial approximation.

5. 3D Interactivity Results

A fully interactive application was created featuring the chewing simulation and muscle information.

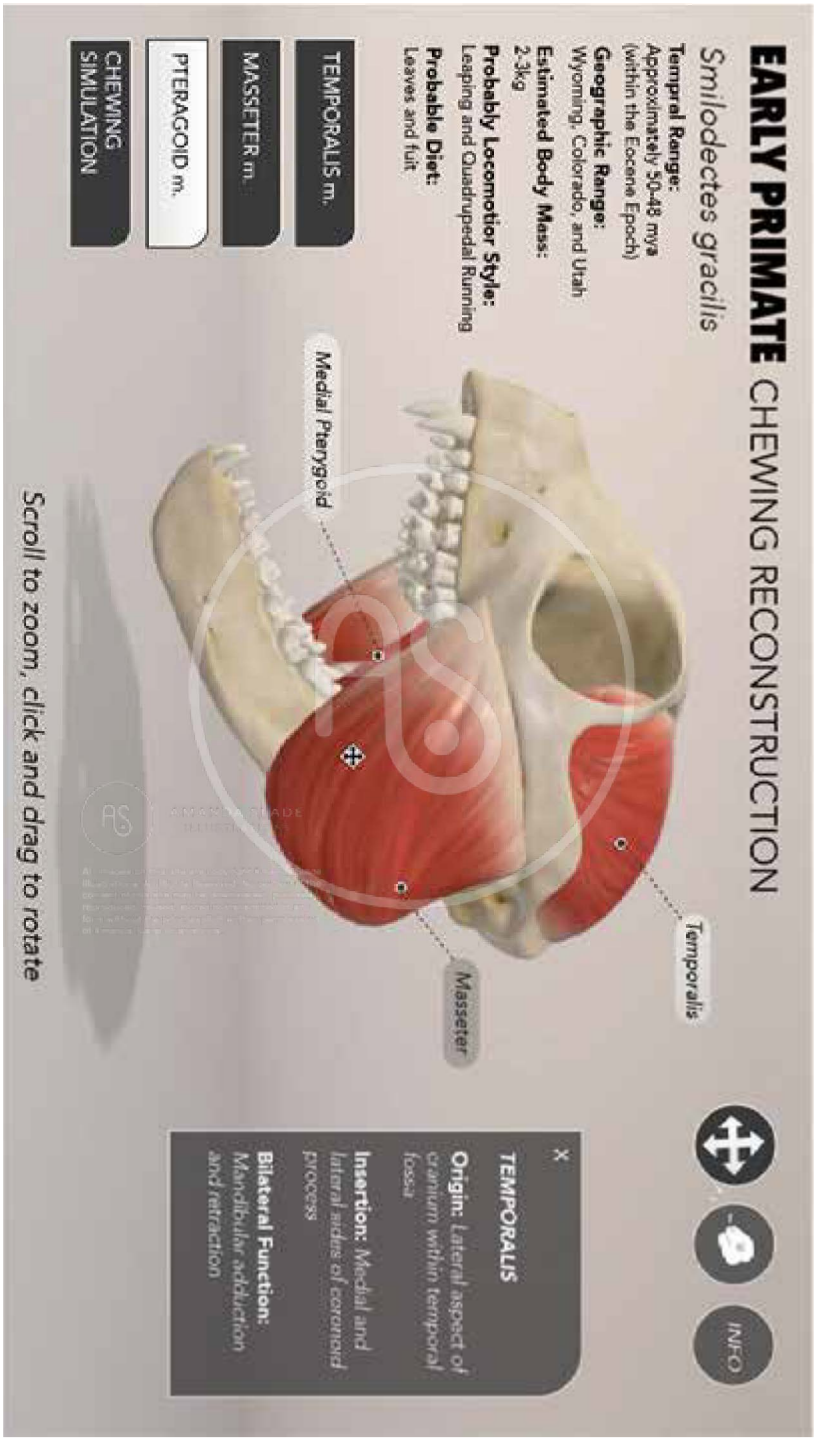

Figure 56. Screen shots displaying the interactive chewing simulation in a web application

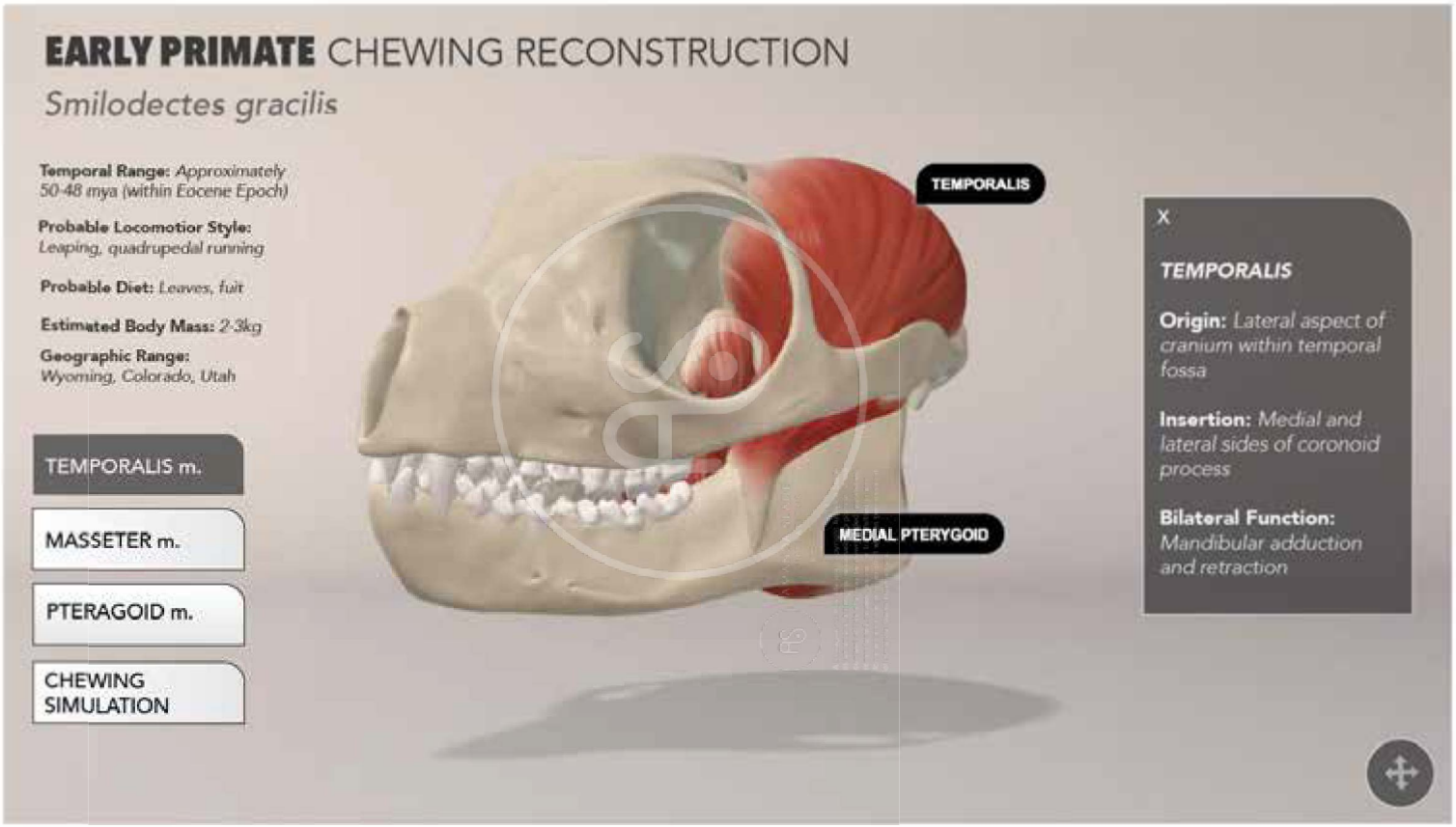

Figure 57. Screen shot displaying the interactive web application, displaying muscle interactivity.

Figure 58. Screen shot displaying interactive web application, displaying muscle interactivity.

6. Work Flow Results

Documentation of the workflow is presented in stages divided by software.

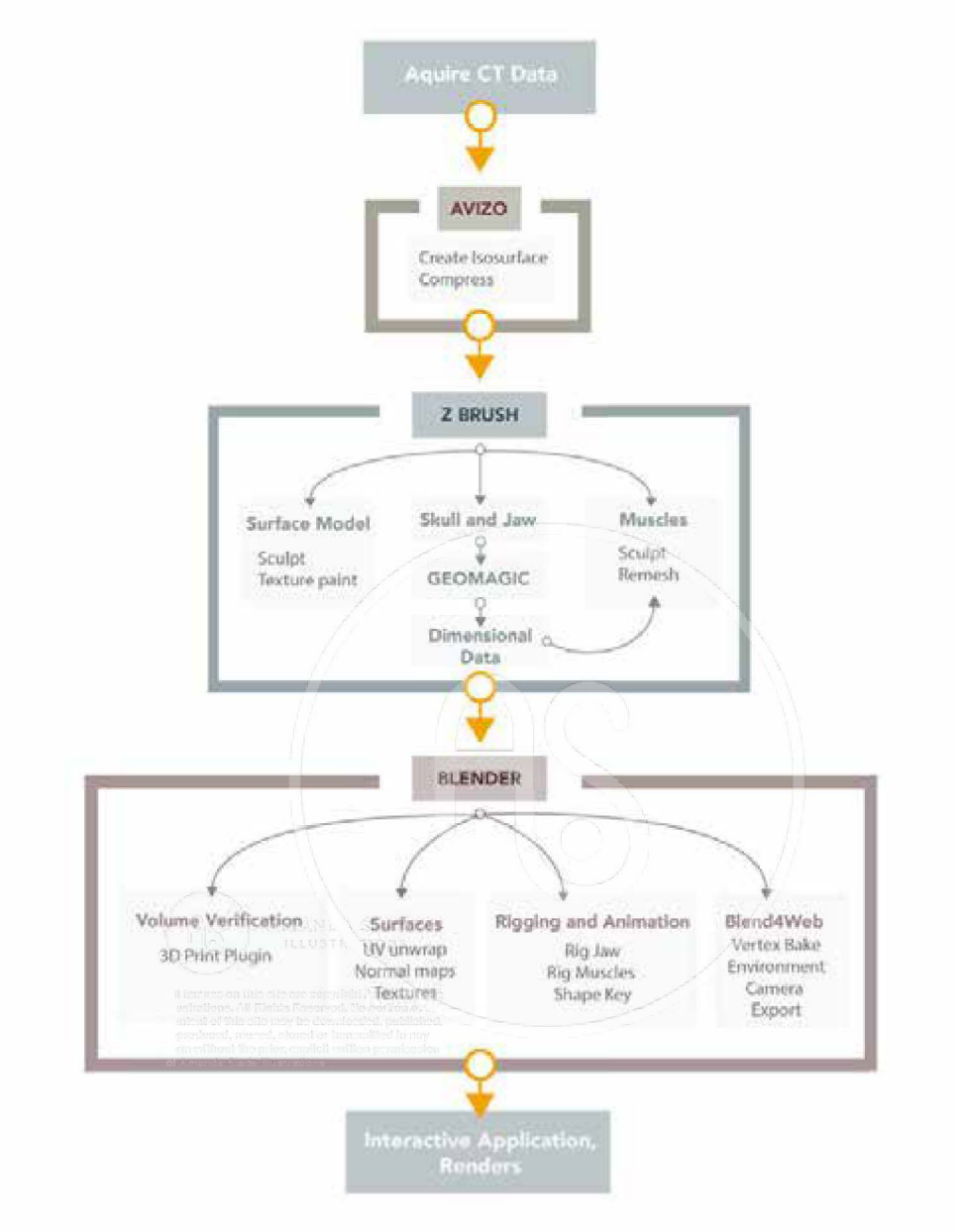

Figure 59. Diagram of the project work flow.

7. Asset Referral Information

Assets can be found at
amandasladeillustration.com and
The Department of Art as Applied to Medicine
Johns Hopkins University
Baltimore, MD

DISCUSSION

The goal of this project as a whole was to create a comprehensive virtual reconstruction of an early primate's chewing anatomy and biomechanics in order to enhance the value of the fossilized cranium and mandibles of *Smilodectes gracili*s as objects of study. This section reviews and discusses what was involved in creating the models, animations, and interactive applications created to achieve the primary goal as well as any drawbacks or limitations that were encountered at each stage.

1. Fossil Reconstruction

The primary goal of the reconstruction of the *Smilodectes gracilis* specimen, was to provide a virtual model of the specimen, free of the damage and distortion that typically encumbers a scientist in making accurate osteological measurements. The *Smilodectes* fossil being studied in this project for example, was so impacted by sediment that certain osteological landmarks, such as the attachment area of the medial pterygoid, were entirely obscured. The virtual reconstruction of the specimen that was produced was unencumbered by these flaws was able to yield the osteolgical dimensions need for muscle reconstruction.

When reconstructing a damaged specimen there is the inherent risk of bias entering the decision making of the changes to make. A fully reconstructed model might sacrifice accuracy for completeness. In the *Smilodectes fossil* specimen used for this project, for instance, a significant portion of the nasal region, as well as parts of the zygomatic arch were missing from the fossil and required reconstruction based entirely on reference material rather than content from the specimen itself. The ambiguity of such reconstruction techniques was in some part resolved by utilizing a three stage approach that emphasizes transparency to the changes being made. The reconstruction moved through the stages of first, a segmented model; second, a restored model; and finally, a fully reconstructed model. The techniques and software used are described in the **Materials and Methods** section. This three stage approach allows for any changes made or anatomy added to be entirely clear to the viewer. A scientist interested in this species or early primates in general has full access to virtually analyzing the anatomy of a nearly unaltered fossil of the species or a fully reconstructed approximation of the bony morphology without risk of mistaking reconstructed data for raw data.

2. Muscle reconstruction:

Reconstructing the chewing musculature for *Smilodectes gracilis* was achieved both numerically and virtually. The numerical dimensional data for muscle size calculated for this study generally suggest that

the jaw adductor muscles of this species were large, although further analysis is needed.

Some literature suggests that large muscle mass indicates a folivorous diet (Taylor and Vinyard 2009). Perry's study (2015) states that if the estimates for PCSA (physiological cross sectional area) for Adapis and Leptadapis ," are large, then this would provide support for a folivorous diet (Perry, 2015, p. 3)". *Smilodectes*, *Adapis* and *Leptadapis* are all adapiform primates and it is reasonable to assume a large PCSA in *Smilodectes* would also provide support for the species having a folivorous diet. This would in turn, support the dental analysis that *Smilodectes* was a foliovore (Rose, 1974). There is also literature that suggests that "Truly massive jaw adductors are expected if a primate must ingest large objects that are also very resistant to breakage because these animals simultaneously require long fibers and forceful adductors with great PCSA (Taylor and Vinyard, 2009, Perry 2015)" If the jaw adductors on this specimen of *Smilodectes gracilis* were deemed as truly "massive" then further inferences might be made about its diet including large, resistant objects. The data, however, would need to be analyzed further before it could be presented as solid support for a particular diet.

The virtual 3D reconstructions of the jaw adductors were able to provide a visual verification that the numerical dimensional data were realistic. When the reconstructed musculature was attached to the virtual skull reconstruction, the volumetric relationship between muscle and skull were not obviously disproportionate. That is, they more or less resembled cadavers of primates in the muscle-to-bone size relationship. In addition, there were no osteological constraints that made the reconstructions impossible. The muscle reconstruction generally fit the skull in a believable way. This was confirmed by Dr. Perry at the Department of Functional Anatomy and Evolution and generally conforms to anatomical evidence from strepsirrhine primate dissection photographs (Perry, 2008).

The combination of numerical dimensional reconstruction and virtual 3D reconstruction provides a clearer picture of the jaw adductors for Smilodectes gracilis than has ever been provided before. The data collected have the potential to inform inferences on the diet and perhaps support the dental analysis that the species was a foliovore.

3. Chewing model and Animation

The primary purpose of creating a chewing model of an extinct primate was to virtually demonstrate the digital jaw adductor models in action and thus provide visual validation that the muscle volume predictions were reasonable. This was achieved in that the musculature when put to motion did not behave in a way that would invalidate or put into question the volumetric estimates. This was confirmed by Dr. Perry as well.

The secondary goal of this endeavor was to create a fully articulated and rigged, digital model that would allow parameters such as joint constraints or jaw angle to be input, and then cause the chewing musculature to respond. Such a model demonstrates a unique option for studying chewing biomechanics. The model successfully used numerical inputs, a virtual simulation of movement. The inputs used for this simulation were approximations of the chewing cycle of primates supplied by published literature (Ross and Diaz, 2014, Kay and Hiiemae, 1974). The parameters that allow numerical input include: rotation of the jaw, displacement within the temporomandibular joint, and time.

Although hard data were not produced from the model, it set the stage for future studies in jaw biomechanics. The success of the simulation also validates the time and effort spent virtually reconstructing and rigging the models.

4. Facial approximation

This project lent itself to an artistic reconstruction of the face of *Smilodectes* as the animal might have appeared in life. With so much of the facial anatomy reconstructed in previous stages of the project, much of the science based work in facial approximation had been completed. The result is a virtual model of a realistic animal that brings an extra layer of imagination and inspiration to the project.

The added benefit of this facial approximation being a virtual 3D model allows it to be used in a variety of ways. It can be posed and lit in within all artistic 3D software to create 2D still images or animations. It can also be loaded onto any online 3D viewing platform such as **Blend4Web** which dramatically increases its accessibility.

Paleoart has always been a driver of the public's interest in the field of paleontology, and it could be argued to be a driver of its funding as well. This final layer added to the reconstruction of *Smilodectes gracilis* has the potential to inspire further studies of early primates.

A secondary result is a documented process of how the facial approximation was achieved. The relationship between scientist and artist when creating paleoart has little reproducible documentation. The technique is largely dependent on the artist's and/or scientist's personal aesthetics and preference. This project documents the scientific foundation upon which the approximation was based and makes clear the degree to which the approximation was based on scientific data and the degree to which it was left to artistic interpretation.

5. Web application and Interactively

All models and animations created in this project: the three stages of fossil reconstruction, muscle anatomy, chewing simulation, and facial approximation were made into interactive HTML web applications. An interactive option for the project was chosen to increase accessibility. The application allows for anyone with an internet connection to access the models . The models can be rotated and enlarged, allowing scientists to appreciate the three dimensionality inherent to fossils and fossil reconstruction.

The interactive applications created are self-contained HTML websites that do not considerably request data from the server. The performance relies entirely on the local GPU and CPU upon loading (Li, 2017). Several parameters can be taken into account in order to optimize the performance for WebGL. Polygon count, light sources, shadows, and ambient occlusion can affect the performance. To optimize performance, environmental objects were kept at a very low poly count; only the model was allowed a shadow and ambient occlusion was disabled. The models' meshes themselves were optimized as described in the **Materials and Methods** section. During testing the application loaded and ran well on a 2016 iMac (Processor 3.3 GHz Intel Core i5; Graphics: AMD Radeon R9 M395X 4096 MB).

6. WebGL using Blend4Web

WebGL is a recent technology having been released in only 2011 and whose second iteration was last year (January 2017). WebGL frameworks and libraries have been developed since in order to utilize the technology for interactive web application development (Li, 2017; "List of WebGL frameworks", 2016). 3D game engines, for example, have been starting to incorporate engine based WebGL frameworks such as **Unity** and **Blender**. This is especially useful for the people interested in using the technology but who have no background in coding, as opposed to the popular open-source framework three.js. These frameworks also have the advantage of well developed user interfaces that are familiar to 3D artists.

Although Unity is a well-used 3D game engine its WebGL capabilities have not yet been well-developed (Bezuhoff, 2015). **Blende4web** however, is unique in that it was developed as a new "mode" within Blender that allows artists to build 3D scenes and export them directly to WebGL. It also features a logic node editor and interactive functions that can be embedded on objects without coding (Li, 2015). A drawback is that 2D elements within the web application are better created with coding using JavaScript. This script, however, is arguably much easier to learn than others such as C++ or C#. As such, less complex projects that do not rely heavily on 2D assets can still be created without any coding, as this project was.

Blend4Web is an add-on of **Blender** and therefore shares the same interface; however, its functionalities are different when operating in **Blend4Web**. **Blend4web** is completely based on JavaScript for browser-based real-time rendering and uses its own render engine as opposed to the default render engines within **Blender** (**Blender Render** and **Cycles Render**). The primary differences that this project encountered were the differences in animation capabilities. This project required animation to take place on multiple objects each of which utilized armature animation and **Shapekey** animation. **Blend4web** does not support simultaneous use of these animation functions. The workaround required the **vertex baking** option described in the **Materials and Methods** section. While **vertex baking** was a success, it did require the model to be processed in a different way.

An additional animation challenge that was encountered was the need for multiple objects to be animated simultaneously. Although the playback of these could be programed to play at the same time with the node editor, the results were not reliable and objects would become out of sync (masseter muscle would flex at a different rate than jaw movement, for example). The solution required combining all objects and animating them as a single object; this process is described in the **Materials and Methods section**. The solution was successful; however, it sacrificed control over individual aspects of the animation. While researching solutions to the animation problems encountered, it became clear that the **Blend4Web** team is prioritizing advancing the animation capabilities for future **Blend4Web** versions, as many users were encountering similar issues.

7. Working in Blender

Blender is a free 3D open source software. Any techniques documented in this project are therefore accessible without budget being a limiting factor. Because of its accessibility, a significant community that uses it and presents tutorials and techniques which were used in this project. The large and diverse population of **Blender** have also created a range of add-ons, many of which are also for free. This project utilized the 3D printer add-on and the **Blend4Web** add-on. These add-ons aided workflow in that the different stages of the project did not require separate software for their completion. Measuring the volume of the muscle models for instance, could be completed within **Blender** using the 3D printing add-on rather then needing to be exported to a separate 3D printing software.

8. Working in Z Brush

This program has maintained its place as the best sculpting software for years and this project

could do nothing but confirm its standing. This program was instrumental in the success of creating realistic, detailed, and aesthetic reconstructions. Its mesh optimizing capabilities were also important for creating low poly models that could easily be unwrapped during the UV unwrapping process, described in the materials and methods section. By being able to process and sculpt up to a billion polygons, it also permitted the reconstruction of the fractured skull. Finally, during the creation of the facial approximation, the tools in **Z brush** allowed for realistic and aesthetic rendering to be created.

9. Reproducible Workflow

The workflow created in this project covers three different programs and utilizes a variety of tools within each. The workflow is streamlined in that the movement through each of the programs is linear. Each stage is contained within a specific software. The workflows within each software are also useful in isolation. For instance, the **Z Brush** stage could be skipped and a fossil could be brought directly into **Blender** for processing and uploading onto the internet. This workflow offers a road map for not only biocommunicators, but those interested in virtual paleontology which is quickly taking over the field.

CONCLUSION

This project gave rise to the first dynamic fully articulated, manipulable, animated and interactive model of an extinct primate's masticatory apparatus, featuring a reconstructed fossil skull, jaw adductor musculature and facial approximation. A full range of digital processing software was utilized and information across disciplines was integrated. The models incorporate data from comparative anatomy, functional morphology, and biomechanics. The project utilized the full range of digital processing to complete the project including CT imaging, 3D sculpting, rigging, animation, and finally online interactive software. This project not only pushed the boundaries of the study of early primate chewing architecture and dynamics but also documented a novel workflow that demonstrates a future direction of paleontological imaging and represents the full power of combing art and science.

REFERENCES

1. Abel, Richard Leslie, Laurini, Carolina Rettondini, and Richter, Martha 2012. A palaeobiologist's guide to 'virtual' micro-CT preparation. Palaeontologia Electronica, 15: 17; palaeo-electronica.org/content/issue-2-2012-technical-articles/233-micro-ct-workflow.
2. Berge, et al. 2009. A new reconstruction of Sts 14 pelvis (Australopithecus africanus) from computed tomography and three-dimensional modeling techniques. Journal of Human Evolution, 58: 262-7.
3. Brown MA, Kane JF, William GP. 2009. Methods in Preparation: Proceeding of the First Annual Fossil Preparation and Collections Symposium: 4-11.
4. Brunet M, Guy F, Pilbeam D, Mackaye HT, Likius A, Ahounta D, Beauvilain A, Blondel C, Bocherens H, Boisserie J-R, De Bonis L, Coppens Y, Dejax J, Denys C, Duringer P, Eisenmann V, Fanone G, Fronty P, Geraads D, Lehmann T, Lihoreau F, Louchart A, Mahamat A, Merceron G, Mouchelin G, Otero O, Campomanes PP, De Leon MP, Rage J-C, Sapanet M, Schuster M, Sudre J, Tassy P, Valentin X, Vignaud P, Viriot L, Zazzo A, Zollikofer C. 2002. A new hominid from the Upper Miocene of Chad, Central Africa. Nature, 418:145-151.
5. Cartmill M., 1974. Rethinking Primate Origins. Science, 184: 436 – 442.
6. Cartmill, M., 1972. Arboreal Adaptations and the Origin of the Order Primates. The Functional and Evolutionary Biology of Primates, RH Tuttle, Aldine-Atherton: 97-122.
7. Covert HH. 1986. Biology of Early Cenozoic primates. In: Swindler DR, Erwin J, editors. Comparative Primate Biology, Volume 1: Systematics, Evolution, and Anatomy. New York: Alan R. Liss: 335-359
8. Dunn RH, Rose KD, Rana RS, Kumar K, Sahni A, Smith T. 2016. New euprimate postcrania from the early Eocene of Gujarat, India, and the strepsirrhine–haplorhine divergence. Journal of Human Evolution, 99: 25-51.
9. Early Primate Evolution: The First Primates. Received Feb 2 2018 from www2.palomar.edu/anthro/earlyprimates/early_2.htm.
10. Fleagal JG. 1999. Primate Adaptation and Evolution. Second ed. New York: Academic Press.
11. Gilbert GC, Jungers WL. 2017. Comment on relative brain size in early primates and the use of encephalizaiton quotients in primate evolution. Journal of Human Evolution, 109: 79-87.

12. Gingerich, Philip D. 1979. Phylogeny of Middle Eocene Adapidae (Mammalia, Primates) in North America: Smilodectes and Notharctus. Journal of Paleontology, 53: 153–163.

13. Gregory, WK (1920) On the structure and relations of Notharctus, an American Eocene primate. Mem. Am. Mus. Nat. Hist. 3: 49-243.

14. Gunnell, Gregg F. 2002. Notharctine Primates (Adapiformes) from the Early to Middle Eocene (Wasatchianâ Bridgerian) of Wyoming: Transitional Species and the Origins of Notharctus and Smilodectes. Journal of Human Evolution, 43: 353–380.

15. Harrington RH, Silcox MT, Yapuncich GS, Boyer DM, Bloch JI. 2016. First virtual endocasts of adapiform primates. Journal of Human Evolution, 99: 52-78.

16. Harrington, Arianna. 2016. From First Virtual Endocasts of Adapiform Primates. Morpho Source Media, 99.

17. Hiiemae KM. 1976. Masticatory movements in primitive mammals. In: Anderson DJ, Matthews B, editors. Mastication. Bristol: JohnvWright & Sons:105–118.

18. Kay RF, and Hiiemae KM. 1974. Jaw Movement and Tooth Use in Recent and Fossil Primates. American Journal of Physical Anthropology, 40: 227–256.

19. Kovelenov y, Nyman R. 2014. Blend4Web: The Open Source Solution for Online 3D. Retrieved March 5 2018 from https://hacks.mozilla.org/2014/10/blend4web-the-open-source-solution-for-online-3d/

20. “Lanzendorf PaleoArt Prize” . 2015. GNSI, Guild of Natural Science Illustrators. Society of Vertebrate Paleontology. Retrieved April 20 2018 from https://gnsi.org/resources/grants-awards/lanzendorf-paleoart-prize.

21. Lebatard, 2008. Cosmogenic nuclide dating of Sahelanthropus tchadensis and Australopithecus bahrelghazali: Mio-Pliocene hominins from Chad. Proceedings of the National Academy of Sciences of the United States of America 105, 3226-3231.

22. Leiggi P, May P. 1994. Vertebrate Paleontological Techniques: Volume One. Cambridge: Cambridge University Press, xiii.

23. Linnaeus, Carolus 1735. Systema naturae, sive regna tria naturae systematice proposita per classes, ordines, genera, & species. Leiden: Haak: 1–12.

24. McGwire, Kenneth, and Stephanie Livingston. 1998 Developing Digital Paleontological Collections: Searching, Visualizing, and Measuring Virtual Specimens. National Science Foundation

25. Molhar J. 2009. How Giant Reptiles Flew: Visualizing Quaprupedal Launch in Pterosaurs. MA Johns

Hopkins University, Baltimore, MD: 3-5.

26. Perry JMG 2008. The Anatomy of Mastication in Extant Strepsirrhines and Eocene Adapines. Ph.D. Dissertation, Duke University: 490.

27. Perry JMG, Hartstone-Rose A, Wall CE. 2011. The jaw adductors of strepsirrhines in relation to body size, diet, and ingested food size. Anatomical Record 294: 712-728.

28. Perry JMG, St Clair EM, Hartstone-Rose A. 2015. Craniomandibular signals of diet in adapids. American Journal of Physical Anthropology 158: 646-662.

29. Perry JMG. 2018. Inferring the diets of extinct giant lemurs from osteological correlates of muscle dimensions. The Anatomical Record 301:343-362.

30. Prakhov, A. 2016. Blend4Web vs Unity: WebGL Performance Comparison. Retrieved March 10, 2018 from https://www.blend4web.com/en/community/article/280/

31. Rasmussen, D.T., Sussman, R.W., 2007. Parallelisms Among Primates and Possums, Primate Origins: Adaptations and Evolution, Ravosa, MJ, Dagosto, M, Springer Science and Business Media: 775-803.

32. Ravosa MJ. 1996. Mandibular form and function in North American and European Adapidae and Omomyidae. Journal of Morphology 229 171-190.

33. Rose, Kenneth D. The Beginning of the Age of Mammals. The Johns Hopkins University Press, 2006.

34. Ross C, & Iriarte-Diaz J. 2014. What Does Feeding System Morphology Tell Us About Feeding? Evolutionary Anthropology Issues News and Reviews. 23: 105-120.

35. Ross, Callum F., et al. 2012. Innovative Approaches to the Relationship Between Diet and Mandibular Morphology in Primates. International Journal of Primatology, 33: 632–660.

36. Ryan TM, Burney DA, Godfrey LR, Gohlich UB, JUngers WL, Vasey N, Ramilisonia, Walker A. 2008. A reconstruction of the Vienna skull of Hadropithecus stenognathus. Weber proceedings of the National Academy of Science 105: 31

37. Smithsonian National Museum of Natural History. 2018. What does it mean to be human? 3D Collection. Retrieved from http://humanorigins.si.edu/evidence/3d-collection

38. Soriano, Marc. “Skeletal Animation”. Bourns College of Engineering. Retrieved January 2018.

39. St Clair EM, Reback N, Perry JMG. 2018. Craniomandibular variation in phalangeriform marsupials: functional comparisons with primates. The Anatomical Record 301: 227-255.

40. Sussman RW, 1991. Primate Origins and the Evolution of Angiosperms, American Journal of

Primatology 23: 209-223.

41. Sussman RW, Raven PH. 1978. Pollination by Lemurs and Marsupials: An Archaic Coevolutionary System. Science, 200: 731-736

42. Sutton M, Rahman I, Garwood R. 2016. VIRTUAL PALEONTOLOGY—AN OVERVIEW. The Paleontological Society Papers, 22: 1-20

43. Sutton, Mark D., et al. Techniques for Virtual Paleontology. John Wiley & Sons, 2014.

44. Tavares, Gregg. 2012. "WebGL Fundamentals". HTML5 Rocks. Retrieved March 2018. https://www.html5rocks.com/en/tutorials/webgl/webgl_fundamentals/

45. Yao L. 2017. Lymphatic Voyage: Communicating 4D Immune Cell Dynamics and Lymph Node Architecture using WebGL-based Animation and Interactivity. MA Johns Hopkins University, Baltimore MD

Vita

Amanda Slade was born in Portland, Oregon. She spent her childhood in inner city Portland going to Grant High School where she swam competitively, played in the wind ensemble and graduated as a Valedictorian with a focus in Biology in 2006. Amanda went on to study Biology at Portland State for two years before transferred to Oregon State University where she received her Bachelors of Science in Biology in 2010.

During her time at Oregon State she completed two summer internships; the HHMI (Howard Hughes Medical Internship), with the Tanugay Lab and the PROMISE internship with Oregon Sea Grant. Oregon Sea Grant hired her on as a full time employee after graduating, and it was there that she first became acquainted with biological illustration. She created public outreach materials against invasive species which included pen and ink illustrations for a species identification guide for invasive tunicates.

Amanda has always had a love of travel and after completing a year with Oregon Sea Grant she moved to South Korea to teach English for the next year. This experience allowed her to gain tools that would help her throughout her career including education, project management, and the ability to work outside her comfort zone. She only returned to the mainland US for a short time before traveling again, this time to the Big Island of Hawii to work on a series of organic farms with the WWOOF (World Wide Opportunities on Organic Farms) program.

After three months of working on farms she returned home and began working as a veterinary technician. Amanda has always been passionate for veterinary medicine and it became a wonderful opportunity to learn about the field and about medicine in general. While she worked went to school for art and anatomy in preparation for application to all four of the North American Schools for Medical Illustration.

Upon completing her masters from Johns Hopkins she will be moving to Athens Georgia to complete the Comparative Medical Illustration Certificate Program which focuses on two subjects she is deeply passionate about: Medical illustration and Veterinary Medicine.